International Symposium on Fire Safety Research

on the occasion of the retirement of Leen Twilt in cooperation with EGOLF

Syllabus

Monday, 14 March 2005

TNO Environment and Geosciences

TNO Knowledge for business

International Symposium on Fire Safety Research

On the occasion of the retirement of Leen Twilt in cooperation with EGOLF

Monday, 14 March 2005
Delft, the Netherlands

Syllabus

Editors

Joris Fellinger
TNO Centre for Fire Research
P.O. Box 49, 2600 AA DELFT, The Netherlands
Phone: +31 152763487
Fax: + 31 152763025
E-mail: Joris.Fellinger@tno.nl

Kees Both
TNO Centre for Fire Research
P.O. Box 49, 2600 AA DELFT, The Netherlands
Phone: +31 152763480
Fax: + 31 152763025
E-mail: Kees.Both@tno.nl

Copyrights

Contents

Foreword

Fire safety, actually a strange name for a very interesting part of science in our modern society. The primary goal of fire safety is not to save the fire, rather the opposite. Notice the word science: a couple of decades ago, fire safety was merely practiced performing fire tests in furnaces. Quite a step we all made since then. Fire safety nowadays, still includes (of course!) fire testing, but also advanced calculation and fundamental research into e.g. fire spread and combustion processes. One of the pioneers in making these steps has been Leen Twilt.

Since Leen Twilt will make his final steps in fire safety, an organizing committee composed of colleagues, decided to organise an international symposium on that occasion. In this booklet, both the presentations given at the symposium are presented, as well as background articles of some of the speakers. The background articles also give an impression of the variety of fire safety issues, Leen Twilt has been involved in. The articles and presentations cover:

- fire testing, both according to standards as well as to non-standard fire testing and modelling of these tests national and international fire safety projects;
- projects resulting in a pragmatic, more or less directly applicable outcome and projects describing a first phase of more fundamental research;
- research into improving materials and systems for modern buildings and cultural heritage;
- the established fire safety experts and the promising talents;
- and more.

Although some articles and presentations deal with the reliability (and repeatability and reproducibility) of test and models or touch upon (the effects of) active fire safety measures, one could easily observe that the majority of the work presented addresses deterministic approach towards passive fire safety measures, with an emphasis of structural integrity issues. The legacy of Leen Twilt leaves challenges to all experts in the fire safety field: the development and promotion of the rational fire safety combining active and passive measures.

The organising committee hopes you will enjoy glancing through or studying in the articles and presentations provided in this booklet. We herewith thank all the speakers and authors, and last but not least, our gratitude extends towards Leen Twilt, for being a most inspiring, driven and motivated, intelligent and vigorous colleague and friend.

On behalf of the organising committee,

editors: Joris Fellinger and Kees Both

Note: These proceedings will be published officially via special issues of Heron, a joint publication of Delft University of Technology and TNO.

The Single Burning Item (SBI) test method – a decade of development and plans for the near future

Rudolf van Mierlo
TNO Centre for Fire Research, Delft, the Netherlands
Email: rudolf.vanmierlo@tno.nl, Phone: +31 15 276 3490

Bart Sette
Ghent University, Dep. of Flow, Heat and Combustion Mechanics, Ghent, Belgium

Harmonised technical specifications are needed to create a single European market. Although many test methods were available to assess the reaction to fire performance of building products, no set of existing test methods was both politically and technically acceptable. As a result the Single Burning Item (SBI) test method has been developed . For about 80% of the building products on the European market this assessment will be, and partly is already, compulsory. The paper describes the development process of the SBI test method, including the result of the second recently finalised round robin exercise. Items for further development are discussed with the emphasis on some uncertainty aspects of the test method.

Key words: Reaction to fire, SBI, test methods, round robin

1 Introduction

Through the use of harmonized technical specifications, thus removing technical barriers between Member States, the Construction Product Directive (CPD) [24] aims to create a single European market. It applies to all construction products that are produced for, or incorporated within, building and civil engineering construction works. It harmonises all construction products subject to regulatory controls for CE marking purposes.

The CPD defines six "Essential Requirements", from which one is the "Safety in case of fire". While in other Directives the essential requirements are directed to the products themselves, the CPD relates to the essential requirements of the works. The link between the requirements of the works and the technical specifications for building products is established through the "Interpretative

Documents". One of the fire characteristics for construction products to assess is the reaction to fire performance.

The CPD provides for a "Standing Committee on Construction" (SCC), which assists the European Commission in its implementation. The SCC members are representatives of the Member States. In general the SCC is a consulting body to the Commission, but for certain items indicated in the CPD it is a regulatory body. The SCC has set up a technical working group to assist in the interpretation of the Directive in fire safety related matters: the "Fire Regulators Group" (FRG), recently re-established and named "Experts Group on Fire issues under the CPD" (EGF).

One of the characteristics for construction products to assess is the reaction to fire performance. This characteristic is present in the national regulations of all European member states and plays an important role in evaluating possible uses of building products. The basis for the European reaction to fire classification, the EUROCLASSES, was put in place in 1993 by the Fire Regulators Group. The classification system was based on the performance of products under different fire conditions: the attack of a small flame; exposure to a fully developed fire; and some intermediate level. Due to the nature of fire under the influence of gravity forces, two basic applications of products were distinguished: products applied on a floor and all other products.

All but one of the tests needed in this new classification system were known international standard test methods. No existing test method representing the intermediate level that was both politically and technically acceptable. The missing test method, including the apparatus, representing the scenario of a Single Burning Item - to test building products excluding floor coverings - had to be designed from scratch. The apparatus soon got called the SBI [1].

The SBI test method was planned to assess the performance of building products in a (real scale) room corner scenario. The ISO 9705 Room corner test [5], which is a full-scale test method intended to evaluate the contribution to fire growth provided by a surface product applied in a room, was put forward as the reference test for this scenario. The main development objective therefore was that the product ranking in the SBI would have a high correlation with the ranking obtained in the ISO Room corner test. The second development objective followed from the requirement that the method had to be capable of measuring the required characteristics in a repeatable and reproducible way.

This paper describes major steps in the development of the SBI method, recent results acquired and the need for further improvements. For convenience a short description of the test method is given here.

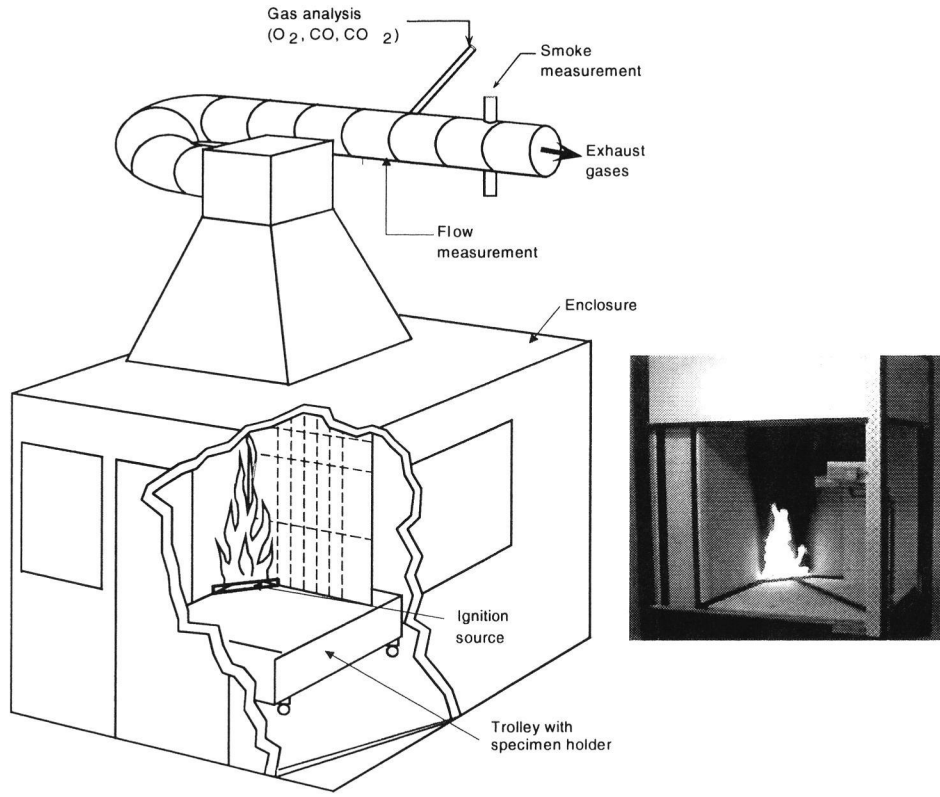

Figure 1 The Single Burning Item test set up in the normative 3 x 3 m² test room.

The SBI test simulates a single burning item burning in a corner of a room. The test apparatus is presented in Figure 1. The total exposed specimen surface area is 1,5 m x 1,5 m. The specimen consists of two parts (height 1,5 m, width 0,5 and 1,0 m) which form a right-angled corner. Eventual corner joints as applied in end-use conditions form part of the product under test[1]. A triangular shaped propane diffusion gas burner running at 30kW acts as heat and ignition source representing a burning waste paper basket. It is placed at the basis of the specimen corner. The performance of the specimen is evaluated during 20 minutes. There is a floor in the test configuration but no ceiling. Floor, specimen and burner are installed on a trolley that can be

---

[1] *Due to specimen construction and size, construction behaviour like mechanical deformation may be of major importance for product performance in the SBI test method. This in contradiction to many other reaction to fire tests.*

removed from the room for easy mounting of the specimens. The combustion gases are collected in a hood and transported through a duct. The duct contains a measurement section with a differential pressure probe, thermocouples, a gas sample probe and a smoke measurement system, to measure heat and smoke production.

2 Development of the basic method

The development of the SBI test method was assigned by the European Commission and carried out under direct guidance by the Fire Regulators Group. A group of seven, later nine, fire laboratories from an equal number of EU member states was formed in 1993 with the development task. The aim was to develop a test method that produces results representative for the behaviour of building products when exposed to one single object, e.g. a coach or a litter basket, on fire placed in the corner of a room. A specific irradiance level that falls onto the specimen was prescribed.

Many design aspects were considered in the early stages. The major ones being:

- Type of heat source: Four heat sources were considered, leading to two serious candidates: a diffusion type burner and a gas fired radiant panel. The selection of the propane diffusion sandbox burner was finally made on the basis of practical aspects, repeatability and discrimination capability.
- Closed or open arrangement of the test apparatus: For reasons of reproducibility and operator protection a closed configuration was chosen. Preliminary CFD calculations showed no significant influence of the walls of the enclosure at the chosen size.
- Inclusion or not of a ceiling in the specimen arrangement. A specimen arrangement without ceiling was chosen based on the absence of a significant effect of the ceiling on the discrimination capability of the test, the measurability of parameters, or the repeatability and reproducibility of the results.

Other parts of the apparatus were taken from other standards: the oxygen depletion measurement technique and accompanying instrumentation were based on the ISO 9705 and ISO 5660 [3] design.

Not only the design of the apparatus received much attention. The test, calibration and calculation procedures were specified in great detail. Unlike the more global description of the calculations in many other standards, the calculations were introduced in detail to facilitate the writing of calculation software without (much) further technical knowledge of the measurement techniques.

After acceptance of the design by the European Commission, some fifteen to twenty additional SBI's were build and installed all over Europe in just a few months to perform a large round robin project. The round robin started in May 1997 with 20 laboratories, testing 30 building products in

threefold. Fifteen laboratories managed to perform the tests in the required very tight time schedule. The result of the round robin was accepted by the Standing Committee in December 1997, as sufficient proof of the ability of the SBI test method to measure the required characteristics in a repeatable and reproducible way, however under the condition of certain improvements.

A further one year of development work resulted in changes to the smoke measurement, to the velocity profile in the exhaust duct and to the calculation and calibration procedures:

- Smoke measurement system improvements concern prevention of soot deposit on the lenses; a reduction of vibration in the optical system; and simple positioning of calibration filters.
- The velocity profile in the exhaust duct at the pressure probe position was asymmetric W-shaped instead of fully developed. Three changes were introduced to the exhaust duct: a shift of the guide vanes further away from the probe position, the introduction of a small orifice immediately behind the guide vanes and the introduction of 0,5 meter additional duct length. The result was a nearly flat profile over the mid half of the duct radius.
- Calculation procedures: two improvements were introduced:
  - Automatic synchronisation of gas analyses data: Since pressure, temperature, oxygen and carbon dioxide concentration, needed to calculate the heat release, have different dead times, a synchronization is needed. A fully automated procedure was introduced to exclude human interpretation.
  - Introduction of validity checks for the burner switch response time; drift in gas concentrations and light attenuation; malfunctioning of thermocouples; and for the deviation in heat and smoke burner output. A failure to meet the criteria invalidates the test result.
- Calibration procedures: nearly all calibration procedures were extensively rewritten; some new ones were introduced.

After five and a half years of development under direct guidance of the European Commission, the draft method was handed over to CEN in spring 1999. There the method was fine-tuned and transferred into a draft CEN standard. No fundamental design changes were introduced. However, a large number of small adjustments improved the standard considerably.
The SBI method was accepted in CEN as a European test method in the Autumn of 2001 and has been implemented in national regulations since then.

3 The reaction to fire classification system

The basis for the European reaction to fire classification, the EUROCLASSES, was put in place in 1993 by the Fire Regulators Group. The classification reflected the needs of the Regulators in the different member states to transpose current national performance levels into new European levels, and not implicitly the urge to design a technically well balanced set of classes. The classification of building products excluding floorings is assessed using four test methods. Three classifications apply: a main classification related to heat production (classes A1, A2, B, C, D, E or F, where A1 represents the highest level ("no contribution to fire") and F has no requirements or "no performance determined"), and additional classifications for smoke production (s1, s2 or s3, where s1 is the best, s3 has no requirements) and for flaming droplets and particles (d0, d1, d2, where d0 is the best, d2 has no requirements). The SBI test method is relevant for the main classes A2-D[2] and all additional classes.

Based on current practice in the member states, the EC choose to take a series of fire characteristics into account in the SBI: an index representing the speed of growth in heat release rate (FIGRA), the total heat released over the first 10 minutes (THR_{600s}), a simple lateral flame spread to the end of the specimen (LFSedge), an index representing the speed of growth in smoke production rate (SMOGRA), the total smoke produced over the first 10 minutes (TSP_{600s}), and a parameter defining three levels of flaming droplets and particles (FDP).

Due to differences in national regulatory needs the characteristics were combined in the three separate classifications mentioned earlier: a main, heat release based, classification, valid for all member states, a smoke production classification and a classification of falling flaming droplets and particles for only a part of the member states.
The FIGRA and SMOGRA indices use threshold values for total heat release and smoke production below which they are set to zero by definition. This in order to eliminate some ambiguous results obtained with very small release rates in the first tens of seconds in the test. Different levels of thresholds were introduced for FIGRA in different classes, leading to $FIGRA_{0,2MJ}$ and $FIGRA_{0,4MJ}$.

A compilation of the SBI criteria[3] in the various classes is given in Table 1[4].

---

[2] *The alternative special requirement option for external non-substantial components in class A1 is not noted.*
3 Some typical examples of product classification according to the criteria: paper faced gypsum plasterboard: A2, s1, d0; steel with thin plastic weather coating C, s2, d0; most wood based products (not fire retardant treated): D, s2, d0; most uncovered not fire retardant treated thermoplastics: D, s2, d2 or E, s3, d2
[4] *The alternative special requirement option for external non-substantial components in class A1 is not noted.*

Table 1 SBI classification criteria.

Main classification		Smoke classification		Flaming droplets/particles classification	
A2 and B	$FIGRA_{0,2MJ} \leq 120$ W/s LFS < specimen edge $THR_{600s} \leq 7{,}5$ MJ	**s1**	SMOGRA ≤ 30 m²/s² $TSP_{600s} \leq 50$ m²	**d0**	No flaming droplets/part.
C	$FIGRA_{0,4MJ} \leq 250$ W/s LFS < specimen edge $THR_{600s} \leq 15$ MJ	**s2**	SMOGRA ≤ 180 m²/s² $TSP_{600s} \leq 200$ m²	**d1**	No flaming droplets/part. persisting > 10 s
D	FIGRA ≤ 750 W/s	**s3**	-	**d2**	-

4 Recent developments

Since its introduction the SBI test has been used extensively in a large number of European fire laboratories and considerable experience has been acquired. The European building sector is now working with the SBI test method to provide their products with a reaction to fire classification, and the particularities of the method have become increasingly apparent ever since.

Several organisations have started to further develop the method. EGOLF, the European Group of Organisations for Fire testing, Inspection and Certification[5], has listed ambiguous and insufficiently defined (parts of) procedures and proposed common solutions and interpretations for them to harmonise the way of working with the method between its members. These proposals, "recommendations" in EGOLF, are not changes to but only additions to the current standard, since EGOLF is not authorized to change the standard. The Fire Sector Group of Notified Bodies (FSG)[6] works along the same lines to support the work of the notified laboratories. Both EGOLF and the FSG send requests for changes in EN 13823 to CEN TC127[7] that has started the formal review of the method. An extensive list of work items has been drafted by TC127. Most purely technical issues already have been solved, but the remaining items might lead to a more or less fundamental change of the method leading to substantially different classifications of products. TC127 still has not decided on the advisability of such a change since guidance by the Commission is still awaited for.

---

[5] *EGOLF members are independent, official, nationally recognised, organisations that test, inspect or certify materials, components and products in support of legislation in Europe; current membership comprises 50 laboratories, of which 47 from EC and EFTA countries.*

[6] *The European Commission supports a structure for the CPD Group of Notified Bodies (third party conformity assessment bodies under the CPD). Fire issues are dealt with in the "horizontal" Fire Sector Group as a general topic relevant for (nearly) all product family related Sector Groups.*

[7] *CEN TC127 is the responsible CEN TC for the development of fire standards under the CPD.*

As major weakness of the method (e.g. in terms of repeatability and reproducibility) is the importance of the mounting and fixing of specimens could be mentioned. However, this is a direct consequence of the CPD principle to test products in their end use application and to test specimen of considerable size where mechanical deformation behaviour plays an important role.
Real weaknesses are recognized in issues like:

- Fallen debris blocking the burner and/or closing the gas supply by blocking the visibility of the flames by the flame detector. The use of a grid to protect the burner only solves part of the problem; it will give no improvement for fluid debris.
- The oxygen analyser is used at the border of its specifications. Regular calibrations, day-to-day checks, good pre-measurement filtering and conditioning of the combustion gases and good maintenance do not solve all the problems here.
- There is no good check of the thermal attack on the specimens. This could be introduced by means of a heat flux measurement or a reference test on a reference material of well known behaviour. The solutions available at present are not reliable enough to override the propane gas supply requirement.

The remaining uncertainties about the accuracy and robustness of the method have lead to the joint initiative of EGOLF and CEPMC (Council of European Producers of Materials for Construction) to organise a second round robin with financial support by the Commission. The round robin was formally set up "to verify the efficiency of the various modifications previously made to the test method and the test procedure after the first round robin in 1997 and to investigate any further remaining deficiencies". The results were reported only recently [23] and can be summarized as follows:

- The repeatability and reproducibility of the continuous classification parameters ($FIGRA_{0,2MJ}$, $FIGRA_{0,4MJ}$, THR_{600s}, SMOGRA and TSP_{600s}), represented by the quotient of the standard deviation estimates (σ_r and σ_R) and the mean value of the parameters (μ), are between 11% and 20% for σ_r/μ and between 21% and 34% for σ_R/μ), when very low[8] mean values are excluded. General proof of improvement of the accuracy of the method in comparison to the first round robin could not be found. Only the reproducibility of the smoke measurements shows some improvements.
- All laboratories show sufficient proof to measure heat release related data in an acceptable way; 90% of them does this acceptably for smoke production related data as well. It takes many laboratories however much longer than expected to comply with the calibrations. This creates concern about the abilities and level of training of the laboratories/operators.

---

[8] *Very low defined as a value 50 % or less of the lowest classification borderline for the Euroclasses A2 – E (i.e.: $FIGRA_{0,2MJ} \leq 60$ W/s, $THR_{600s} \leq 3,75$ MJ, SMOGRA ≤ 15 m²/s² and $TSP_{600s} \leq 25$ m²).*

- Overall the current specified calibration procedure is acceptable and is able to evaluate a laboratories capability to measure heat release rate and smoke production rate in an accurate way. The procedure also helps to highlight problems and to locate them. The round robin shows that there is room for improvement of the calibrations and it is recommended to revise the calibration procedures. Furthermore it is recommended to further develop the calibration of the optical system and to make it normative.
- The results of the visual observations indicate that the set of products used may be a poor discriminator to check the ability of the method to assess the visual observation related parameters. The results however already indicate that large differences in interpretation of visual observations exist.

The round robin clearly shows the benefit of having good calibration procedures, but only if they are applied and laboratory personnel knows how to act when criteria are not satisfied.

The eagerness of industry and fire laboratories to obtain information about the quality of the test results is not the only drive for further attention to the method. Accreditation bodies are increasing the pressure on fire laboratories to include an estimate of measurement uncertainty, other than obtained out of a round robin, in the test report.
According to EN ISO 17025:1999 [8], which sets out the general requirements for the competence of testing and calibration laboratories, and ISO 10012-1 [11], which sets out the requirements for assuring the quality of measuring equipment, uncertainties are to be reported in both testing and calibration reports.

In response to these international standards EGOLF has published a regulation document EGOLF/R4 [4] in 2001. The document provides guidelines by which EGOLF members should interpret and implement the European Standard EN ISO 17025 and the criteria by which they should be subject to accreditation and surveillance against that standard by accreditation authorities.
Different to EN 45001:1989 [9] which prevails EN ISO 17025, the latter makes the estimation and measurement of uncertainty of test results mandatory. Till the release of this new standard, EGOLF had been arguing that reporting uncertainty on fire test results is practically speaking not possible. This belief is still reflected in document EGOLF/R4, but more recent initiatives in EGOLF try to develop means to evaluate uncertainty of measurement for each individual method or family of methods.

In the mean time EGOLF uses the results of round robin exercises as a basis for prove of competence of its member laboratories. This however has some disadvantages:

- It does not differentiate between the uncertainties related to the apparatus, the operator, the product under test, etc.;
- It is costly and time consuming to organise them;
- The results are based on some 'representative' products; in practice however the spread in results may be different.

The round robins result in an estimation of the 'overall' relative repeatability and reproducibility standard deviation making use of the International Standard on Accuracy of Measurement Methods and Results, ISO 5725 [12].

On the other hand, fairly recently, some individual organisations have tried to quantify uncertainty associated with the calculation of heat release rate and smoke production rate [13][20][21][22] on a theoretical basis. However, out of a review of all major round robins, Janssens [14] found that the results suggest that the uncertainty is much greater than the theoretically found values, in particular for intermediate and large-scale tests.

So one of the biggest challenges for the fire community in the coming years, is to work out, for the different test methods, means to evaluate uncertainty of measurement. Due to the actual European harmonisation of fire testing (EN 13501-1 [2]) this is becoming even more important.

5 Determination of uncertainty

The general principles for evaluating and reporting uncertainties are given in the ISO Guide to the Expression of Uncertainty in Measurement (GUM [10]), but need to be adapted to the specific case of fire testing. Today, on the international scene, two entities are active on the subject. The first one is the Swedish national fire institute, SP, and the other one is a working group around the person of Tony Enright. However, in view of the pressure exercised by accreditation authorities, there is an increasing interest of testing laboratories worldwide in the subject.

Despite the initiatives taken, there is still an important way to go before reporting uncertainty along the lines of the GUM document.

The weak points in the work done so far are that:

- Not all relevant phenomena are taken into account, often because people are not aware of them or because they believe they can be neglected. Examples of these are the Reynolds dependence of the velocity pressure probe in the SBI, used to obtain the mass flow of the exhaust gases, and the angular dependence of that same probe.
- The 'guesses' made on uncertainties on the different components since the required statistical information is not readily available. Example of this is that the uncertainty on a gas

concentration measurement is taken as the sum of noise and drift of that gas analyser over half an hour period.

- Dynamic effects of the apparatus have not been taking into account. Due to time constants superseding the data sampling rate, an additional source of error is introduced. This error can not be neglected especially not when considering momentary values like peaks and dips. This is the case in the SBI where the main classification criterion, FIGRA, is defined as the maximum of the quotient of Heat Release Rate by time elapsed to reach that level. To partially eliminate this effect the SBI standard prescribes that the heat release rate first should be smoothened by means of a running average over half a minutes period.
- Covariance's between the different measurands have been neglected. This is not justifiable as can easily be understood from the following example. Suppose a pure substance like for example propane is burnt,

  $$C_3H_8 + 5O_2 \rightarrow 3CO_2 + 4H_2O\,,$$

  we know that for every mole of oxygen consumed, 3/5 moles of carbon dioxide will be formed. So there is a perfect negative correlation between the two (r = -1).
  Furthermore, when there is oxygen consumption, there is heat release and temperature of the exhaust gases will rise with a resulting negative correlation. This negative correlation is also true for the differential pressure measured over the velocity pressure probe, which will increase due to an increased velocity in the exhaust duct when running the equipment at constant mass flow rate.

There is still a wide, unexplored field of research that needs to be filled up in the coming years. The following paragraph highlights some major research topics of interest in the field.

6 Research topics for the near future

Several categories for further improvement of the method still remain. The most important ones are good representation of product performance in practice, good control of the test conditions and determination and limitation of measurement errors. Items from all three categories have been discussed from the beginning of the development of the method, but with an emphasis on the first two. As discussed earlier, research topics in that area have been listed already by CEN, FSG and EGOLF. The third one, "how big are the errors and what can we do about it", has become more important due to the recent uncertainty discussions. Major research topics in that area are highlighted here. Gaining insight in the technique and getting to know its pitfalls, together with a streamlining of the initiatives would greatly improve the accuracy of the method and would allow to obtain a reliable estimation of the uncertainty interval.

6.1 *Gas analysis*

The oxygen concentration is, by far, the most important component to be measured when measuring heat release rate. Evenly important as the concentration measurement itself is the gas sampling and preparation. This includes the sampling, filtering, transport over several meters distance and dehydration. The dehydration is performed in two steps by means of a cooler unit and a desiccant. Since the desiccant is so critical for an accurate measurement of both the oxygen and carbon dioxide concentration, further research is necessary. Indeed, when the partial vapour pressure increases, the measured oxygen concentration lowers resulting in an apparent oxygen consumption and resulting heat release rate. Also some products like Silica gel tend to absorb carbon dioxide initially, while releasing it back further on in the test. This results in a sloppy response curve and can be overcome by using products like Anhydrous Calciumsulphate. Also the problem of saturation – the product must be replaced before the colour indicator warns to do so –, under what circumstances can the product be regenerated and chemical interaction with the combustion gases needs further attention.

The uncertainty related to the oxygen concentration itself includes the calibration method, the calibration gas, ambient conditions like barometric pressure and room temperature, damping, vibrations, etc. The challenge here is to measure variations in concentration of the order of 50 particles per million (ppm) in the range from 17 to 21 Vol.%. These variations are in the same order as the allowed noise level. Although damping of the signal allows to eliminate a great part of the noise, it results in higher response times.

Determination of the uncertainty on the measurement requires much more than for example taking the sum of noise and drift as proposed by Enright [13].

6.2 *Mass flow rate*

Only limited effort has been invested in the accurate determination of the mass flow rate and/or in the improvement of the extraction system (duct diameter, guide vanes, ...). Only a limited number of people within the fire testing community seems to be aware of the impact of the mass flow on the accuracy of the overall heat release rate and smoke release rate measurement. Prove of this are the pre-standards prEN 50399-1 [6], for the assessment of the reaction to fire performance of cables, and prEN 45545-2[7], for the assessment of the reaction to fire performance of materials for railway vehicles. Especially in the second standard, where one wants to measure heat release rates as low as 7 kW and variations of heat release rate smaller than 1 kW making use of hardware designed to cope with fires releasing up to 1 MW (Duct f = 400 mm; extraction rate 1.5 m^3/s at 298 K). The oxygen depletion at the 7 kW level under the given circumstances is only 250 ppm, which almost disappears in the measurement noise.

In general, there is a high degree of 'copy-pasting' from other standards, i.e. ISO 9705, into new developed standards without re-evaluating the method in these new circumstances. ISO 9705 is a full-scale test method intended to evaluate the contribution to fire growth provided by a surface product applied in a room. It goes for itself that appropriate downscaling for small and intermediate scale test methods is necessary.

Besides the improper downscaling, some physical phenomena or the way measurements are taken may increase the overall uncertainty.

6.2.1 Velocity profile – The effect of heating and cooling

The technique for measuring mass flow rate $\dot{m}$ currently used in intermediate to large scale calorimeter tests consists of measuring the velocity on the axis of the duct v_{axis} and to multiply this with a correction factor k_t to obtain the mean velocity. This mean velocity is then multiplied with the mean density $\overline{\rho}$ and the surface area A to obtain the mass flow rate.

$$\dot{m}(t) = \overline{\rho} k_t v_{axis}(t) A$$

k_t is the velocity profile correction factor and is defined as

$$k_t(t) = \frac{\int_A v(t)dA}{v_{axis}(t)A}$$

Since the distribution of the velocity is not known, k_t is approximated and taken as a constant over time. If we knew the velocity distribution, the mass flow rate could be approximated by

$$\dot{m}(t) = \overline{\rho} \int_A v(t)dA$$

which is only correct when the density is uniform over the measuring section. Ideally we would want to measure

$$\dot{m}(t) = \int_A \rho(t)v(t)dA$$

So far, uncertainty studies have disregarded the error made assuming the density is constant. Only recently, a study has been made that tries to quantify the uncertainty related to the ever changing velocity and density profile over the duct section induced by the ever changing combustion gas temperatures and the thermal inertia of the system [19].

The same group of researchers has also discovered that the velocity profile correction factor varies with, what they call, the *'effective' Reynolds number*, which is based on the turbulent viscosity, rather than with the 'instantaneous' Reynolds number [16]. They define the effective Reynolds number as:

$$\mathrm{Re}_{eff} = \frac{\rho U_b D}{\mu_{eff}}$$

with ρ the density, D the inner duct diameter, U_b the bulk velocity and $\mu_{eff} = \mu + \mu_t$ the sum of the molecular and the turbulent viscosity.

6.2.2 The velocity measurement

The velocity measurement is made by means of a so called bi-directional pressure probe which is based on the pitot-static principle. The bi-directional probe [15] was originally designed for measuring the low velocity of (buoyancy-driven) fire induced flows associated with small to medium size fires. It has been 'copy-pasted' into various international standards and is considered to be the state of the art for measuring mass flows in combustion gases.

Although the probe is suited to work both in sooty environments and at elevated temperatures, its main disadvantage however is that it overestimates the measured velocity by approximately 1% per degree pitch or yaw angle initially [17]. This can be caused by improper alignment of the probe with the flow or by a radial velocity component in the exhaust flow.

The probe used in the SBI standard, which is a slightly modified design, is less angle sensitive but is, in contradiction with the standard bi-directional probe, Reynolds dependant. Due to the ever changing temperatures of the combustion gases and the varying velocity of said gases, the Reynolds number related to the probe outside diameter will vary, in most fire tests, in the range from 3.10^3 to 3.10^4 approximately. Further details can be found in [17].

So far, these effects have been disregarded resulting in a too low estimate of the uncertainty interval.

As a result of these findings, further research has been undertaken which has resulted in a new velocity pressure probe design that combines a low angular sensitivity and a Reynolds independency over a wide range [18].

6.3 *Transient error*

An additional source of error is introduced by the response times of the measuring devices. The gas analysis system – from sampling to analysis – has a time constant τ in the order of 10 seconds. This introduces a non negligible transient error which, in the case of oxygen, equals

$$\delta = \tau \frac{dXO_2}{dt}.$$

Inverse techniques may help to restore the 'real' variation of oxygen concentration over time. This however needs further investigation and, if used, a general agreed consensus on how to do it.

In a nutshell the procedure is as follows. The gas analysis system works as a (first order) low pass filter with transfer function H(s). Taking the inverse in the Laplace domain $H(s)^{-1}$, allows us to restore the original signal if not that the high frequency disturbances like noise were to disturb the process. Indeed, the inverse system $H(s)^{-1}$ works as an amplifier for the high frequencies.

So inverse techniques should only be used with great care and will require appropriate filters to remove the high frequency noise from the measured signal. This will require a complete redesign of the data acquisition as we know it now, i.e. one sample taken every three seconds.

7 Conclusions

The SBI test method has had a turbulent history of development and strong, both political and economical, interests have governed the debates. The standard has been published early 2002 and people are getting used to the particularities of the test method. Over the years, the test method has also gained confidence both in test institutes and in industry.

It is our believe that it is now time to have a major revision of the test method and its calibration procedures based on both new theoretical insights and on experience gained during the second SBI round robin exercise.

The revision should not lead to a new test method, though to a higher measurement accuracy and an increased confidence. It should also lead to a guidance document that allows laboratories to include reliable uncertainty estimates in their test reports.

A multiplier effect can/will be that, in a first stage, all heat release rate related fire test standards will be revised to obtain higher measurement accuracy and to include guidance on the estimation of uncertainty. In a second stage, all other fire test standards would be revised to include guidance on uncertainty estimation.

References

[1] SBI; European Standard - Reaction to fire tests for building products - Building products excluding floorings exposed to the thermal attack by a single burning item. EN 13823:2002. CEN Central Secretariat, Brussels 2002

[2] Classification Standard; European and International Standard – Fire classification of construction products and building elements – Part 1: Classification using test data from reaction to fire tests. EN 13501-1:2002; CEN Central Secretariat, Brussels (2002)

[3] Cone Calorimeter; International Standard – Reaction-to-fire tests – Heat release, smoke production and mass loss rate – Part 1 : Heat release rate (cone calorimeter method) ; ISO 5660-1:2002

[4] EGOLF/R4; Accreditation of Fire Test Laboratories – Interpretation of the European Standard EN ISO/IEC 17025:1999 when applied to Fire Test Laboratories; EGOLF / R4:2001

[5] ISO Room Corner; International Standard – Fire tests – Full-scale room test for surface products; ISO 9705:1993; International Organisation for Standardisation, Geneva, 1993

[6] Vertically Mounted Cable Test; European Standard – Common test methods for cables under fire conditions – Heat release and smoke production measurement on cables during flame spread test – Part 1: Apparatus; prEN 50399-1; CENELEC project 15315

[7] Railway Standard; European Standard - Railway applications - Fire protection on railway vehicles - Part 2: Requirements for fire behaviour of materials and components; prEN 45545-2:2004; CENELEC project 12281

[8] European and International Standard – General requirements for the competence of testing and calibration laboratories. EN ISO/IEC 17025:2000.; CEN Central Secretariat, Brussels (2000) and International Organisation for Standardisation, Geneva (1999)

[9] European Standard – General criteria for the operation of testing laboratories; EN 45001:1989; CEN Central Secretariat, Brussels 1989

[10] GUM, Guide to the expression of uncertainty in measurement; BIPM/IEC/IFCC/ISO/IUPAC/OIML; ISBN 92-67-10188-9

[11] International Standard – Quality assurance requirements for measuring equipment – Part 1: Metrological confirmation system for measuring equipment. ISO 10012-1:1992; International Organisation for Standardisation, Geneva (1992)

[12] International Standard – Accuracy (trueness and precision) of measurement methods and results – ISO 5725 Parts 1 to 6; International Organisation for Standardisation, Geneva, 1996-1998

[13] Enright P., and Fleischmann C.; Uncertainty of Heat Release Rate Calculation of the ISO 5660-1 Cone Calorimeter Standard Test Method; Fire Technology, Vol. 35, 1999, pp. 153-169

[14] Janssens M.; Variability in Oxygen Consumption Calorimetry Tests; Thermal Measurements: The Foundation of Fire Standards, ASTM STP 1427, ASTM International, West Conshohocken, PA, 2002

[15] McCaffrey B.J. and Heskestad, G.; A Robust Bidirectional Low-Velocity Probe for Flame and Fire Application; Combustion and Flame 26, 125-127 (1976)

[16] Merci B., Theuns E., Sette B., Vandevelde P.; Numerical Investigation of the Influence of Gas Heating and Cooling on the Velocity Profile Correction Factor in the SBI-Configuration; Fire and Materials; Under review

[17] Sette B.J.G.; Critical considerations on the use of a bi-directional probe in heat release measurements; Fire and Materials; Accepted December 2004

[18] Sette B.J.G.; Development of a Velocity Pressure Probe; Fire and Materials; under review

[19] Sette, B., Theuns E., Merci B., Temperature effects on the mass flow rate in the SBI and similar Heat Release Rate Test Equipment, Fire and Materials, Under review

[20] Axelsson J., Andersson P., Lönnermark A. and Van Hees P.; Uncertainty in Measuring Heat and Smoke Release Rates in the Room/Corner Test and the SBI; SP Report 2001:04; Swedish National Testing and Research Institute, Borås, Sweden, 2001

[21] Dahlberg M.; Error Analysis for Heat Release Rate Measurements with the SP Industry Calorimeter; SP Report 1994:29; Swedish National Testing and Research Institute, Borås, Sweden, 1994

[22] Enright T.; Heat Release and the Combustion Behaviour of Upholstered Furniture; Fire Engineering Research Report 99/17; ISSN 1173-5996; University of Canterbury, Christchurch, New Zealand, 1999

[23] Part A: Final Technical Report; Project for the European Commission: Enterprise Directorate-General; "SBI (Single Burning Item) Second Round Robin"; Call Identifier ENTR/2002/CP11; Applicant: EGOLF, 2005

[24] The Construction Products Directive; Council Directive 89/106/EEC of 21 December 1988 on the approximation of laws, regulations and administrative provisions of the Member States relating to construction products; European Commission, Enterprise, 1989

Modelling of fire spread in car parks

Leander Noordijk
TNO Centre for Fire Research, Delft, the Netherlands
E-mail: leander.noordijk@tno.nl, Phone: +31 15 276 3299

Tony Lemaire
TNO Centre for Fire Research, Delft, the Netherlands

Currently, design codes assume that in a car park fire at most 3-4 vehicles are on fire at the same time. Recent incidents in car parks have drawn international attention to such assumptions and have raised questions as to the fire spreading mechanism and the resulting fire load on the structure. E.g. a recent fire at Schiphol Airport showed a much faster fire spread and a larger number of vehicles on fire at the same time than was normally assumed. To understand and predict the fire spread in a car park a, for the time being deterministic, model is being developed based on the effects of the governing radiative heat transfer. With this model it will also be possible to quantify the effects of different relevant parameters.

Keywords: fire spread, car park, radiation

1 Introduction

In this research the focus is on fire spread in the case of a fire in a car park. The current, empirically founded, assumption is that during a fire in a car park at most 3-4 vehicles are on fire at the same time [3].. In a recent fire (10-2002) in a car park near Schiphol airport [1] however, around 30 cars were on fire at the same time. Also the fire spread was much faster than currently assumed. However, the fire occurred in a car park of a car rental company, which led to some specific circumstances that might have caused the more rapid fire spread than normally expected.

- All cars were parked on a small distance of each other, which can enhance fire spread from car to car.
- All cars were new and new cars contain more plastic parts than older cars. Plastics can be ignited more easily and produce more heat.
- All fuel tanks of the cars were completely filled, leading to a high fire load.
- The fuel tanks were made of plastic and started leaking fuel, creating pool fires which can also cause spreading of fire, by draining away under other cars.

Some of those specific conditions can however also apply in normal (public) car parks and the exact contributions of each of the effects are unknown. To quantify these effects, a deterministic model is being developed. The deterministic model is intended to be used together with a probabilistic approach, because a large number of input parameters is quite uncertain and occurs in a wide range. The choice of a probabilistic approach in combination with a deterministic model limits the possibilities for the deterministic model. CFD for example can give a detailed and accurate solution for a specific case with specific parameters, however it is too time consuming to be used in combination with a probabilistic approach. Furthermore the reliability of such a solution should not be overestimated, because large uncertainties are introduced by the uncertain parameters.

Figure 1 Picture after the fire in the car park near Schiphol airport (picture from [1])

The model focuses on fire spread by radiation, because this accounts approximately for the heat transfer of 30-40% of the heat released by the fire. Therefore, radiative heat transfer is expected to have the largest influence on fire spread. Furthermore radiative heat transfer does not require mass exchange or direct contact between the heat exchanging bodies and is described by well-known equations which can easily be solved. However, there is still the possibility to add the effects of the pool fires (due to the leakage of fuel from the fuel tanks) in the model, when the results based on radiative heat transfer turn out to be insufficient.

This study is to be seen as a first step to approach the trends which to a large degree undermine the current safety concepts: closer parking distances, large cars, more cars, application of more

combustible materials, more electrical appliances (increasing the probability of short-circuits and self-ignition) and so fort. The probability and the consequences of large(r) fires seem to increase; this underscores the necessity to initiate the development of more fundamental research into fire spread in car parks.

2 Description of model

2.1 *Introduction*

Mainly two different types of fire spread can be distinguished: fire spread inside a car and fire spread from car to car. Currently the major interest is in the fire spread from car to car. Fire spread from car to car can occur in various ways, for example directly by flames or by means of convective or radiative heat transfer. This is illustrated in figure 2.

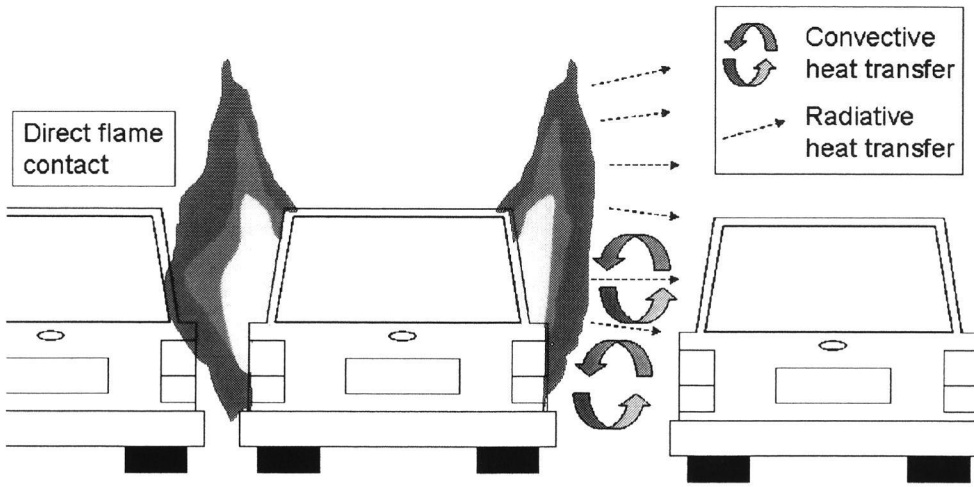

Figure 2 Different ways of fire spread; on the left direct fire spread by flame contact, on the right indirect fire spread by heating due to convection and radiation

When a car or other object is on fire, the flames emit a significant part of the total heat release by means of radiation. The radiation is transferred through the surrounding air towards other cars or objects. The parts of other cars absorb some of the incoming radiation, which causes heating of those parts. Because of the heating, the temperature will rise and when the ignition temperature is exceeded, those parts start burning too.

Three different processes can be distinguished: the emission of the radiation, the heat transfer through the air (transmission) and the absorption of the radiation. In the following sections those three processes are described in detail.

2.2 *The emission of radiation*

In the model, all objects are built of surfaces. Some of the surfaces are burning. A solid surface can burn, when inflammable gases evaporate out of the surface material (pyrolysis) and burn in flames after they have left the surface. The mass loss rate of gases evaporating out of the surface depends on the heat transfer towards the surface. When the gases burn, heat is released. A significant part of the total heat release is emitted by radiation.

The mass loss rate $\dot{m}''$ of a surface, caused by pyrolysed gases, is defined as [4]:

$$\dot{m}'' = \frac{\dot{q}''_e + \dot{q}''_{fr} + \dot{q}''_{fc} - \dot{q}''_{rr}}{\Delta H_g} \tag{1}$$

where $\dot{q}''_e$ is the external heat flux, $\dot{q}''_{fr}$ the radiative heat flux of the flame towards the surface, $\dot{q}''_{fc}$ the convective heat flux of the flame towards the surface, $\dot{q}''_{rr}$ the outgoing radiation of the surface and ΔH_g the heat of gasification. The values of the heat flux from the flame towards the surface have been estimated using literature values for the maximum heat flux (unlimited oxygen available) from the flame towards the surface. Note that ignited surfaces without any external incidental radiation flux can still burn because of the heat flux of the flame towards the surface. The calculated mass loss rate can be used to calculate the heat release rate, by multiplying the mass loss rate with the heat of combustion and a parameter to take into account the incomplete combustion. About 30-40% of this heat release rate is emitted as radiation. The rest is used to heat up the burning products and the entrained air.
The part of the total heat release rate which can be regarded as radiation is emitted by the flames. This is described by the equation:

$$\dot{Q} = \varepsilon A \sigma T^4 \tag{2}$$

where $\dot{Q}$ is the emitted amount of energy, ε the emission coefficient of the flame, A the area of the flame, σ the Stefan-Boltzmann constant and T the absolute temperature of the flame. The flame will have a different size (and shape) than the burning surface.

In the model the mass loss rate of a surface is calculated, as stated before, as a function of the radiative heat flux on the surface. In the model the temperature of the flame and the emission coefficient are simply fixed. For a given radiative heat flux, the area of the flame can be calculated using equation (2).

2.3 *Heat transfer by radiation*

The radiative heat transfer between two surfaces of a certain temperature depends on the thermal and geometrical properties of the surfaces. The important thermal properties are the temperatures,

emission and absorption coefficients. The geometrical properties are the shape, the orientation and the position of the two surfaces.
The radiative heat transfer between two surfaces can be described by analytical expressions. The expressions are quite simple for rectangular surfaces orientated perpendicular or parallel to each other. Furthermore in a car park the surfaces of most objects are orientated that way and most shapes can be approximated using rectangles. So in this model, it is assumed that all objects are built of rectangular surfaces orientated perpendicular or parallel to each other, which makes the calculations much more efficient.

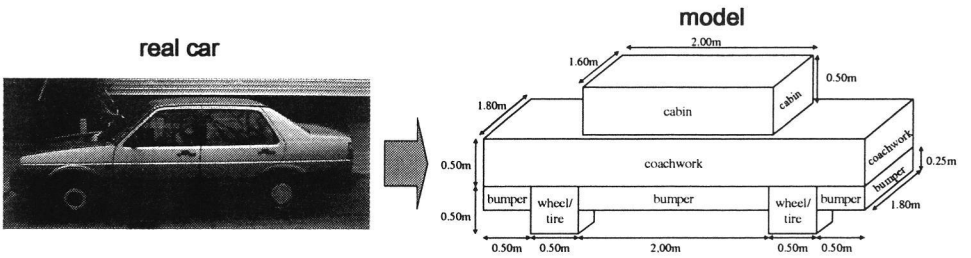

Figure 3 Example of a car built of rectangular surfaces orientated perpendicular or parallel to each other

The model is chosen such that the main parts that contribute to the fire development can be treated separately and, if desired, in relative great detail.

This means the cars in the car park are built of rectangular surfaces orientated perpendicular or parallel to each other. The surfaces have different properties, depending on the material used. In figure 3 is shown how a car can be built of this kind of surfaces. The exact size and location of the parts in a car can be chosen which results in a different type of car. The car can also be 'refined' by building it of more, smaller rectangles resulting in a more detailed model. The cars can now be placed in the car park, but again all surfaces have to be orientated perpendicular or parallel to each other, which results in four possible orientations for a car with respect to another car.

The radiation flux on a surface is the result of a number of visible (hot) surfaces close to it. Those surfaces have a constant temperature. Let's now consider the radiative heat transfer between two surfaces. The discussed procedure can easily be extended if there are more hot surfaces (which are not located 'behind' each other) by taking the sum of all fluxes as the total radiation flux on a surface, which is also done in the model.
The radiation flux on a surface is calculated in a few points (infinitesimal small surfaces) on the surface in so-called sensor points and depends on the thermal properties of both surfaces and the position and orientation of the surfaces. The position and orientation of the surfaces can be

combined in one coefficient: the view factor or configuration factor, which resembles the part of the total solid angle covered by the other surface. This leads to the following equation for the incoming radiative flux in a sensor point A_{d1} (on a surface A_1) caused by a (hot) surface A_2:

$$Q''_{2\to d1} = a\varepsilon\sigma A_2 T_2^4 F_{d1\to 2} \tag{3}$$

where $Q''_{2\to d1}$ is the radiation flux per unit area at the location of the sensor point (d1) on surface A_1 caused by surface A_2, a the absorption coefficient of surface A_1, ε the emission coefficient of the emitting surface A_2, σ the Stefan-Boltzmann constant ($5.67\text{x}10^{-8}$ $Wm^{-2}K^{-4}$), A_2 the area of surface A_2, T_2 the temperature of surface A_2 in Kelvin and $F_{d1\to 2}$ the view factor from the infinitesimal small surface A_{d1} to surface A_2. Note that the fixed values for the flame temperature and emission coefficient, introduced after equation (2) , do not necessarily change the results. Because equation (3) can be seen as the absorption coefficient times the amount of radiation from a flame reaching the receiving surface, which is actually the product of the radiation heat release by the flame (equation (2)) and a geometrical factor. The geometrical view factor takes into account the part of the radiation from the flame reaching the receiving surface and within certain limits this factor would not change much for different flame heights.

As mentioned before the view factor depends on the geometrical properties of the two surfaces relative to each other. In Appendix A some simple view factors are described for the interested reader.

2.4 *Absorption of radiation, heating and ignition*

The incoming radiation flux $Q''_{2\to d1}$ resembles the amount of energy entering a infinitesimal small area on surface A_1. There is also energy leaving the surface by radiation and convection. The energy flux leaving the surface by radiation $Q''_{rad,loss}$ can simply be found to be:

$$Q''_{rad,loss} = \varepsilon\sigma T_1^4 \tag{4}$$

where ε is again the emission coefficient of the emitting surface, σ the Stefan-Boltzmann constant and T_1 the temperature of the emitting surface in Kelvin. The energy flux leaving the surface due to convection $Q''_{conv,loss}$ is:

$$Q''_{conv,loss} = \alpha(T_1 - T_0) \tag{5}$$

where α is the convective heat transfer coefficient, T_1 the temperature of the surface and T_0 the ambient temperature.

The difference between the energy entering and the energy leaving the surface causes heating or cooling of the surface. The temperature at the next time step can be calculated with a simple energy

balance. When the calculated temperature exceeds the ignition temperature the surface will start burning the next time step.

In figure 4 the time to ignition is shown for different plastics as a function of the radiative heat flux on the surface (data from [5]). In the figure the large spreading can be seen between the different materials.

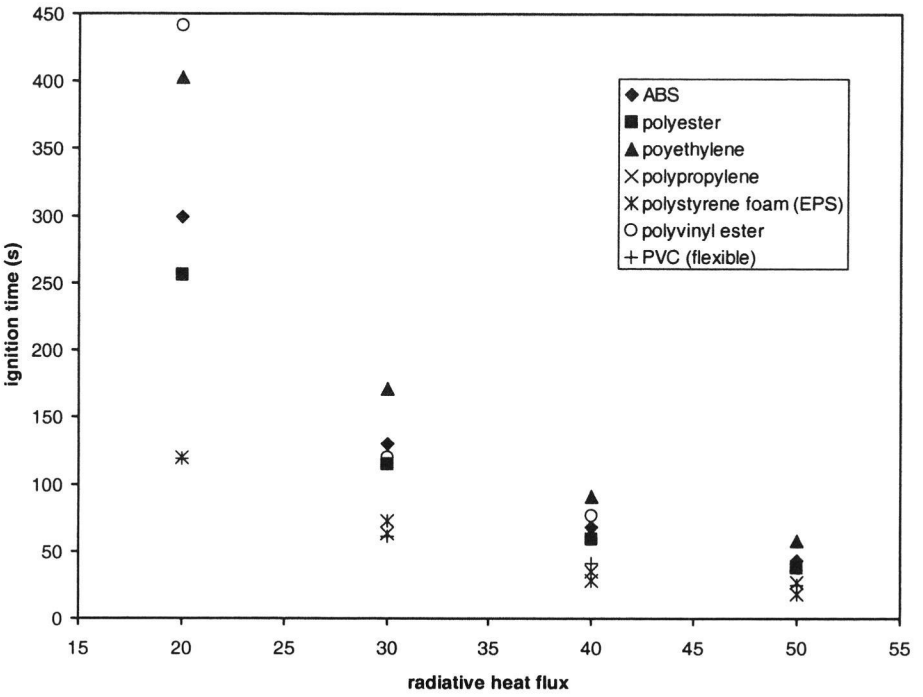

Figure 4 The time to ignition as a function of the radiative heat flux on the surface for different plastics.

3 Results

The development of this model is in an early stage and the model is not validated yet. Nevertheless the first results show realistic ways of fire spread and realistic temperature predictions. A few qualitative pictures are presented here to show how the results of the model can look like.

Note that in the current model each part of a car is built of surfaces, but the surfaces have to be the faces of a block. So a complete bumper is made of three faces on a block. The blocks are used to model fire spread within a car, for example from one side of the bumper to another side of the bumper. Currently the fire spread within a block is not really modelled, because a whole block will

be in fire when one of the surfaces starts burning. This will significantly increase the fire spread, but this will be changed in a later version.

A fire starts with a burning car in a car park, which can ignite other cars. In figure 5 an example of a car park with 6 cars is showed after some time. The dark surfaces in the figure are on fire and the second car from the left was initially on fire. In the figure, it can be seen that at the current time the compartment of the car in the front is on fire too. In the figure the *surfaces* are showed. Note that the burning surfaces have a different height than in the initial (non-burning) situation. This represents the flame height, which depends on the mass loss rate, which on its turn depends on the incoming radiation flux.

In figure 6 the same car park with 6 cars is showed, only from a different point of view. In this figure all blocks (resembling car parts) are showed. The dark blocks now represent car parts that are on fire. In this figure it is much easier to see which parts are burning. Now can be seen that even the bumper of the car parked behind the initially burning car is on fire.

Normally the showed figures are in colour, where the colour is a measure for the temperature and state (not yet burning, burning, finished burning) of the block or surface.

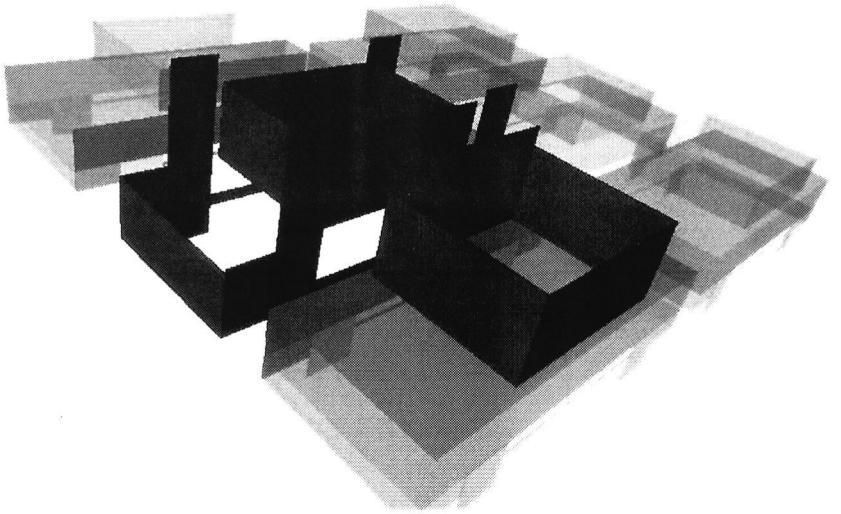

Figure 5 The surfaces on fire after a certain time. The dark surfaces are on fire, note that the height of a burning surface represents the flame height and is based on the heat release rate.

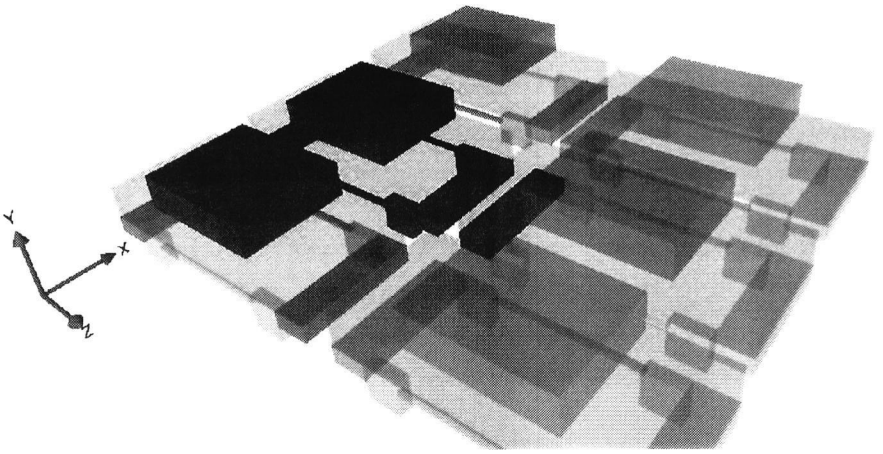

Figure 6 Parts on fire in the car park after a certain time. The dark parts are on fire, the lighter parts are non-burning. This only indicates whether or not a part is burning.

4 Perspectives for further research

This model is in the development phase. However it has promising features in the sense of quantifying the effects of different parameters like the distance between cars, the influence of material properties (e.g. different types of plastics). and car dimensions. Furthermore a number of additions or modifications can easily be made, because of the modular and flexible structure.

A number of modifications are planned:

- Fire spread within a surface
  - A more realistic representation of fire spread within a surface is needed
  - Currently a complete surface starts burning when at one of the sensor points the ignition temperature is reached, which can lead to a too fast fire spread
  - Using a simple quadratic growth model the fire spread on one surface of a car part can be described in more detail
  - Data of the research project on fire spread in cars by MVFRI and NHTSA [2] can be very useful here to obtain a more realistic description of the fire spread on a surface
- Fire spread within a car
  - A more realistic representation of fire spread within a car is needed
  - Currently a complete car part starts burning when one of the faces start burning, which leads to a too fast fire spread

- It is more realistic to let a (non-ignited) face of a car part start burning after some time, maybe when the initially ignited face is completely on fire (as described before)
- Again data of the research project on fire spread in cars by MVFRI and NHTSA [2] can be very useful here to obtain a more realistic description of the fire spread in a car

- Shadow effect
  - The shadow effect, the effect that a surface behind another surface is not (completely) visible, should be taken into account. Not taking it into account can lead in extreme cases to a too fast fire spread
  - There are algorithms available to take this effect into account
- Smoke layer
  - A hot smoke layer above the parked cars can enhance fire spread by radiation towards the cars from above
  - Currently no smoke layer is taken into account, which leads to a slower calculated fire spread
  - A smoke layer can grow and parts of cars can become surrendered by hot smoke, which can lead to heating of not yet ignited parts. On the other side a smoke layer, which surrenders car parts, can shield those car parts from radiation.
  - A smoke layer can possibly be introduced by solving simple mass and energy balances, as done in the current zone models

It is expected that more and larger fires will occur in the near future. With a view to better understand the phenomena involved and hence the possible (combination) of countermeasures, the model will be further developed. Any interest is highly welcomed, please feel free to contact the authors for questions, suggestions etc.

5 Appendix A: View factors: the base of the model

This part describes the calculation of view factors and is intended for the interested reader. This part is not essential for the understanding of the model.

5.1 Introduction

View factors are used in the calculation of the radiative heat transfer between the different surfaces. In this model only the view factors from infinitesimal small surfaces to finite surfaces are evaluated. Furthermore those surfaces are only orientated perpendicular or parallel to each other. The view factors are really the base of the model, because the main heat transfer mechanism is assumed to be radiation and the factors determine the amount of radiation energy leaving or entering a surface.

Actually only two different view factors for the most standard configurations are important, all other view factors can be calculated by adding or subtracting those standard view factors. In this appendix first the expressions for the two standard view factors are evaluated and finally in an example is shown how the standard view factors can be used in more complex configurations.

5.2 *Standard view factors*

The left part of figure 7 shows the configuration for the calculation of the standard view factor in the case of perpendicular orientation. The accompanying expression for the view factor $F_{d1\to 2}$ is:

$$F_{d1-2} = \frac{1}{2\pi}\left[\tan^{-1}\left(\frac{1}{C}\right) - \frac{C}{Y}\tan^{-1}\left(\frac{1}{Y}\right)\right] \tag{6}$$

with $A = \frac{a}{b}$, $C = \frac{c}{b}$ and $Y = \sqrt{A^2 + C^2}$ where a, b and c are defined as in the figure. The right part of Figure 7 shows the configuration for the calculation of the standard view factor in the case of parallel orientation. The expression for the view factor $F_{d1\to 2}$ is now:

$$F_{d1-2} = \frac{1}{2\pi}\left\{\frac{A}{\sqrt{(1+A^2)}}\tan^{-1}\left[\frac{B}{\sqrt{(1+A^2)}}\right] + \frac{B}{\sqrt{(1+B^2)}}\tan^{-1}\left[\frac{A}{\sqrt{(1+B^2)}}\right]\right\} \tag{7}$$

with $A = \frac{a}{c}$, $B = \frac{b}{c}$ and a, b and c again defined as in the figure. Note that this expression is symmetric in A and B as can be expected from the symmetry in the configuration.

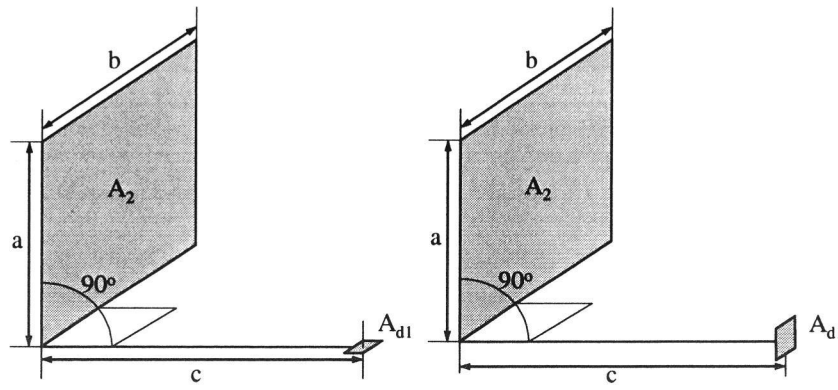

Figure 7 The configurations for the standard view factors in the case of a perpendicular and a parallel orientation of the surfaces

5.3 *View factors in non-standard configurations*

The two standard view factors introduced before can be used to calculate the view factor in all configurations built simply and solely of perpendicular and parallel orientated rectangles. This is

done by decomposing configurations to combinations of the standard configurations. It is important to note that view factors are additive: if a surface 2 can be decomposed into two parts 2a and 2b, which together make the total surface 2, the total view factor $F_{d1\to 2}$ can be written as $F_{d1\to 2} = F_{d1\to 2a} + F_{d1\to 2b}$.

To illustrate the use of this property the view factor in the situation shown in figure 8 is calculated. The non-standard view factor $F_{d1\to 2}$ of the infinitesimal small surface A_{d1} to the surface A_2 is calculated. This is done by defining a surface A_3 as shown in the figure and a combined surface $A_{2,3}$ defined as the surfaces A_2 and A_3 together. The view factors $F_{d1\to 3}$ and $F_{d1\to 2,3}$ can be calculated using the standard view factor for perpendicular orientated surfaces given in Figure 7 . Furthermore can be found that $F_{d1\to 2,3} = F_{d1\to 2} + F_{d1\to 3}$, which leads to the expression for the view factor $F_{d1\to 2} = F_{d1\to 2,3} - F_{d1\to 3}$.

In this way all possible perpendicular and parallel orientations can be evaluated and it works out that all those configurations can be solved using the two standard view factors and the additive property of the view factor.

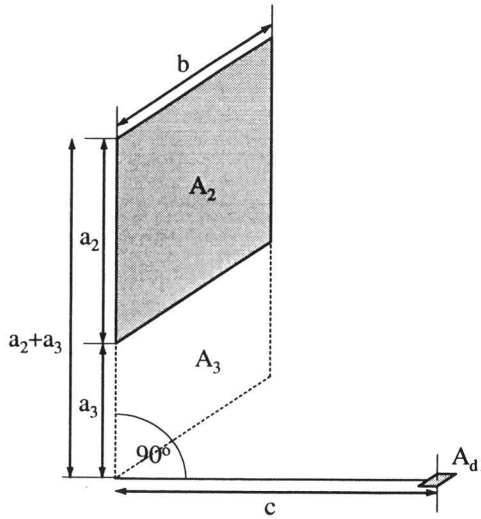

Figure 8 A relatively simple non-standard configuration, where the view factor to the surface A_2 can be found using the view factors to the combined surface $A_{2,3}$ and the surface A_3.

References

[1] Brandweer Haarlemmermeer (2004) 'Onderzoeksrapportage parkeergarage brand te Schiphol, gemeente Haarlemmermeer' on http://www.brandweerkennisnet.nl/cms/show/id=536221/contentid=40842.

[2] DOT/GM Research project: Evaluation of Motor Vehicle Fire Initiation and Propagation by U.S. Department of Transportation and General Motors (GM). More information: Motor Vehicle Fire

Research Institute (http://www.mvfri.org) and National Highway Traffic Safety Administration (http://www.nhtsa.gov).

[3] Joyeux, D., J. Kruppa, L.G. Cajot, J.B. Schleich, P. van de Leur and L. Twilt (2002) *Demonstration of real fire tests in car parks and high buildings*, European Commission

[4] Drysdale, D. (1985) *An introduction to Fire Dynamics*, New York: John Wiley and Sons

[5] Babrauskas, V. (2003) *The ignition handbook*, Issaquah, USA: Fire Science Publishers.

Scientific background to the harmonization of structural Eurocodes

Joël Kruppa
CTICM, Paris, France
Email: jkruppa@cticm.com, Phone: +33 1 30 85 20 86

Daniel Joyeux
CTICM, Paris, France

Bin Zhao
CTICM, Paris, France

Structural Eurocodes are a set of 58 different parts dealing with all the aspects of the design of buildings and civil works. Among them are some parts devoted to the structural fire design. This paper gives some background information from various research projects which were carried out during the last decade to improve or fill some gaps in the knowledge to be able to understand the entire structural behaviour of a building when submitted to a real fire. Focus is made on the so called "natural fire safety concept" and on projects dealing with composite (steel + concrete) structures, as well as steel members.

Structural Eurocodes, fire design, natural fire, fire safety engineering, heat transfer, mechanical behaviour, modelling

1 Introduction

The Eurocodes are a series of European standards which provide a common series of methods for calculating the mechanical strength of elements playing a structural role in construction works (hereinafter 'structural construction products'). Those methods make it possible to design construction works, to check the stability of construction works or parts thereof and to give the necessary dimensions of structural construction products [1].
The Eurocodes provide common design methods, expressed in a set of European standards, which are intended to be used as reference documents for Member States to [2]:

- prove the compliance of building and civil engineering works or parts thereof with Essential Requirement n°1 *Mechanical resistance and stability* (including aspects of Essential Requirement n°4 *Safety in use*, which relate to mechanical resistance and stability) and a part of Essential

Requirement n°2 *Safety in case of fire*, including durability, as defined in Annex 1 of the Construction Product Directive

- express in technical terms these Essential Requirements applicable to the works and parts thereof
- determine the performance of structural components and kits with regard to mechanical resistance and stability and resistance to fire, insofar as it is part of the information accompanying CE marking (e.g. declared values).

In the end of 2004, the 58 different parts which formed the Eurocode set are all nearly reaching the stage of EN (European Norm) and will be implemented, as wished by the European Commission and the Members States, within some years throughout the European Union, the Economic European Area and, also, in a lot of other countries. Among these parts, 7 dealt with "structural fire design".

As far as these "fire parts" of Eurocodes are concerned, to reach this stage, a huge amount of work, involving many European research institutes and experts, was needed. Generally based on existing recommendations developed, for instance, by European Commission for Constructional Steelworks (ECCS), Fédération Européenne du Béton (FEB), Fédération International de la Précontrainte (FIP)... the European Commission have set a group of 13 experts [3] in 1988 to write the first drafts of Eurocode fire parts.

In mid-1990 a series of parts dealing with actions on structures exposed to fire and with fire resistance design of structures made in concrete, steel, composite and timber were officially presented in a seminar on 25 to 27 June 1990 in Luxemburg to the potential users.

At this time, the European Commission took the decision to forward the further development of these Structural Eurocodes to the Comité Européen de Normalisation (CEN) and in 1993-1995, new versions of these fire parts were issued, under the reference ENV 1991-2.2 to ENV 1999-1.2 [4, 5]. These "pre-standards" were used in some European countries and decision was taken, at the end of the 90's to convert them to "full European standards", leading now to the series of EN1992-1.2 to EN 1999-1.2.

To illustrate the progress made in each version, table 1 presents the content of the annexes of the various versions of Eurocode 1 on actions in case of fire, from 1990 to 2002.

The current final version of the Eurocode fire parts are given a wide range of tools for designing entire structures or parts thereof for any kind of fire scenario. These tools can be very simple when based on tabulated data, user friendly when based on analytical formulae or very efficient when based on advanced calculation method such as the finite element method at elevated temperatures.

Table 1: Comparison of the content of annexes of Eurocode 1- 1.2

Item	"Chapter 20" – 1990	"ENV 1991-2.2" - 1995	"EN 1991-1.2" – 2002
Fire load density	5 pages in annexes 0 and 3	5 pages – annex D	7 pages – annex E
Fire modelling	4 pages in annexes 1 and 2	None	2 pages – annex D
Parametric fires	None	3 pages – annexes A and B	3 pages – annex A
Equivalent time of fire exposure	1 page – annex 5	2 pages – annex E	2 pages – annex F
Thermal actions for external members	6 pages – annex 6	8 pages – annex C	9 pages – annex B
Localised fires	none	none	3 pages – annex C

Hereafter, some examples are given of research projects carried out, showing the output they have provided. They dealt with:

a. Natural fire safety concept to provide in-depth background information for assessment of the behaviour of either large structural volume or car park structures when submitted to real fire development
b. Fire design of steel structures either made with stainless steel or lightweight structural elements
c. Fire design of composite structures either for beams or slabs.

2 Natural Fire Modelling

When dealing with realistic fire scenarios, the fire safety design is based on physically determined thermal actions. In contrast with conventional fire design, parameters like the amount of fire load, the rate of heat release and the ventilation factor play an important role in the fire design. The specification of appropriate and realistic design fire scenarios is a crucial aspect of fire safety design. The assumptions made with regard to these factors have a major influence on the thermal conditions within a compartment and have a significant impact on the fire design.
The design fire scenarios used for the analysis/development of a building fire have to be deduced from all the possible fire scenarios. In most buildings, the number of possible fire scenarios is infinite and need to be reduced. Only "credible worst case fire scenarios" will be studied. If the

design fire scenarios are chosen, a number of fire models are available to calculate the thermal actions.

Different characteristics relevant for the assessment of design fires are listed by a working group led by Leen Twilt et al [27]. Regarding the methods for assessing the fire severity, different levels of fire calculation methods are relevant to the various stages of fire development. When a fire is initiated, it is localised within a compartment and, according to the characteristics of the compartment and of the fire load, it can remain localised or becomes generalised to the whole compartment.

In many cases of small compartments or small opening regarding the compartment size, the fire develops into to a fuly developed fire.

Mainly three levels of modelling are available for each situation, as shown in table 2.

Table 2 – Different levels of fire models

Levels of the model	Localised fire	Generalised fire
Simplified	Hasemi model Heskestad model	Parametrical fires
Zone models	2-zone model	1-zone model
Filed model	CFD	CFD

The simplified models are generally empirical models. The zone-models take into account all the main parameters controlling the fire, but introduce simplified assumptions that limit the domain of application.

The field models are rather complex for being used as a general design tool and should be limited to specific cases. Field models are the only tools valid for a complex geometry. The last European Community of Steel and Coal research projects were focussing on the improvement or the development of empirical and numerical tools [15, 17, 22].

When the conditions of flashover or generalised fire are not reached, a fire remains localised. In this condition, a two-zone model is used to estimate the general effect of the smoke layer. The local effect near the fire is also studied by empirical models developed in a previous research' natural fire in large compartments' [13]. Hasemi [18, 19, 20, 21] performed experimental investigations to determine the localised thermal actions from a fire, from which a simplified method was developed. The combination of both models allows for the determination of the temperature field near and far away from the fire. The main results of the models are the thermal actions to the structure.

2.1 *Hasemi model*

In a research project devoted to large compartments [17], a calculation method was developed to estimate the temperature field and the temperature of structural elements in case of a localised fire. This method combines:

- Hasemi's model for localised fire [18], and
- Two-zone model

These two models have been implemented within the software Ozone within a European research project [15].

The validation of this calculation model has been made for both large compartments [17] and car parks [22, 23]. Because Hasemi's model was originally developed for small scale test results with rates of heat release less than 1 MW, additional validations were performed for larger fires, from 2 MW to 60 MW. For example the figure 1 shows a comparison between calculated and measured temperatures of an IPE 600 beam above a car fire, showing a relatively good agreement.

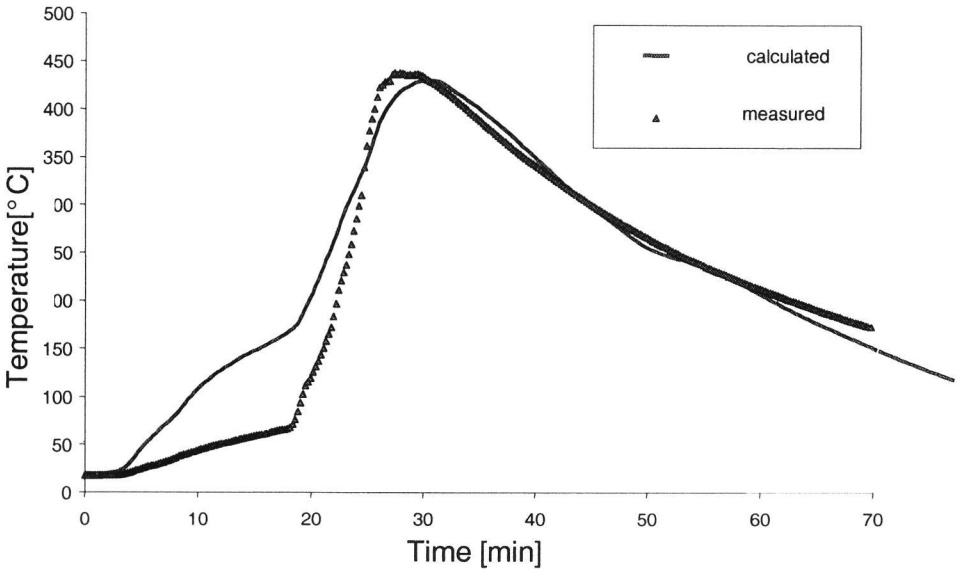

Figure 1 : Comparison between calculated and measured temperatures of a steel beam above a localised car fire

2.2 *Heskestad model*

When the flames are not impacting the ceiling, an empirical method has been developed to determine the thermo-dynamic data of an open fire [6]. These empirical equations are the basis of the equations (C1) to (C3) of the revised final draft of Eurocode 1 part 1.2 (EN 1991-1.2 : 2002). The first correlation obtained from axially symmetric open fire dealt with the flame height, which is

representative of the height along the axis of the flame where the average temperature is 520°C. The second empirical non dimensional correlation is given for the temperature along the axis of the plume.

The application is not considered for low flame height to diameter ratio, where a single plume does not exist. A limit of 0.5 for this ratio may be used.

Historically, these empirical equations have been developed from small scale test results. Firstly, the determination of centreline temperature equation was determined to model the plume, i.e. above the height of the flame. Further, several research works on small scale tests (less than 1000 kW) [6, 7, 8 ,9 ,10] have been carried out to verify the previous equation but also to extend their results to the flaming region. These researches have led to very similar equations with similar values of the coefficients validated on the flaming regions. In addition, these experiments have shown that the mean temperature along the axis of a turbulent open fire is never higher than 900°C.

Then, European research projects have validated the equations for large fires. Large scale test results have been used [14]. In figure 2 comparisons are made between measured and calculated temperatures along the axis for a 20 MW fire performed in 1998 in a large industrial hall [14, 22], and in one of the largest experimental test with temperature measurements with a 60MW fire performed in 1994 in an 28m high exhibition hall [11, 13].

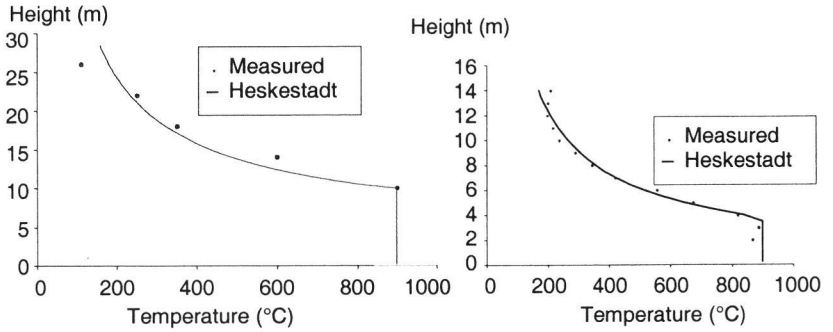

Figure 2 : comparisons between centreline calculated and measured temperatures for a 60MW fire (left) and a 20MW fire (right)

2.3 *Parametrical fires*

The parametric fires are relevant to the determination of temperature within a compartment in case of generalized fire. However, even if it is a strong improvement compared to the standard "ISO-fire", these parametric fires, as shown in the following figures, are not yet able to provide a very accurate answer of the fire severity, consequently it is recommended to use them only for pre-

design calculation. These parametrical fires presented in the ENV1991-2-2 have been improved to include the multi-layer wall effect since they took into account only single layer wall, limiting the application domain; the improved version has been implemented in the EN1991-1-2 [28].

The second main improvement made for parametrical fires is the introduction of the fuel control condition, by using minimum fire duration, generally assumed as 20 minutes. This fuel control condition leads to a minimum value of O, the ventilation factor, calculated from the 20 minutes fire duration. This allows withdrawing the case of high speed fire leading to unsafe temperature.

The following figure shows the improvement for a fuel control fire, of a hotel fire test [40].

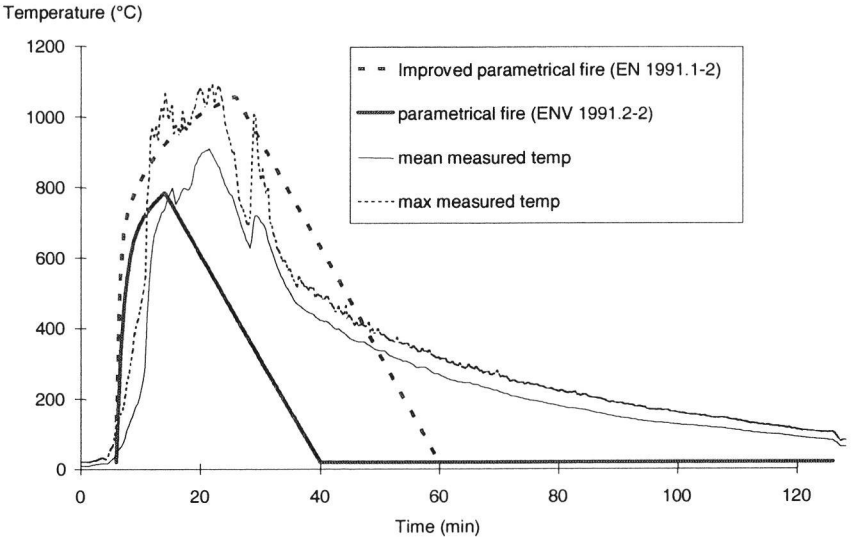

Figure 3: Effect of the improvement of the parametrical fires: comparison with experimental results of a hotel fire test

2.4 *Zone models*

Two types of zone models exist:

- 1-zone model assuming a generalized fire
- 2 zone model assuming 2 layers: a hot upper zone and a cold lower zone.

A large number of zone-models exists in the world, the background of these models or the code source are often not available [24, 25]. A zone model, OZONE, has been developed within an ECSC research project [15]; it allows jumping from a two-zone model leading to a one-zone model when hot gas layer reaches some specific conditions (of temperature and/or height). This zone model was then validated by comparison with another existing one-zone model (NAT [16]) and with more than 100 experimental tests.

Large scale fire tests have been performed and are used for validation. The figure 4 shows, as example, the temperature-time curve comparison between tests and zone model.

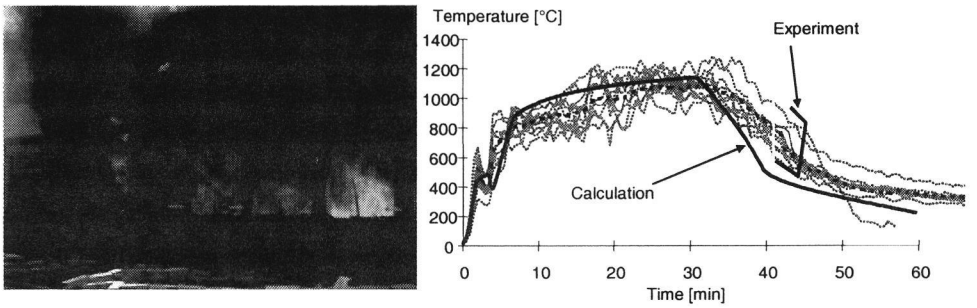

Figure 4 : Comparison between calculated and measured temperatures of generalized fire in a school room

2.5 *Characteristics of the fire compartment*

2.5.1 Boundary elements of the compartment

One of the assumptions generally made is that the fire in one compartment will not spread to other compartments. Whether this is true, depends on the fire behaviour of the boundary constructions (floors, walls [including doors], etc.). Consequently, it is necessary to understand this behaviour in order to assess their capability to act as fire barriers.

To carry out such assessment, the following options could be used:

- Calculations

  Concerning some rather simple situations, it is possible to perform heat transfer and mechanical behaviour calculations for the relevant time-temperature curve to be developed within the compartment. Such an approach need to be, preliminary, correlated with some existing test results on the same kind of separating element; however these test results mainly refer to standard fire conditions, which not allows to a wide spread of knowledge as far as the influence of the severity of fire on the behaviour of separating elements is concerned. It is why this approach needs to be linked with "expert judgments".

- Ad-hoc tests

  The separating element can be exposed, in a furnace, to a temperature-time curve resulting from a calculation with a fire model taken into account the parameters related to a worst-case fire scenario. However the number of fire tests needed may be very large.

- Expert judgement

This approach makes use of the available test-data of ISO-resistance tests on separating elements. In combination with calculation procedures, the behaviour under natural fire conditions can be assessed by identifying the influence of the main parameters which could lead to more onerous situations.

- Direct use of ISO-requirements

National rules define fire compartments with ISO ratings for fire resistance of walls, ceilings, doors and floors, depending on the use and the geometry of the building. Since this kinds of requirements mean implicitly that a fire will not grow beyond the fire compartment, it could be assumed that any separating element fulfilling these ISO requirements will be able to maintain the fire within the compartment for any other fire scenarios.

2.5.2 Thermal characteristics

The heat loss by convection, radiation and conduction from the compartment is an important factor for the temperature determination. Through the separating element, according to the thermal inertia of the wall (insulated or not), this heat loss is within the range of 30 % to 90% of the total amount of heat released within the compartment by the combustion of fire load, and consequently the thermal properties of the walls have to be known.

The three main parameters characterising the thermal properties of a material are:

- heat capacity c_p
- density ρ
- conductivity λ

The conductivity and the heat capacity depend on temperature. It is suggested to neglect the effect of water content since this will generally be on the safe side.

The table 3 gives the thermal characteristics of some materials, other than those already covered by Eurocodes, usually used in building.

Table 2: Typical values of the thermal properties of relevant materials for the compartment envelop.

Material	Temperature (°C)	λ (W/m/K)	ρ (kg/m³)	c_p (J/kg°K)
Ceramic Wool	20	0,035	128	800
	200	0,06	128	900
	500	0,12	128	1050
	1000	0,27	128	1100
Cement	20	0,0483	200	751
	250	0,0681	200	954
	500	0,1128	200	1052
	800	0,2016	200	1059
Calcium Silicate	20	0,0685	450	748
	250	0,0786	450	956
	450	0,0951	450	1060
Bricks	20	1,04	2000	1113
	200	1,04	2000	1125
	500	1,18	2000	1135
	1000	1,41	2000	1164

3 Fire behaviour of steel structures

For more than three decades, there was an enormous financial effort by the steel industry to investigate the "weakness" of constructional steel structures subjected to fire and a number of design rules have been developed in this field which were incorporated within Structural Eurocodes. With respect to this situation, the recent research works have been orientated towards other types of steel structures such as stainless steel structures as well as steel and concrete composite structures. In addition, as far as local instability, for instance, the local buckling of thin wall element, is concerned, very few works were performed before 90's.

Consequently two research projects have been carried out on stainless steel [29, 30], in which the fire behaviour of stainless steel members were investigated. It was known for many years that stainless steel has a much better fire performance than carbon steel, nevertheless, no systematic study was made to clarify the fire behaviour of stainless steel members used in buildings. To provide a technical basis for fire design of stainless steel members both material mechanical properties of different stainless steel grades and the related structural behaviour are investigated not only through various experimental works but also from numerical simulations.

A huge number of tests have been carried out in order to investigate mechanical properties of stainless steel at elevated temperatures (figure 5). Based on the experimental results obtained for different steel grades, an analytical investigation was made which has led to the establishment of a mathematical model for describing stress-strain relationships of stainless steel at elevated temperatures.

The relevant parameters necessary to cover a temperature range from 20 °C to 1000 °C have been given for five stainless steel grades studied in these research projects. The stainless steel material model was then used to simulate the fire behaviour of various kinds of structural elements; in general their comparison with test results gives good agreement [31] (figure 6). The material model for stainless steel at elevated temperatures obtained in these projects has been incorporated in the informative annex C of the fire part of Eurocode 3 for steel structures [32].

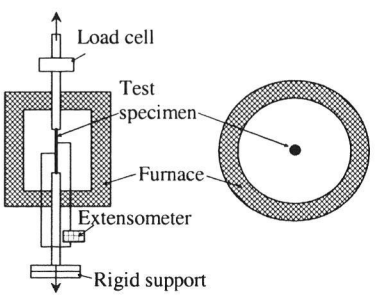

Device for tensile tests

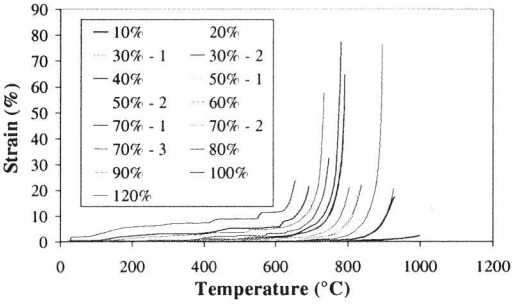

Anisothermal test results of stainless steel

Figure 5: Anisothermal test of stainless steel at elevated temperatures

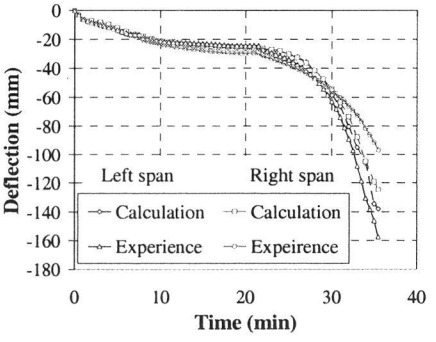

Continuous stainless steel beam

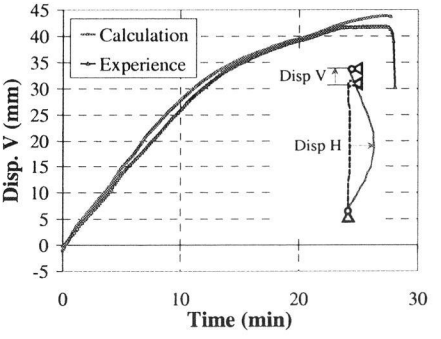

Stainless steel column

Figure 6: Comparison between fire tests of stainless structural members and numerical modelling

In parallel to above research projects on stainless steel, important works have been carried out for investigating the fire behaviour of cold formed lightweight steel structures [33, 34, 35] because of their increasing use not only as non-load bearing structural members, such as in fire partition walls, but also as load bearing structural members such as in housing or rack structures. The main objective of these works was to get deep information about the performance of this type of steel structure subjected to fire condition. The main feature of such structure elements is their important sensitivity to local buckling due to the very thin wall sections, and in the ENV version of Eurocode 3, no calculation rule, except a fixed critical temperature of 350 °C, is provided.

The research project dealt with the following items

- mechanical properties of cold worked lightweight steels at elevated temperature,
- assessment of the fire behaviour of fully engulfed lightweight steel studs,
- assessment of the fire behaviour of steel studs maintained by boards with fire on one side of the partition,
- development of design rules to be implemented into the European standards.

The advanced numerical modelling developed in this research project, taking account of corresponding material model, is fully valid for predicting the fire behaviour of cold worked lightweight steel (figure 7). For the time being, the results of this work has been partially included in informative annex E of the fire part of Eurocode 3 [32].

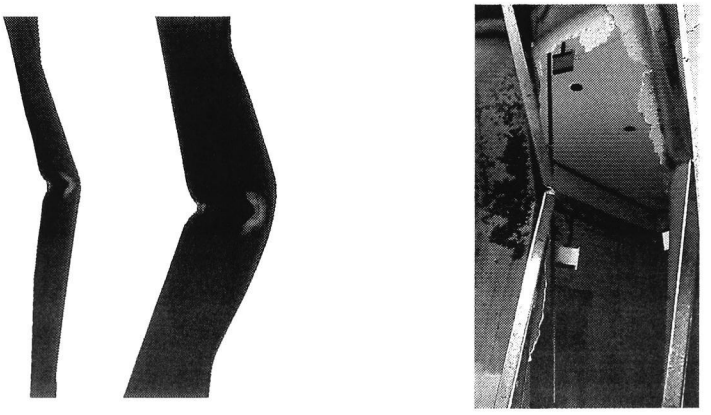

Deformed shape simulated for steel stud

Deformed shape of studs in fire test

Figure 7: Comparison between fire tests of cold worked lightweight steel structural members and numerical modelling with developed material model

4 Fire behaviour of composite structures

The steel and concrete composite structures have shown important advantages regarding the fire performance. The first version of the fire part of Eurocode 4 appeared in the middle 80's and should be at that time the first code in the world in which a full design procedure is provided. Although different design rules have been available in this version, some of them remained still either incomplete or not fully accurate. For that reason, an important research project has been conducted from 1988 in which the first design rules of Eurocode 4 with respect to steel and concrete composite slabs and beams were fully investigated by means of both experimental and analytical studies [36]. This project sponsored by ECSC, accompanied by other independent works [37, 38], has led to improve design rules for composite slabs and beams.

Regarding steel and concrete composite slabs, the design rules derived from above research works allow to give much more accurate results compared to old design rules of the ENV version of the fire part of Eurocode 4. For the insulation criterion, figure 8a a comparison is made between the outcomes of the new simple calculation method and of an advanced calculation model. A similar comparison, based on the rules given in the previous version of the fire part of the Eurocode 4, is presented in figure 8b.

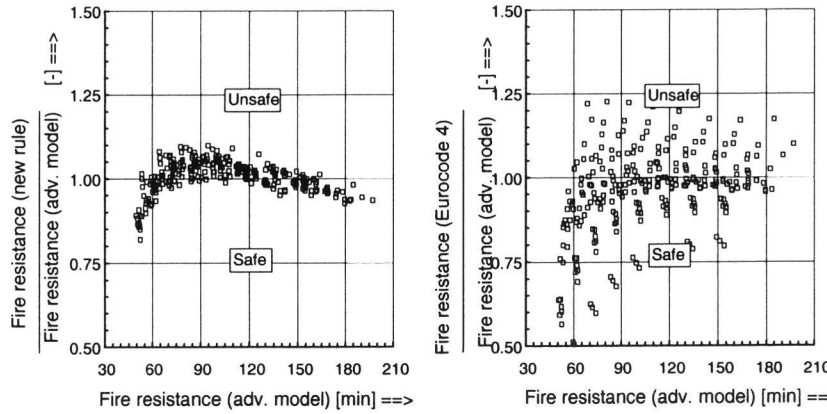

(a) assessment according to new rule

(b) assessment according to old rule

Figure 8: Comparison of simple calculation methods for the insulation criterion of composite slabs to the outcomes of an advanced calculation model [37]

Another example concerns the temperature assessment of reinforcing steel in composite slabs; in figure 9, one can find that the new rule gives better estimation than the old rules of Eurocode 4. All

these rules and, in addition, the rules related to mechanical resistance model have been incorporated in the latest version of the fire part of Eurocode 4.

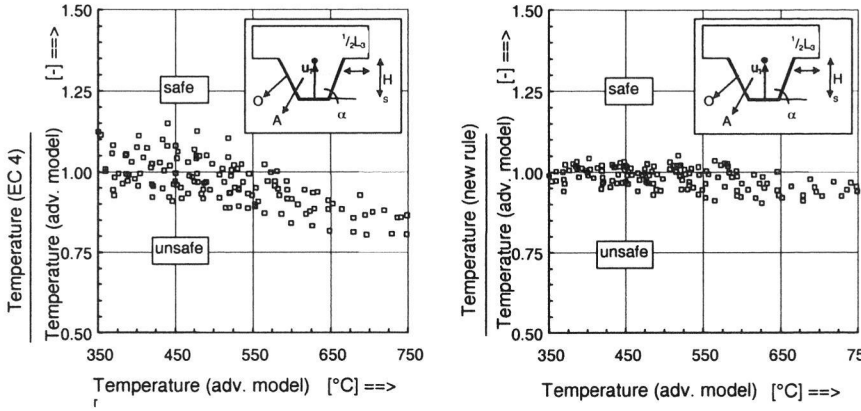

(a) assessment according to old rule

(b) assessment according to new rule

Figure 9: Comparison of the simple calculation methods for temperature of reinforcing steels of composite slabs to the outcomes of an advanced calculation model [37]

Another steel and concrete composite member dealt with in above research project concerns composite beams. In the old version of fire part of Eurocode 4, the design rules permitted only to predict the fire resistance of simply supported and full shear connected composite beams. However, in reality, more and more composite beams are made with partial shear connection. In addition, the use of continuous composite beams could provide much better fire resistance than simply supported beams. As a consequence, the research work performed was based on both fire tests and numerical modelling, providing a solid technical background for the establishment of design rules regarding shear connection resistance (figure 10), and regarding the mechanical resistance of composite beams with hogging moment (figure 11). The derived corresponding design rules have been included in current section 4 of the main part and informative annex E of Eurocode 4 [39].

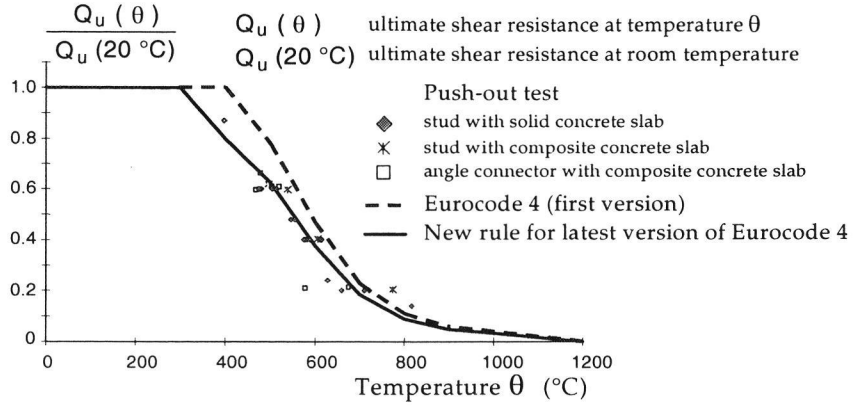

Figure 10: Shear of resistance of connectors at elevated temperatures

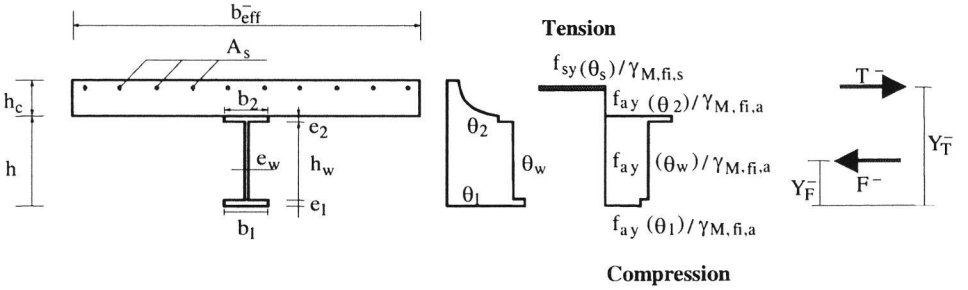

Figure 11: Design rules for calculation of hogging moment resistance

5 Conclusions

Over 15 years or so, a team of European experts were able to develop new calculation rules for the behaviour of steel and composite structures in any fire situations.

These calculation rules were mainly based of a huge amount of research projects carried out with the sponsoring the ECSC.

Within the last version of the fire part of Eurocode 1 "actions in case of fire", it becomes obvious that an accurate assessment of the fire safety level of a building needs to consider realistic fire scenarios and that the use of the previous ISO-fire needs to be limited to the ranking of construction products.

The design rules in the last version fire parts of Eurocode 3 and 4 become more accurate and cover more types of structural members in fire situation due to the numerous research projects carried out during last twenty years as presented above. Nevertheless, some work is still necessary to enlarge

the application field of Eurocodes for a full available fire safety engineering assessment of steel and composite structures.

Acknowledgement

The authors wish to thank all the fire experts who have worked with enthusiasm and abnegation to allow reaching the current stage of fire parts of Eurocodes and the European Commission for having (and continuing to) sponsored a large amount of research projects.

References

[1] European Commission (11 December 2003) 'the implementation and use of Eurocodes for construction works and structural construction products' in *Commission Recommendation*, 887/EC.

[2] European Commission (2003) 'Guidance Paper L (concerning the Construction Products Directive)' in *Application and use of Eurocode*, 89/106/EEC

[3] Dotreppe, J. C. ; C. Hahn, B. A. Haseltine, M. Kersken-Bradley, L. Krampf, J. Kruppa, M. Law, J. Mathez, E. Pedersen, P. Schaumann, J. B. Schleich, G. Storti, L. Twilt (April 1990) 'Actions on structures exposed to fire' in *Commission of European Communities*, Eurocodes Chapter 20.

[4] Kruppa, J. (5 December 1994) 'Presentation of Eurocode parts on structural fire design' in *Symposium on fire standards in the international marketplace*, Phoenix, Arizona.

[5] Kruppa, J. (24 – 26 September 1996) 'Performance-based code in fire resistance : first attempt by Eurocodes' in *International conference on performance-based codes and fire safety design method*, Ottawa, Canada.

[6] Audouin, L. and J.M Most (1995) 'Average centreline temperatures of a buoyancy pool fire by image processing of video recordings' in *Fire Safety Journal*, Vol 24 n°2.

[7] Heskestad, G. (September, 1988) 'Fire plumes' in Society of fire protection engineers (Eds) in *The handbook of Fire Protection engineering*.

[8] Mac Caffrey, B.J. (1979) 'Purely buoyant diffusion flames' in *NBSIR*, 79-1910.

[9] Hasemi, H. and M. Nishita (1988) 'Fuel shape effect on the deterministic properties of turbulent flames' in *Fire safety science* .

[10] Annarumma, M. (1989) 'Modélisation numérique et validation expérimentale des flammes de diffusion turbulentes dominées par les effets de gravité', in *Thèse de doctorat*.

[11] Leborgne, H. Research Report n°94R-242, *CTICM France*.

[12] Leborgne, H. Research Report n°98R-406, *CTICM France*.

[13] Joyeux, D. (1995) 'Simulation of the test of Parc des expositions de Versailles', *CTICM France*, INC-95/34-DJ/IM.

[14]Joyeux, D. (September 2001) 'Validation of the Equations C1 to C3 of the annex C of Eurocode 1 part 1.2', *CTICM France*, INC – 01/303b – DJ/NB.

[15]Schleich, J_B.; L-G. and A-L. Cajot (1994-98) 'Competitive steel buildings through natural fire safety concept' in *Draft Final Report July 2000*, Part 1 to 5, ECSC Research 7210-SA/125,126,213,214,323,423, 522,623,839,937, B-D-E-F-I-L-NL-UK & ECCS.

[16]Curtat, M. ; P. Fromy (mars 1992) 'Prévision par le calcul des sollicitations thermiques dans un local en feu. Première partie: le modèle et le logiciel NAT' in *Cahiers 2565* du CSTB.

[17]ARBED- LABEIN- TNO- CTICM – Université de Liège- (February 1997) 'Development of design rules for steel structures subjected to natural fires in Large Compartments' in *Final report CEC Agreement* 7210/ SA210, 317,517,618,832.

[18]Hasemi, Y. and T. Tokunaga (1984) 'Flame Geometry Effects on the Buoyant Plumes from Turbulent Diffusion Flames' in *Fire Science and Technology*, Vol.4, n°1.

[19]Ptchelintsev, A.; Y. Hasemi and M. Nikolaenko (1995) 'Numerical Analysis of Structures exposed to localized Fire' in *ASIAFLAM's 95*, Hong Kong.

[20]Wakamatsu, T.; Y. Hasemi, Y. Yokobayashi, A. Ptchelintsev 'Experimental Study on the Heating Mechanism of a Steel Beam under Ceiling exposed to a localized Fire'.

[21]Hasemi, Y.; Y. Yokobayashi , T. Wakamatsu, A. Ptchelintsev (1995) 'Fire Safety of Building Components Exposed to a Localized Fire' in *ASIAFLAM's 95*, Hong Kong, Scope and Experiments on Ceiling/Beam System Exposed to a Localized Fire.

[22]Joyeux, D. (March 2002) 'demonstration tests in large compartment and car parks' in *ECSC European research project*, INC-02/410c-DJ/IM pp. 25 – CTICM - France.

[23]Joyeux, D. (March 2002) 'Méthode simplifiée d'échauffement d'un élément soumis à un feu localisé' INC-00/62-DJ/IM – CTICM - France.

[24]DIFT - (22 July 1992) *ARGOS Theory Manuel* (draft 5), Danish Institute of Fire Technology.

[25]Peacock, Jones, Bukowski and Forney (June 1991) 'Technical Reference Guide for the Hazard I Fire Hazard Assessment Method' in *NIST Handbook 146*, Volume II, Version 1.

[26]Quintiere, J.G. (21st -23rd August 1995) 'Predicting fire growth'-'First European Symposium on Fire Safety Science' Abstracts, Institute for Structural Engineering, CH - 8093 Zurich.

[27]Twilt, L.; L.G. Cajot, D. Joyeux, P. Van de Leur, J. Kruppa, J.B. Schleich (March 1996) 'Input data for natural fire design of building structures' in *Proceedings IABSE conference Delft*.

[28]CEN (2002) 'Actions on Structures - Part 1.2 : Actions in case of fire' in *EN 1991-1.2, Eurocode 1*.

[29]CTICM/UGINE (March 2000) 'Development of the Use of Stainless Steel in Construction, WP 5.1: Material Behaviour at Elevated Temperatures' in *Final report*, ECSC project 7210-SA/327.

[30]CTICM/UGINE/VTT (December 2004) 'Structural design of cold worked austenitic stainless steel, WP6: Elevated temperatures' in *Final report*, ECSC project n° 7210-PR/ 318.

[31]Zhao, B. and F. Conrad (May 2004) 'Stress-strain relationships of stainless steel at elevated temperatures' in *Proceedings of stainless steel experts seminar*, London.

[32]CEN (2004) 'Design of steel structures – Part 1-2: General rules – Structural fire design' in *EN1993-1-2 Eurocode 3*, Brussels.

[33]Outinen, J. (1995) 'Transient state tensile results of structural steels S235, S355 and S350GD+Z at elevated temperatures', Helsinki University of Technology.

[34]Ranby, A. (February 1999) 'Structural fire design of thin wall steel sections' in *PhD thesis*, Lulea University of Technology, Sweden.

[35]CTICM/ARBED/CORUS/LABEIN/SBI/VTT (March 2004) 'Calculation rules of lightweight steel sections in fire situation' in *Final report*, ECSC project n° 7210-PR/ 254.

[36]CTICM/TNO (July 1995) 'Fire Resistance of Composite Slabs with Profiled Steel Sheeting and of Composite Steel Concrete Beams'.

[37]Both, C. (1998) 'The Fire Resistance of Composites Steel-Concrete Slabs' in *Dissertation TU*, Delft.

[38]Zhao, B. (July 1994) 'Modélisation numérique des poutres et portiques mixtes acier-béton avec glissements et grands déplacements - Résistance à l'incendie' in *PhD Thesis*, INSA de Rennes.

[39]CEN (2004) 'Design of composite structures – Part 1-2: General rules – Structural fire design' in *EN1994-1-2 Eurocode 4*, Brussels.

[40]Joyeux, D. (July 1998) 'Etude expérimentale de feux caractérisant un hôtel' INC-98/24-JK/IM, CTICM – France.

Building evacuation, rules and reality

Peter van de Leur
DGMR Raadgevende Ingenieurs BV, Den Haag, the Netherlands
Email: le@gmr.nl, Phone +31 70 350 3999

The paper discusses some of the problems surrounding the simulation of the evacuation time in buildings. Building regulations offer little guidance to the designer in dealing with these problems, but good and safe solutions can easily be described qualitatively.

Key words: Evacuation, phased evacuation, tenability, waiting time

1 Introduction

The safe evacuation of the building occupants is the pre-eminent objective of fire safety measures required by building regulations. There is a substantial body of knowledge on the different stages of the evacuation process, on effective evacuation strategies, and on how the building design influences the possibilities of the occupants of a building to safely evacuate; see SFPE[4] for an overview of the state of the art. Applying that knowledge in the design of buildings has the potential to lead to optimised designs in terms of the level of safety, architectural freedom and costs. Traditional building rules targeting safe evacuation are however in most cases based on a much simplified model of the evacuation process, which does not allow the use of the currently available knowledge.

A general fire engineering design methodology does allow for any sound available knowledge to be introduced in the design. Whereas performance based building codes embrace the fire engineering methodology, the level of acceptance of such generalised methodologies, especially with authorities responsible for building permits, is still limited. Often, anything beyond the simplified approach is met with reluctance. This may be attributed on the one hand to the authorities being unfamiliar with the methodologies. It should however be recognized that the use of poorly validated methods and tools by engineers has done little to increase confidence.

There are what could be called isolated successes where advanced calculation tools have gained a level of acceptance. Examples of these are the highly graphical computer models for calculating evacuation times based on following individual escape paths. The application of these tools is not without problems, especially where their results are to be coupled to the requirements of the building code.

This paper identifies and discusses a number of these issues, related to evacuation under fire conditions. The issues have come to attention in actual design processes occasionally but have, under the pressure of the "standard simplified approach" not been solved to any degree of satisfaction. Where the discussion involves building regulations, references are to the Dutch Building Decree and associated rules, see Bouwbesluit [1]. While many of the problems discussed will be present in other countries as well, the corresponding situation outside the Netherlands is beyond the scope of this paper.

2 Evacuation issues

2.1 Full or partial evacuation

One of the essential concepts of fire safety in buildings is the rapid and adequate evacuation of all the occupants of the building in case of fire. Many of the fire safety measures introduced in the design and operation of the building are aimed at ensuring that the occupants can safely leave the building before they are overtaken by heat and toxic products, and before the building collapses. The Dutch building regulations –as many other national building codes- assume that an unchecked fire will grow to involve the whole building, necessitating its complete evacuation. The fire department will normally be able to limit the extent of the fire to within one fire compartment; the probability of failure in this objective is however too high to count on successful repression and to let occupants of other fire compartments stay in the building.

Only in exceptional cases where it is sufficiently probable that the building can survive a fire, where fire compartmentation is rigorous, and where a full evacuation would take too much time, do some building codes accept a "defend in place" strategy. High rise buildings are an example where building codes (not the Dutch one!) allow to design according to this alternative strategy. Other examples are easily found where a full evacuation is unnecessary, such as large, spread-out building complexes with very limited connections between compartments. Actually, even medium rise apartment buildings are in practice almost never evacuated completely, since due to the high level of compartmentation a fire is easily contained to within one or two dwellings.

In cases such as described above a full evacuation can be shown to be unnecessary if not counterproductive: people may be put at risk when escorting them to safety through hazardous areas, where they would be better off staying in place while the fire is suppressed; the consequences of fire could easily grow much larger if the emergency teams have to spend part of their resources to rescue efforts instead of fighting the fire. In those cases it should be allowed to base the design, including the egress capacity, on the partial evacuation that is shown to be safe and practicable.

2.2 *The application of advanced computer models*

The escape time t_{escape} in a fire situation has three main components, according to Marchant [3]:

$$t_{escape} = t_{perc} + t_{aware} + t_{travel}$$

where t_{perc} is the time between ignition of the fire to perception of the emergency, t_{aware} the time between perception and awareness of the need to escape, end t_{travel} the travel time to a place of safety. Much of the knowledge and design tools that have been developed on evacuation over the last decades have focused on the mathematical modelling of the escape process, i.e. t_{travel}. This has lead to the emergence of more or less sophisticated software packages, that are increasingly being applied in building design. The computer models do allow better prediction of the travel time than the traditional simplified "hydraulic" approaches, but not of the other components of the evacuation time. More often than not, the other components are at least as large as the travel time, and vary substantially over the building.

The "advanced" programs also contain at best a crude model for the decision-making process of individual occupants. Getting reasonable travel times therefore requires significant input and "steering" by the operator of the computer program. The reverse side of this is a severe limitation of the predictive capability of the program. Two examples of the need for manipulating the simulations are given in the figures below.

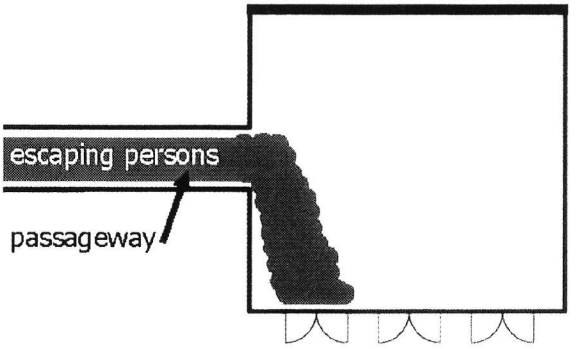

Figure 1: An example of the need for manipulation in advanced evacuation simulations. The distance map allocates all persons coming from the passageway on the left of the drawing to the first of three double exit doors. The other two doors are left unused. This had to be solved by arbitrarily allocating a third of the persons who were going through the passageway to each of the three exits.

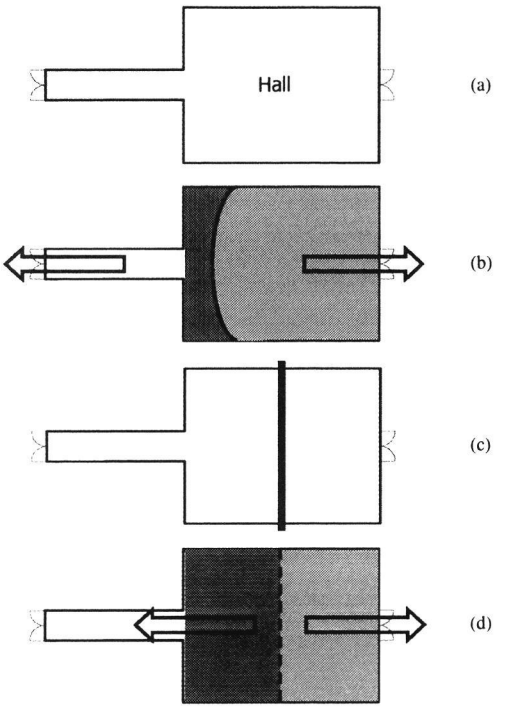

Figure 2: An example of the need for manipulation in advanced evacuation simulations. The figure shows artificial plan views An assembly hall with two exits, one at the end of a corridor (a)Each person is allocated to the exit closest to him on the basis of a calculated "distance map" . In the example, virtually everybody in the hall is allocated to the exits on the right (b). By adding a "virtual wall" halfway in the drawing (c) an even distribution over both exits is obtained (d).

These issues, as well as the fact that two major components of the escape time are not included in the computer simulations, could be dealt with in a crude fashion by introducing a safety factor on the RSET (the Required Safe Egress Time, i.e. the result of the calculation of evacuation time), before balancing it with ASET (Available Safe Egress Time). See Fahy [2] for a detailed discussion of the use of safety factors to compensate for uncertainty and bias in evacuation model results.

When evaluating the results of an advanced model, there is a tendency to compare the calculated evacuation time for a space or a building with the maximum time requirement set by the regulations. That maximum time requirement is in its origin directly associated with a simple hydraulic type travel time calculation. It should not come as a surprise that the more advanced

model comes up with larger evacuation times, as it takes into account at least some of the complicating factors that the simple hydraulic calculation ignores completely.

The evacuation times calculated by the more advanced model being in general larger than the hydraulic results has proven to be a strong impediment to the application of the advanced model: Instead of profiting from the added effort in applying better knowledge, the user is penalised by being allowed less persons inside the building.

It could be argued that the more accurate prediction by the more advanced model requires a smaller safety factor on results than the hydraulic model.
In order to enable such a procedure in the Dutch regulatory context, it would be necessary to separate the implicit safety factors in the regulations from the requirements. In a simplified representation, the Dutch requirements come down to the following time requirements:

Table 1: Egress time requirements according to the Dutch regulations

Evacuation of :	Maximum time	
Room, smoke compartment[1]	1 minute	To be calculated taking into account the total available door width, assuming a flow capacity of 1.5 person per second per meter[2] of door width
Complete building	15 minutes	To be calculated taking into account the total available door, corridor and stair widths, assuming a flow capacity of 1.5 person per second per meter of door or corridor width, and 0.75 person per second per meter of stair width

The 1 minute requirement for a smoke compartment could be thought of as consisting of a time requirement of say, 3 minutes, combined with a safety factor of three to be applied to the actual evacuation time calculated with the simple rule as stated in table 1. A more advanced model that

---

[1] *A fire compartment is subdivided in smoke compartments such that the maximum walking distance to the nearest exit is limited to (30..40 m, depending on occupancy). Smoke compartments are separated by smoke resisting structures.*

[2] *In evacuation calculations within the scope of Dutch regulations, widths of doors, corridors, stairs are always actual or structural widths; as opposed to effective widths where a boundary layer is subtracted from the actual widths. In international literature flow capacities are mostly correlated with the effective width.*

takes into account complicating factors such as the internal layout of the spaces and differences in mobility characteristics of the occupants could be rewarded with a reduction of the safety factor from, again say, 3.0 to 2.0[3]. In that case, an evacuation time of 1.5 minutes calculated by the advanced model would still be acceptable. In general, the better a model can be demonstrated to predict actual evacuation times, the smaller the safety factor that should be applied to its results.

2.3 *Simultaneous or phased evacuation*

The standard concept of full evacuation is often accompanied by the notion that all occupants of the building start evacuating at exactly the same time. For the design of egress provisions, this has important consequences. This is due to the notion that any smoke compartment must be emptied within one minute (after alarm). Circulation spaces used by multiple smoke compartments as the primary area that exits lead to must then be sized to hold the occupants of all the associated smoke compartments who are allocated to that circulation space, before they continue their evacuation to a place of safety. In reality, there is a need for the fastest possible evacuation only in the smoke compartment where the fire originates, as smoke can fill the compartment in a very short time. The occupants of other smoke compartments are not subjected to a direct threat (fire, smoke, collapse) until much later, since the smoke compartment boundaries constitutes a firm barrier against the entrance of smoke and heat. A situation can therefore be considered safe where the circulation space is sized to allow the smoke compartment of origin to empty into it within the first minute. The other smoke compartments have to wait until space becomes available as the circulation space empties into exits, stairs etc. Reasonable values of the delay of the alarm may be 1 – 2 minutes, and 2 – 5 minutes for the time after which the other compartments are empty.

The above issue is especially consequential for assembly buildings such as cinemas and theatres that can hold large numbers of people. If they are to be designed for simultaneous evacuation, the central lobbies need much more surface area than if they are designed for phased evacuation. Quite traditional designs cannot comply with the requirements if simultaneous evacuation is to be taken into account. A phased evacuation can safely take place in the cases mentioned since the compartments have a high level of fire separation from each other and from the escape routes, reducing hazards arising from delaying the evacuation.

It is clear that in practice there is a strong bias towards an earlier start of the evacuation in the compartment where a fire starts, as these occupants normally become aware of the need to evacuate before the occupants of other smoke compartments. The problems associated with a simultaneous

---

[3] *The safety factors in this section represent merely examples. Actual proposals should be founded on rigorous study.*

evacuation will in practice only occur with a general alarm triggered by an automatic detection system.

An unanswered but highly interesting question is which forms of phased evacuation can safely be introduced in a design, and which conditions should be satisfied. Factors that should influence the decision to allow phased evacuation in the design are:

1. How probable it is that occupants of the other compartments can remain unaware of the evacuation of the compartment of origin; an evacuation alarm system should support the phasing by delaying the evacuation alarm in the compartments that "compete for circulation space" with the compartment of origin by an amount of, say, 1 or 2 minutes. Only adequate and audible spoken-word evacuation alarm systems can deliver this kind of support. The fire or an evacuation in progress in the compartment of origin should also not be visible from within adjacent compartments through transparent separating structures;
2. The openness of the compartment of origin; if a fire breaks out in a compartment where people are working in separate rooms with closed doors, it is unlikely that the occupants will start to evacuate at the same time as they will become aware of the fire at different times. An automatic fire alarm system can compensate for this. In an open-plan office, an automatic fire alarm is not needed to make all occupants aware of the emergency at about the same time.
3. The use of the building should favour phased evacuation. A continuous and intensive circulation between the compartments makes a successful phased evacuation less likely; dwellings and other occupancies where people may be asleep or otherwise unable to respond quickly to an alarm condition should never be designed for simultaneous evacuation since it is highly unlikely that all occupants need the same evacuation space at exactly the same time.

Phased evacuation can take different forms. Examples are:

1. Phasing between compartments on the same storey, where a building has multiple smoke compartments on a storey. The main evacuation route from all smoke compartments passes through a common circulation zone where the escape staircases are located. A special form of this type is where the compartment of origin and the compartments directly adjacent to it are evacuated, while the rest is evacuated later;
2. Phasing between storeys. This is the simplest and least controversial form of phasing. The whole fire storey empties into the staircases before the non-fire storeys are alarmed. With fire resistant staircases and floors, both on the aspect of the threat to the non-fire compartments and of the risk of simultaneous evacuation taking place after all, this option scores high.

Dutch regulations allow phased evacuation as a basis for design in a general statement only; concrete requirements and "determination methods" are based on simultaneous evacuation. The

above section provides arguments that may be used to defend a building permit request based on phased evacuation. An example of the effect of phased evacuation is shown in fig. 3 below

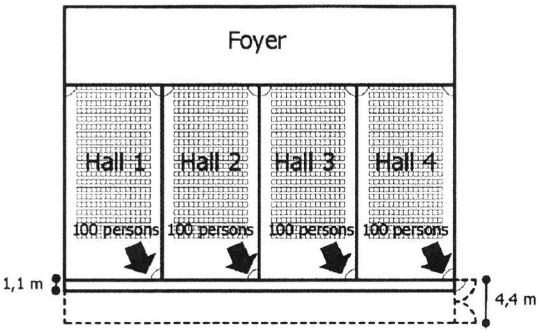

Figure 3: Example: a cinema with four halls of 10 x 20 m, 300 seats each, accessed through a central lobby. 100 persons in each hall allocated to an emergency exit giving access to a common passage with a single exit. A design was approved where the passage area and exit door width were sized for 100 persons (25 m²/1.1 m, phased evacuation). If simultaneous evacuation would have been obligatory, the passage would have to be sized for 400 persons (100 m²/4.4 m)

2.4 *Waiting time*

A hot topic in evacuation time calculation is the question whether a design may be such that people are forced to wait, e.g. in front of an escape staircase, for a prolonged period of time before they can enter the staircase and continue their evacuation. The official Dutch building regulations do not forbid such a situation to occur, as long as the occupants can leave the building within the required 15 minutes.

An informal design guide from the Dutch Ministry of the Interior states that "a group of people in motion shall not be slowed down extremely". This is mostly interpreted as saying that people should always feel that they are moving if they are to avoid panic reactions. In this view, forcing people to wait for more than half a minute before they can enter a staircase is not acceptable. The background of these concerns appears to be the incidents in mass gatherings where large numbers of people have been hurt or killed (Hillsborough football stadium, the yearly Hadj gatherings in Mecca). Obeying this rule leads to escape routes, including staircases, that have a more or less equal flow capacity over their total length. Whereas that may be in fact quite desirable from a safety point of view, it is at odds with many traditional designs for high occupancy buildings such as schools.

While the concerns raised must be considered real enough in the extreme occupancies mentioned as examples, they seem rather exaggerated in buildings with much smaller occupancy numbers.

Factors that should be taken into account when deciding whether people can be forced to wait on their escape route are:

1. The number of people that need to make use of the route in question;
2. The level of threat that the waiting people perceive from the incident. If they see flames approaching, or if they are engulfed by hot smoke, or even if they have a hot smoke layer above them, they may feel directly threatened; clearly, a physical smoke-resistant or fire resistant barrier between the fire and the waiting area can be extremely effective in reducing the perceived level of threat. To what extent a heat and smoke venting system does a similar job when it maintains a smoke layer above the waiting area is doubtful. The height of the interface and the smoke temperature will certainly be of influence;
3. The waiting time; the acceptable waiting time depends on the level of threat. This could be expressed in terms of the dose of radiative or convective heat, or toxic gases, that may be accumulated;
4. The freedom they have or perceive in taking alternative routes; if people can move, and feel that they can possibly reach another route, even under the same level of threat they will be less given to panic than if they have no options other than wait in line;
5. Visual contact with the place of safety. If people know that the place of safety is close by, they may accept the direct threat more easily than if they have no idea how far beyond their view they have to move before they are out of reach of the threat.

2.5 *Scenario-dependent or scenario-independent treatment*

The requirements in table 1 are –implicitly- scenario independent. This means that no assumption is made as to the location of a fire or as to its development in time. Since the requirements are in terms of the total free door width, it is assumed that all escape routes are available.
These assumptions are consistent with a scenario where the occupants of a smoke compartment of origin become aware of a fire sufficiently fast to allow them to leave the compartment before the path to the closest compartment exit becomes untenable.

In more detailed approaches, specific scenarios are analysed in which the fire is assumed to block escape routes, forcing occupants to choose a different route. By analysing all relevant positions and developments, it is possible to check the design for weaknesses causing excessive evacuation times.

It is important to note that when dealing with specific scenarios, the standard scenario-independent acceptance criteria (the 1 / 15 minutes, ref. to table 1) should not be applied. The scenario-independent evacuation time is the shortest possible one, all actual scenarios represent less optimistic situations. In a design where the scenario independent building evacuation time just

remains below 15 minutes, it should be accepted that actual scenarios lead to evacuation times above 15 minutes.

A good design from the perspective of evacuation will not show excessive evacuation times for any realistic fire scenario. While the regulatory requirements allow quite bad designs in this respect, the designer should try to avoid these.

3 Recommendations

The present paper aims at promoting a more advanced, and less regulations-limited view of the evacuation process when designing buildings for safe egress. It identifies and discusses a number of factors which are in themselves well known, but which are virtually always ignored in building design in favour of the traditional model calculations dictated by the Dutch building regulations. Taking into account these factors enables much better designs, both from the point of view of safety and of economics. It also addresses main advantages and drawbacks of advanced models and implicitly provides areas for further discussion and research. Examples are the improvement of the predictive capabilities evacuation models by including psychological elements such as way finding, familiarity with the building and adaptive routing.

References

[1] Bouwbesluit (2003), official text of the Building Decree 2003 as published in staatsblad 2001, 410, after modifications published in Staatsblad 2002, 203; Staatsblad 2002, 516 and Staatsblad 2002, 518.

[2] Fahey, R.F. (2002) 'Tools for the simulation of human behaviour' in *SFPE Fire Protection Engineering*, Fall 2002, Nr. 16, pp. 19-22.

[3] Marchant, E.W. (1976) 'Some aspects of human behaviour and escape route design' in *Proc. 5th International Fire Protection Seminar*, Karlsruhe, September 1976.

[4] SFPE (2002) 'SFPE Handbook of Fire Protection Engineering', 3d ed. , sections 3.12 – 3.14, 2002, edited by NFPA

Multi-storey steel framed buildings under natural fire conditions

Gert van den Berg
TNO Centre for Fire Research, Delft, the Netherlands
Email: gert.vandenberg@tno.nl, Phone: +31 15 276 3394

Joris Fellinger
TNO Centre for Fire Research, Delft, the Netherlands

Pascal Steenbakkers
Arup Fire, London, UK

Ton van Overbeek
TNO Centre for Fire Research, Delft, the Netherlands

In this article, a methodology is presented by which the structural behaviour of composite steel framed building under natural fire conditions can be analysed. As a first step, a fire model is employed in order to predict the temperature development in the fire compartment. Secondly, a thermal response model is used to calculate the temperature distribution and development in the various structural elements. Finally, by means of a mechanical response model and given the thermal response, the structural performance of the full structure is predicted. This methodology is demonstrated by means of two case studies on two existing high-rise buildings in The Netherlands.

Key words: fire resistance, natural fire conditions, composite steel frame structures

1 Introduction

Traditionally, the fire resistance of load-bearing structures is assessed by considering the behaviour of single structural components, rather than the composite behaviour of a complete structure. In the traditional approach, the elements which are considered to be critical are isolated from the whole structure. The fire resistance is assessed on the basis of the behaviour under fire of this isolated element. This assessment could either be based on an existing design rule. Or, when such design rule is not available, the isolated element is taken to a furnace for fire testing. In order to perform the fire test, the single element is incorporated in a test rig and thus subjected to a certain set of boundary conditions. Also, a certain schematised loading is applied. By this approach, the

composite behaviour of a whole construction is not taken into account properly. In a complete structure, the boundary conditions of a single element is influenced by the behaviour of the surrounding structure, also the loading on the single element can be variable depending on the deformation of the structure.

Also in the single structural component approach, strongly schematised, standard fire conditions are taken into account. Whereas in reality, fire conditions can be quite different from case to case. Depending on various parameters, such as the amount of flammable material and the ventilation in the fire compartment etc., the fire development in a compartment can differ significantly, both in the time and the temperature regime. This is not taken into account in the standard approach for fire resistance testing.

The Cardington Demonstration project has shown that, under well monitored, fully developed fire conditions, the floors and steel beams of composite steel framed buildings may remain unprotected, without failure of the building structure [1]. In order to use these results for practical design purposes and the conditions under which such conclusions hold were specified more precisely in a subsequent research project. This research project is referred to as the "Cardington (2) project". As a results of this project, operational design guidance with regard to the structural behaviour of multi-storey composite steel framed buildings under natural fire conditions were obtained. The approach developed in the Cardington (2) project is presented in this article.

For a complete analysis of the structural behaviour of composite steel framed building under natural fire conditions, the following models are needed:

- a fire model, by which the temperature development in the fire compartment is predicted as function of the various parameters involved (dimension & lay out of the fire compartment, fire load density, ventilation conditions etc.);
- a thermal response model, by which the temperature distribution and development in the various structural elements (beams, columns, slabs) is predicted, given the thermal loading;
- a mechanical response model, by which the structural performance (deflections, deformations, moment distribution etc.) is predicted, given the thermal response.

These models are further explained in Chapter 3. However, in order to complete the history of this research program, a brief summary of the Cardington Demonstration project is presented first, see Chapter 2. Finally, in Chapter 4, the presented methodology is illustrated with two case studies, which are taken from two existing high-rise building located in The Netherlands.

2 Full-scale fire tests

In the past various full-scale fire tests have been performed. The fire tests which were used in order to calibrate the present modelling are referred to as the Cardington Demonstration project [1].

Within this Demonstration project, a total of 6 full-scale fire tests were carried out within the eight-storey steel framed structure located within the BRE Large Building Test Facility at Cardington, Bedfordshire, United Kingdom. See Figure 1 for a picture of this structure.

The fire tests, which were performed can be summarised as follows:

- Test 1 – restrained beam — unprotected beam, heated over 8 meter of its 9 meter length at a controlled speed of approx. 3 – 10 °C per minute.
- Test 2 – plane frame — unprotected beams and protected columns over the entire width of the building, heating was controlled by a furnace.
- Test 3 – 1st corner — area of the fire compartment was 76 m^2, fire load 45 kg of wood per square meter.
- Test 4 – 2nd corner — area of the fire compartment was 54 m^2, fire load 40 kg of wood per square meter.
- Test 5 – large compartment — area of the fire compartment was 340 m^2, fire load 40 kg of wood per square meter. This compartment was located between rows A – C and rows 1 – 4, see Figure 1.
- Test 6 – simulated office — area of the fire compartment was 135 m^2, containing "normal" office materials, fire load equivalent of 46 kg of wood per square meter. This compartment was located between rows D – F and rows 3 – 4, see Figure 1.

In Figure 1 a typical floor plan of the building is shown in which the locations of the various fire tests are noted.

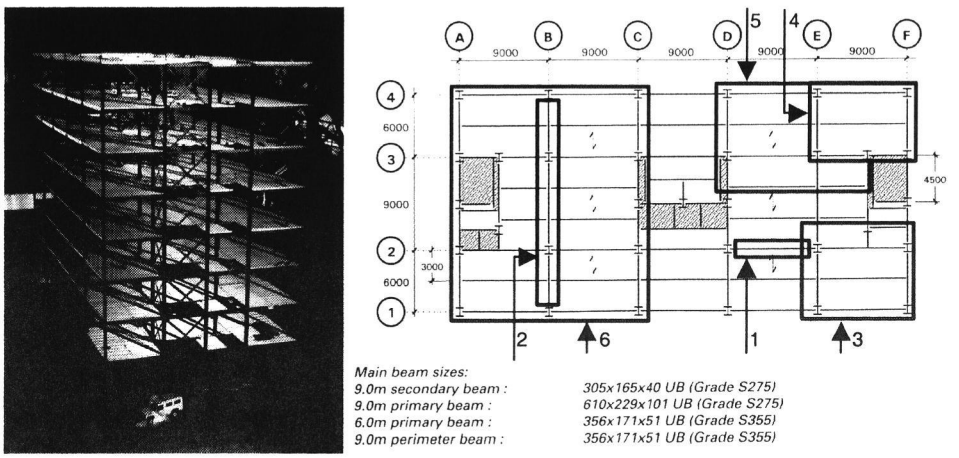

Figure 1 Photo of the steel framed structure at Cardington (left) and floor plan with locations of various fire tests (right).

The most important finding of the demonstration project was that the eight-storey steel framed structure in Cardington, in which the fire tests were performed, possessed a very significant degree of inherent fire resistance even although the steel floor beams remained entirely unprotected against fire attack.

3 Modelling

3.1 Fire model

The fire model utilised for the analyses presented in chapter 4 is composed of a one-zone and a two-zone model as well as a model to switch from the two-zone to the one-zone model [2]. Within the main model, various sub-models are adopted which enable the evaluation of:

- The heat and mass transfer between the inside of the compartment and the ambient external environment through vertical and horizontal openings and boundaries and forced vents (vent model).
- The heat and mass produced by the fire (combustion model).
- The mass transfer from the lower to the upper layer by the fire plume (air entrainment model).

Figure 2 shows a schematic view of the two-zone model and its sub-models for heat and mass transfer. In the two-zone model, the compartment is divided in an upper and a lower layer. In each layers the gas properties (temperature, density, etc.) are assumed to be uniform. The pressure is assumed to be constant throughout the whole compartment volume, except when it is evaluated that mass exchanges through vents.

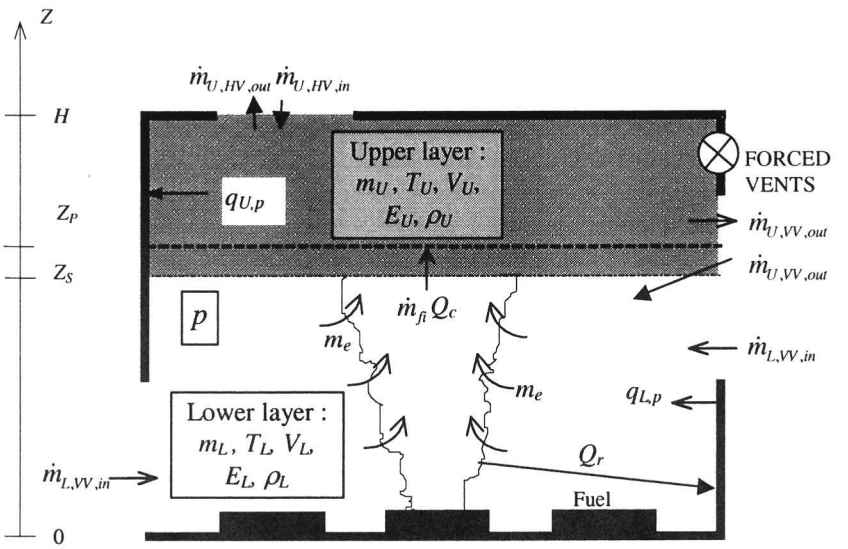

Figure 2 Schematic view of two-zone model and associated sub-models

Some switch criteria are defined so that they represent a limit beyond which one-zone model assumptions becomes closer to the physics of the fire situation than the two-zone model. The switch is made so that the total energy and mass present in the two-zone model system at time of switch are fully conserved in the one-zone model system.

Figure 3 shows a schematic view of the one-zone model and its sub models for heat and mass transfer. In the one-zone model, a single zone represents the compartment. In this zone the temperature and density are assumed to be uniform. The pressure is assumed to be constant on the whole compartment volume (except while evaluating mass exchange through vents). The zone is supposed to be opaque. Radiative and convective heat transfers connect partitions to it.

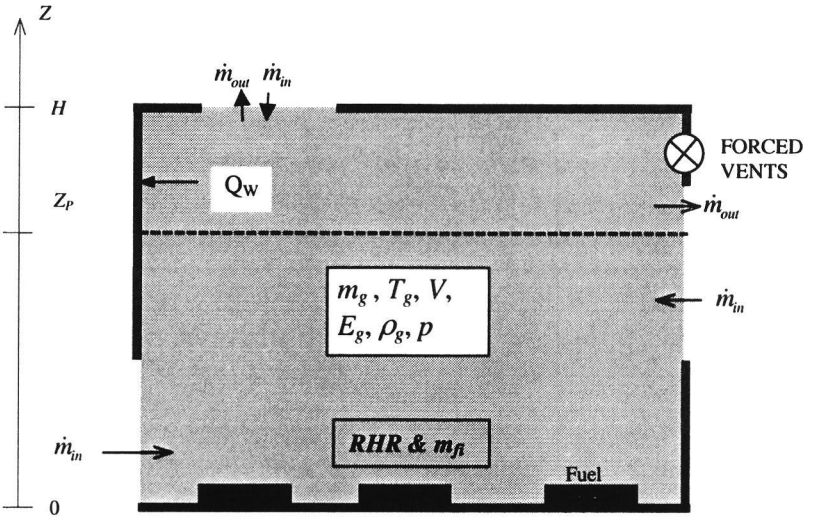

Figure 3 Schematic view of one-zone model and associated sub-models

3.2 *Thermal response*

From the fire model, based on various input parameters, the temperatures in the fire compartment are predicted. From these predicted air temperatures, the structural response will be assessed. This is carried out on the following steps. Firstly, the temperature distribution in the structural members are calculated (thermal response). Secondly, based on the calculated temperatures of the structural members, and given the mechanical loading, the mechanical behaviour of the structure is calculated (mechanical response).

The thermal analysis is performed while the structure is exposed to fire. For a complex structure, the sub-structuring technique is used, where the total structure is divided into several substructures and a temperature calculation is performed successively for each of the substructures. The thermal analysis is made using 2-D solid elements, to be used later on cross sections of the finite elements

which will be used in the analysis of the mechanical response. For the calculation of temperatures in beams, the temperature is non-uniform in the sections of the beam, but there is no heat transfer along the axis of the beams. For shells, the temperature is non-uniform through the thickness of the shell, but there is no heat transfer in the plane of the shell.

3.3 *Mechanical response*

For the analyses presented in Chapter 4, the finite element model DIANA is employed [3]. DIANA is a general-purpose three-dimensional finite element programme, suitable for the simulation of the thermal and structural response of structures including physical and geometrical non linear behaviour, dynamic effects and time and temperature dependent problems.

The physical non-linear behaviour of steel has been modelled with a Von Mises yield contour including hardening according to Eurocode 4 [4]. Concrete stress-strain behaviour has been modelled with a Drucker-Prager yield contour for compression including hardening. After evaluation of the effect of the inclusion of cracking, it appeared that the effect on the response was minimal while the effect on the numerical stability was detrimental. Therefore, in the analyses, no additional cracking criterion was applied. Later on, in the newest version of DIANA (8.1), the numerical instability was overcome and cracking could be applied, see the case study of the *Delftse Poort* in chapter 4.

In the modelling as presented, steel members such as beams and columns and ribs of steel-concrete composite slabs are being modelled with numerically integrated curved beam elements. These beam elements can be subdivided into zones to describe the actual cross sectional shape. Over each zone a time dependent temperature and temperature gradient are prescribed. The slabs have been modelled with numerically integrated curved shell elements, also provided with temperatures and temperature gradients. In both beam and shell elements, embedded reinforcement was placed where appropriate.

If two structural elements are connected to the same node, all degrees of freedom, i.e. the displacements and rotations, are compatible. If appropriate, the joints between structural elements have been modelled as hinges or with different nodes that were tied only for the required degrees of freedom. Figure 4 shows the adopted finite element mesh, which is used to model a typical section of the composite steel/concrete floor. The distribution of the various elements to model this section of the composite floor is primarily chosen with the aim to obtain a proper temperature distribution of the modelled structure.

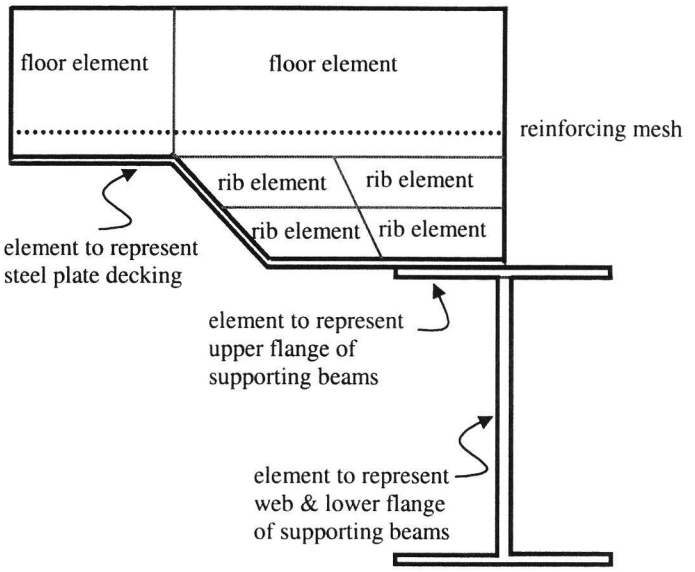

Figure 4 Schematic view of finite element mesh of a typical section of the composite steel-concrete floor

The simulations have been carried out in an incremental-iterative way. First the mechanical load has been applied. Hereafter, time has been increased incrementally. In each time step, the temperatures increase according to the results of the thermal response analyses. The temperature increase results in thermal expansion and degradation of the mechanical properties. Within each time or load step, the equilibrium has been searched in an iterative way using a secant stiffness approach. Within each iteration, the strain decomposition in each element is also carried out in an iterative way.

4 Examples

4.1 Case: Rembrandt Tower Amsterdam

4.1.1 Introduction

As a first case, the Rembrandt Tower in Amsterdam, see Figure 5, was analysed using the tools described in the previous paragraphs [5] and [6]. This high-rise office building has a height of 135 m. It consists of a steel frame structure with steel columns in the faced braced by a square concrete core in which the vertical transport systems are incorporated. The floors are made of composite decks using steel sheets supported on steel beams. A typical storey is 3.4 m high and each storey consists of one fire compartment.

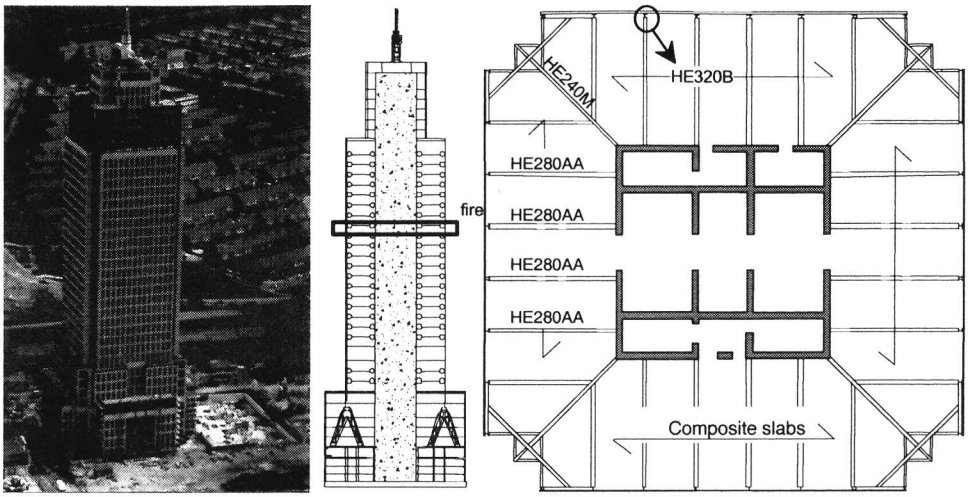

Figure 5 Photo of the Rembrandt tower office building in Amsterdam (left),cross section of the structural system with the fire exposed storey (mid) and floor plan of the structural system (right).

Dutch regulations require an equivalent fire safety level in for building beyond 70 m as for buildings lower than 70 m. However, no method is prescribed to assess the safety level. Therefore, one has to use general fire safety engineering principles and tools to meet the requirements. From fire safety engineering it is known that several aspects need special consideration in high rise buildings:

- The smoke movement is affected by the chimney effect, i.e. a natural draught exists in the building which can hamper the smoke spread control.
- Fire spread to other compartments can not be stopped by the fire brigade from the outside of the building. The fire brigade can only attack the fire through the building.
- High hydrostatic pressure differences exist in the suppression systems
- A complete evacuation of the building is takes more time than for a normal building if it is possible at all.

The consequences of an eventual collapse with respect to the urban environment are far greater than for a low rise building.

4.1.2 Approach

A finite element model of the structural system of the tower was developed with the computer code DIANA, in which a fully developed fire was assumed in one fire compartment. In order to achieve a consistency of crudeness between the model for the fire development and the structural model, the standard fire was replaced by a simulation of the fire development of a typical fire compartment in the building with the computer programme Ozone [3], i.e. the model described in chapter 3.

The size of the braced steel columns reduces towards the top because of the lower loads. A simple fire analyses of the columns at each storey, based on the standard fire exposure, showed that the columns at the 21st storey were most critical, see Figure 5. Therefore, this storey was modelled.
In order to optimise the design, the FE model was used for three design scenario's:

1. the insulation of each member according to a standard design analyses of the single element with the initial applied load and the natural fire exposure.
2. no insulation on the beams and 20 mm of Promatect-H on the columns.
3. without any insulation on both the steel columns and the steel beams but partition walls dividing one storey into four fire compartments.

4.1.3 Fire development

The fire development was modelled with Ozone. Since, most office spaces in the tower are furnished without partition walls, one big compartment was modelled of 32.4 x 32.4 m excluding the central core of 14.4 x 14.4 m. Ozone assumes one-dimensional heat conduction through the boundaries. The actual thermal properties of the concrete core, the composite floors and the sandwich construction of the façade (steel sheet – mineral wool - granite) were modelled with nominal values for concrete, steel and mineral wool as given by the programme. The characteristic value with 80 % reliability of the fire load density in standard offices was used of 593 MJ/m^2.
A big uncertainty is the ventilation resulting from the breaking of the windows. A small parameter study showed that the effect of the assumptions for the breaking of the windows on the temperature of the steel members in the compartment is relatively small. The results based on the assumption that all windows break directly at the start of the fire were finally used as input for the finite element model.

4.1.4 Thermal response models

Separate finite element models were made for the determination of the time dependent and non-uniform temperature distribution of cross sections of the steel concrete composite slab, the regular HE280AA beams and the heavy corner beams HE240M. The temperature of the columns was obtained by Ozone, as a uniform temperature distribution could be assumed for these columns which were exposed from all four sides.

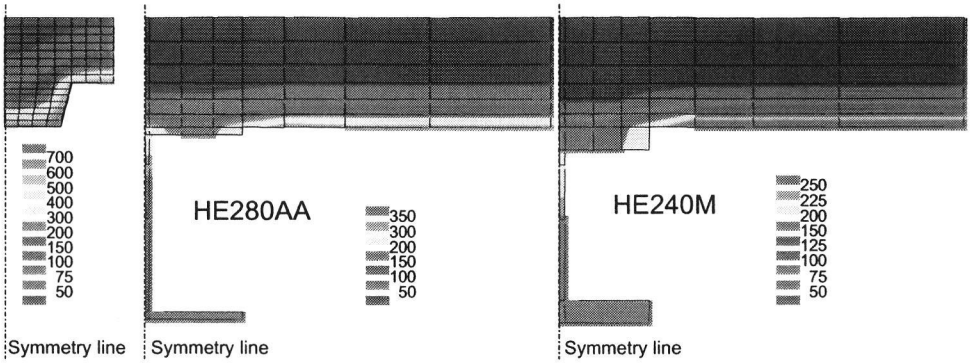

Figure 6 Cross sectional models for the determination of the thermal response of the steel concrete composite deck after 75 min. of fire exposure (left), the bare regular beams after 50 min. (mid) and the bare corner beams also after 50 min. (right)

4.1.5 Structural response model

The entire floor of the 21st level was modelled including the columns. For the scenario in which the fire compartment was reduced to ¼ of the floor area of that storey, one additional floor was modelled on top of the fire exposed construction representing the rest of the building in order to simulate the capability of the higher floors to redistribute the vertical loads to the unexposed columns.

At the bottom side and top side, the columns were modelled with clamped supports, the top side allowing for vertical displacements. At the top side of the columns, the momentary part of the vertical loads of the rest of the building were applied, considering partial safety factors equal to unity, which is in accordance with the recommended values in national and international codes for the fire situation.

The beams, columns and reinforced ribs of the composite slabs were modelled with numerically integrated beam elements based on the Mindlin-Reissner theory. The reinforced concrete deck was modelled curved shell elements. The steel sheet was modelled as reinforcement, considering a separate temperature development for the lower flange, the web and the upper flange. The non-linear temperature distribution in the ribs and the deck obtained with the thermal response models were simplified to linear temperature distributions over the beam and shell elements. For that purpose the average temperature was taken equal to the average temperature over the symmetry line of the thermal response models and the thermal gradient was derived such that the temperature of the reinforcement in the structural model equalled the temperature of the node in the thermal response model at the location of rebar.

From the structural models it was learnt that the deflections during fire were primarily driven by the thermal deformations rather than the applied loads. In design scenario 1 and 2, no failure occurred during the entire fire duration. In the cooling phase, the deflections reduced. In design

scenario 3, the columns collapsed after 38 minutes. It appeared that the cold construction above the fire compartment was not capable to redistribute the loads sufficiently.

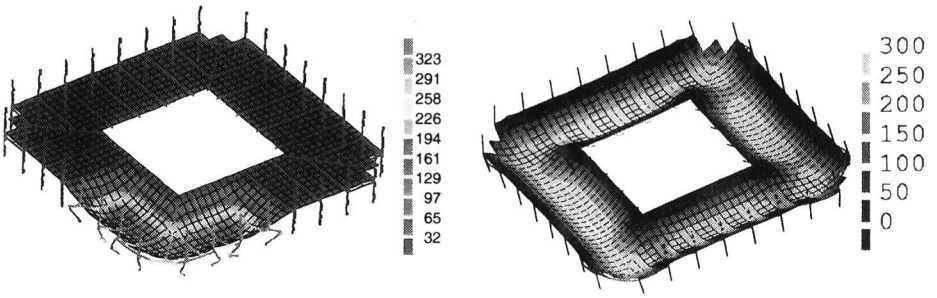

Figure 7 Collapse of the columns after 38 minutes in the scenario with partition walls dividing the floor plan into 4 fire compartments without any insulation on the steel columns and the steel beams (left) and displacements after 95 minutes without for the scenario with no insulation of the beams but 20 mm Promatect-H on the columns (right).

4.2 *Case study Delftse Poort*

The building named *Delftse Poort* (1991) is currently still the highest building (150 m.) of The Netherlands and located close to Rotterdam Central Station. The building comprises four parts constructed of pre-cast concrete. In this case, the fire resistance with regard to collapse in case of a fire at the 25th storey of building part 1, see Figure 8, was studied. The fire compartment that is modelled is in use as an office area. Although the building is equipped with a sprinkler system, in this case study it is assumed that the sprinkler system malfunctions [7].

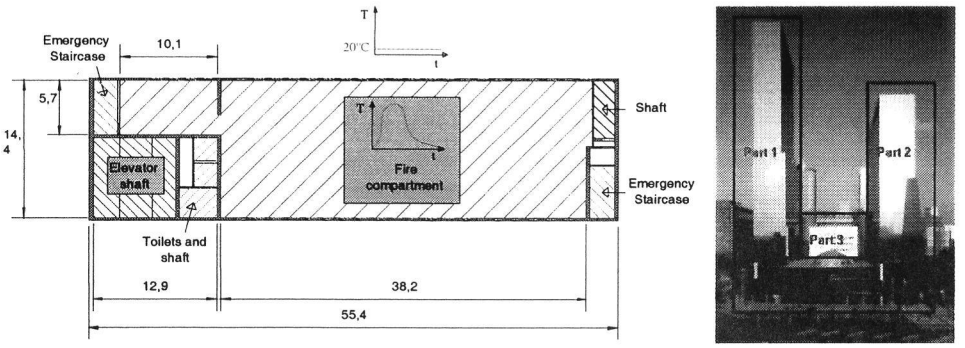

Figure 8 Floor plan of 25th storey. Left: Structural core with e.g. the elevator shaft. Middle: Office area constructed with prefabricated concrete elements. Right: Shaft and emergency staircase

4.3 *Results*

4.3.1 *Natural Fire Model*

Once again, the breaking of the window has an important effect on the development of the fire. However, opposite to a steel framed structure, it was not possible to predict in advance would be most severe. Therefore, three scenario's were evaluated, i.e.

1. Fast fuel controlled scenario
2. Slow oxygen controlled scenario
3. Intermediate scenario

The first two scenarios describe the outer borders of the spectrum of possible time-temperature curves. The third scenario is a best guess based on engineering judgement.

4.4 *Thermal response model*

The fire compartment is not fully taken into account in the system approach. Only that part of the fire compartment that is build up of prefabricated concrete elements is taken into account in the thermal response and mechanical FEM models. The uniform time temperature curves calculated by use of Ozone are applied as a boundary condition to three different thermal response models representing respectively the wall of the 25th storey except for the column, the column of the 25th storey and the floor elements of the 26th storey (see Figure 9). The floor of the 25th storey is considered "cold".

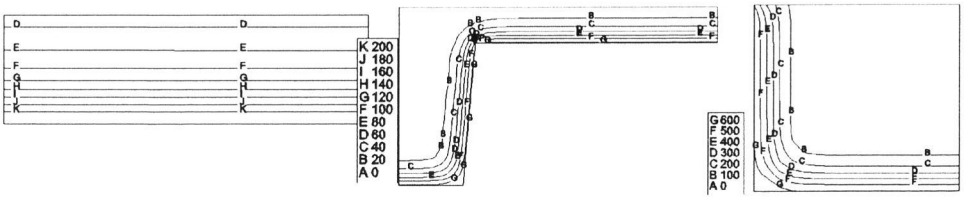

Figure 9 From left to right: wall model – slow scenario, floor model – intermediate scenario and column model – fast scenario, all taken at times at which the maximum air temperature is reached.

4.5 *Mechanical FEM model*

In figure 10 the finite element mesh is presented together with the boundary conditions in a cross-section. The curved shell elements at the bottom and the top of the model represent together with the constraints at the bottom and the top of the model, the structure below and above the model. At the left side of the model, where it meets the structural core of the building, the translation in Z-direction is fixed.

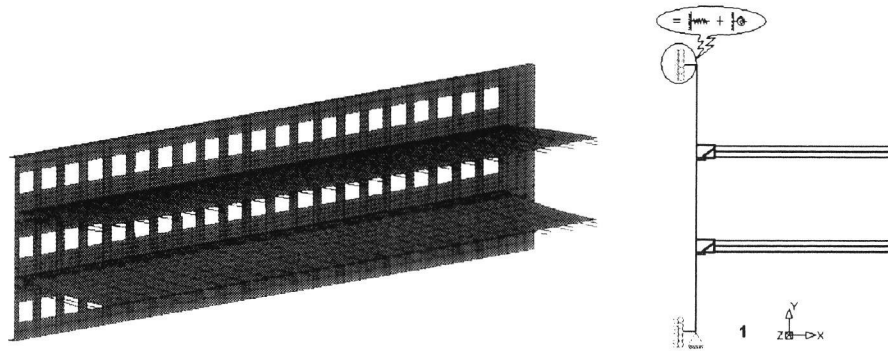

Figure 10 Final mechanical FEM model (left) and boundary condition (right)

When the structure is heated up by the fire the floor expands in both directions. In global X-direction this expansion is more restrained compared to the global Z-direction. This restraint leads to a distributed load on the wall in global X-direction of approximately 350 kN per repetitive structural element of 1.8m'.

Furthermore the upper part of the wall, the column and the lower part of the wall of the 25th storey are heated up by both an average temperature and a temperature gradient. This average temperature has little influence on the mechanical behaviour because the structure just moves upwards. The gradient however leads curvature that is partially restrained by its surrounding structural parts. Consequently a change in the bending moments results.

It is found, that the top part of the column of the 25th storey is a weak part of the structure in case of fire due to a relatively small moment of inertia. Furthermore the distributed load on the wall caused by the restrained expansion of the floor leads to an extra "negative" bending moment at the top of the column. The relatively cold rear side of the column cracks horizontally and the concrete at the hot front side of the column crushes.

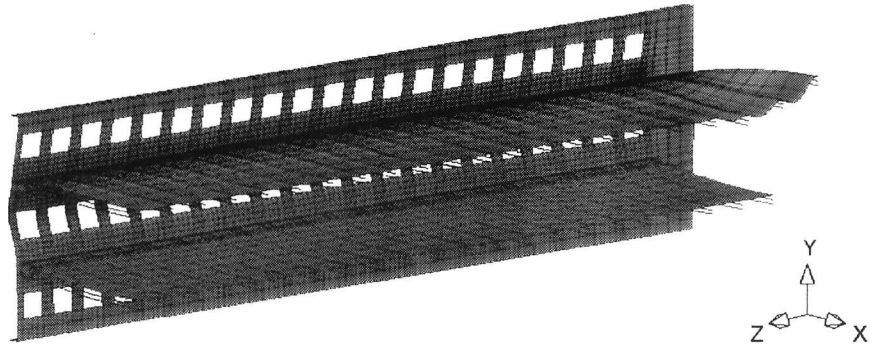

Figure 11 Thirty times enlarged deformation in case of slow –scenario with soft interface configuration

Acknowledgement

The authors wish to thank ECSC for the financial support for the research projects into the Natural Fire Safety Concept as well as both Cardington projects.

References

[1] Martin, D et al. (1999), The behaviour of multi-storey steel framed buildings in fire, Britisch Steel plc, UK

[2] Schleich J-B, Cajot L-G, et al. (2000), Competitive steel buildings through natural fire safety concept, final report of ECSC research project, ECSC Steel Publications, Brussels, Belgium

[3] de Witte, F. (2002), DIANA users manual, Release 8.1, TNO Building and Construction Research, Delft, the Netherlands

[4] prEN 1994-1-2 (2003), Eurocode 4 – Design of composite steel and concrete structures, Part 1-2: General rules – Structural fire design, CEN TC250, Brussels, Belgium

[5] Steenbakkers, P. (2001) Brandveilig Ontwerpen van Hoogbouwconstructies, Deel I – Verkennend onderzoek, Graduation report TU Delft, Delft, the Netherlands (in Dutch)

[6] Steenbakkers, P. (2001) Brandveilig Ontwerpen van Hoogbouwconstructies, Deel II - Case Studie Rembrandttoren, Graduation report TU Delft, Delft, the Netherlands (in Dutch)

[7] Van Overbeek, A.B.M. (2005), System approach on structural fire safety, Graduation report TU Delft, TNO report 2004-CVB-R0378, Delft, the Netherlands

Fire exposed aluminium structures

Johan Maljaars
NIMR, Delft, the Netherlands
TNO Building Structures and Systems, Delft, the Netherlands
Eindhoven University of Technology, Eindhoven, the Netherlands
Email: johan.maljaars@tno.nl, telephone +31 15 276 3464

Joris Fellinger
TNO Centre for Fire Research, Delft, the Netherlands

Frans Soetens
Eindhoven University of Technology, Eindhoven, the Netherlands
TNO Building Structures and Systems, Delft, the Netherlands

Material properties and mechanical response models for fire design of steel structures are based on extensive research and experience. Contrarily, the behaviour of aluminium load bearing structures exposed to fire is relatively unexplored. This article gives an overview of physical and mechanical properties at elevated temperature of frequently applied aluminium alloys, found in relevant literature and discusses mechanical response models currently applied for fire exposed aluminium structures. A comparison is made with steel structures exposed to fire.

Keywords: Physical and mechanical properties of aluminium, fire design of aluminium

1 Introduction

The last decades, more and more load-bearing structures are built in aluminium alloys. The success of aluminium can be attributed to specific properties, such as the low density, good corrosion resistance and the freedom in design thanks to the extrusion process. These and other properties are beneficial in case of structures such as fast ferries, helicopter decks and living quarters on oil platforms.

A wide variety in aluminium alloys and tempers (the temper depends on the treatment) exists. Material properties differ between these alloys and tempers. In general however, aluminium alloys have a high thermal conductivity and low melting temperature, between 580 °C and 650 °C. This combination makes aluminium relatively sensitive to fire exposure.

Although material properties and response of structural elements are well known at room temperature (see e.g. Talat [5], Kammer [18] and Mazzolani [28]), this is not the case under fire

conditions. Lack of knowledge on the behaviour of fire exposed aluminium structures has resulted on the one hand in conservative mechanical response models in standards, such as the European code on fire exposed aluminium structures EN 1999-1-2 [3] and on the other hand in difficulties with getting aluminium structures accepted by approving bodies.
The second section of this article concerns the heating of aluminium sections. Mechanical properties of heated aluminium alloys are discussed in the third section. The fourth section gives an overview of existing mechanical response models for aluminium structures exposed to fire.

2 Thermal response and physical properties

The temperature development in the cross-section of a non-combustible member is given by the well-known Fourier equation:

$$\frac{\partial}{\partial x}\left(\lambda\frac{\partial\theta}{\partial x}\right)+\frac{\partial}{\partial y}\left(\lambda\frac{\partial\theta}{\partial y}\right)+\frac{\partial}{\partial z}\left(\lambda\frac{\partial\theta}{\partial z}\right)=\rho\cdot c\frac{\partial\theta}{\partial t} \qquad (1)$$

Equation (1) shows that the temperature inside the member depends on the conductivity (λ) and the product of density and specific heat (ρ·c), which is called thermal capacitance.
The boundary conditions of equation 1 are determined by the heat flux to the member surface. This heat flux is the summation of heat flux by convection and heat flux by radiation. The latter is directly related to the emissivity of the surface of the heated member.
Thus, besides the thermal properties of the fire itself, heating of an aluminium member depends on the thermal conductivity, thermal capacitance and emissivity of the member. These properties depend on the chemical composition of the material, and may therefore vary per alloy. As the treatment does not change the chemical composition, it is not expected that physical properties depend on the temper, although no tests were found to evaluate this assumption. The relevant physical properties are outlined in the following sections.

2.1 Thermal conductivity

Especially at elevated temperature, the amount of test results on the thermal conductivity found in literature is limited. Tests are reported by Kammer [18], Brandes [10], Holman [17] and in the SFPE Handbook of Fire Protection Engineering [6]. The results are shown in figure 1, together with the thermal conductivity of aluminium alloys according to EN 1999-1-2 [3] and the thermal conductivity of steel according to the European code on fire exposed steel structures, EN 1993-1-2 [2]. From tests carried out it is concluded that the thermal conductivity is different for different alloys.

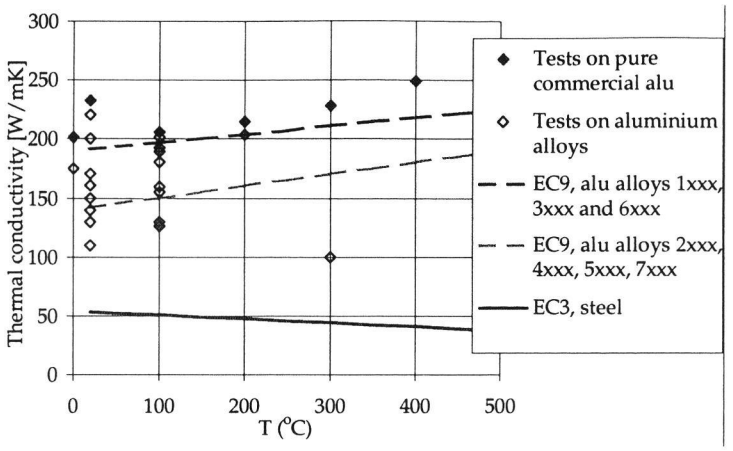

Figure 1: Thermal conductivity of aluminium alloys and of steel

Figure 1 shows that thermal conductivity of aluminium is high compared to steel. Unless a structural element is exposed to fire on some sides and protected at other sides, e.g. by gypsum board, the member temperature can be regarded as uniform. The exact value for the thermal conductivity is then not very relevant.

The high thermal conductivity also leads to elevated temperatures in parts of the structure not directly exposed to fire.

2.2 *Specific heat and thermal capacitance*

Specific heat is the amount of heat needed to raise the temperature of a unit mass of a substance by one degree. Kammer [18] summarises test results on the specific heat. The specific heat resulting from these tests varies little with the type of alloy, but it depends on the temperature. According to data in EN 1999-1-2 [3], the specific heat of aluminium varies from 913 J/kg °C at room temperature to 1108 J/kg °C at elevated temperature, which is 2,1 and 1,7 times higher than that of steel, respectively.

Equation (1) shows that the temperature of an aluminium member is related to the product of specific heat and density. The density of aluminium is 2700 kg/m^3, which is 2,9 times lower than the density of steel. Consequently, the thermal capacitance is lower than in case of steel.

2.3 *Emissivity*

Emissivity of the member can be described as the ease with which a substance radiates its own thermal energy. For ideal grey opaque media, the absorption of radiation equals the emissivity, the rest of the incident radiation is reflected. The emissivity depends on the condition of the surface. The temperature of the aluminium surface is of minor importance for the emissivity (Talat [5]).

In real fires surfaces are almost always (partially) covered with soot. EN 1999-1-2 [3] specifies a coefficient of emissivity of 0.7 for covered (e.g. sooted, but also painted) aluminium surfaces. This coefficient is equal to the value given for covered steel surfaces.
In case of external exposed aluminium members, i.e. members not engulfed in flame, or in case of a 'clean' fire such as in a standard fire test in a gas oven, the member surface is not sooted and the emissivity is related to plain aluminium. The emissivity resulting from tests varies from 0,03 to 0,11 for new, plain aluminium and 0,05 to 0,31 for heavily oxidised aluminium (Kammer [18], Holman [17] and Twilt [31]). The influence of alloying elements on the emissivity coefficient is small (Kammer [18]). Plain aluminium members thus reflect most of the radiative heat emitted by the fire. The coefficient of emissivity of plain aluminium specified by EN 1999-1-2 [3] is 0,3. This value is low when compared to steel: EN 1993-1-2 [2] specifies a coefficient of emissivity of 0.7 for steel.

2.4 *Evaluation of thermal response*

Aluminium heats faster than steel because of the high conductivity and low thermal capacitance. Only in case of plain aluminium, low emissivity prevents very fast heating. As an example, figure 2 gives the member temperature of unprotected steel and aluminium sections exposed to a standard fire. The dark grey lines indicate square hollow sections 50x50x2 mm, light grey indicates the same sections, but with a wall thickness of 0,8 mm. The temperature is determined with the equations in EN 1993-1-2 [2]and EN 1999-1-2 [3], which are based on equation (1):

$$\Delta\theta_t = k_{sh}\frac{1}{c\cdot\rho}\frac{A_m}{V}h_{net,d}\cdot\Delta t \qquad (2)$$

In which:

$\Delta\theta_t$	=	Increase in temperature of the member;
k_{sh}	=	Correction factor for the so-called shadow effect;
A_m/V	=	Section factor for unprotected aluminium members;
$h_{net,d}$	=	Design value of the net heat flux per unit area (determined with EN 1991-1-2);
Δt	=	time interval, which should not be taken as more than 5 seconds.

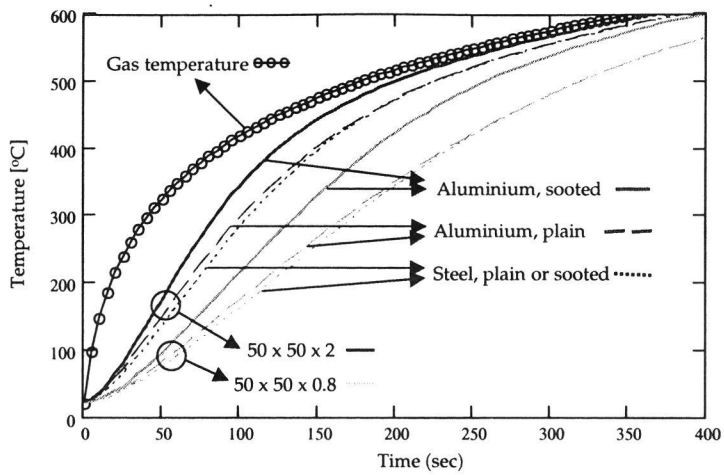

Figure 2: Heating of aluminium and steel square hollow sections

As expected, aluminium sections covered with soot heat faster than steel sections. Apparently, the temperature development in plain aluminium sections is approximately equal to the temperature development in steel sections with the same dimensions (or section factor). Because of specific properties of aluminium, such as extrusion possibility, thin wall thicknesses are applied in many aluminium structures, so that such structures heat fast compared with conventional steel structures.

3 Mechanical properties

A temperature rise in metal structures results in thermal expansion and reduced mechanical properties, which are discussed in this chapter. As the mechanical properties differ per alloy and temper, the chapter starts with a short overview of alloys and tempers.

3.1 Alloys and tempers

Wrought alloys are indicated with a four-digit number according to the international Registration Record administrated by the Aluminum Association. The first digit indicates the dominant alloying element and the other digits indicate a specific alloy. For structural engineering, particularly alloys in series 5xxx (aluminium magnesium alloys) and 6xxx (aluminium magnesium silicon alloys) are of importance because of a combination of moderately high strength, good corrosion resistance and good weldability.

The temper depends on the treatment. Some alloys, such as those in the 6xxx series, are heat treatable. Heat treatment makes use of the property that at higher temperature, more alloying elements can be dissolved in the aluminium matrix than at low temperatures. During production, a large amount of the alloying element(s) is dissolved in aluminium at a temperature just below the

melting temperature. Following, rapid quenching leaves the matrix in a supersaturated, unstable condition. The unstable condition gradually changes in a stable condition by formation of precipitate particles, through which extra strength is obtained (called ageing). For example, tempers starting with T4 indicate that aging takes place at room temperature (naturally ageing). For most alloys, this process takes years. To speed up ageing, it is possible to heat the supersaturated alloy to a moderately elevated temperature (120 to 180 °C) for a specific period of time (mostly several hours). Tempers starting with T5 and higher indicate alloys with this treatment (artificial ageing). For non-heat treatable alloys, extra strength can be obtained through work hardening. Work is done during rolling, extruding, drawing or bending below the recrystallisation temperature. Tempers starting with H indicate work-hardened non-heat treatable alloys.
Alloys that are only annealed and which have not undergone additional treatment are indicated with temper O. An overview of treatment possibilities for various alloy series is given in figure 3. For more information on treatments, see Altenpohl [7] or Kammer [18].

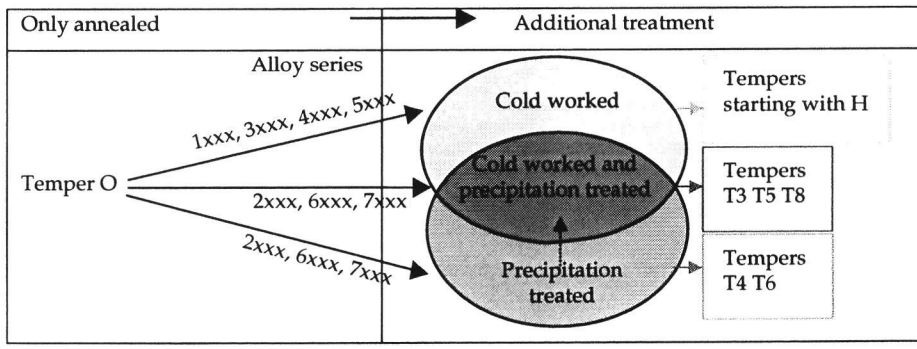

Figure 3: Overview of treatment possibilities

3.2 *Thermal expansion*

Aluminium expands when subjected to an increasing temperature. Thermal expansion of aluminium may lead to significant changes in structural behaviour:

- In cases where expansion of a heated element is restrained (e.g. in case of elements with a temperature gradient) high internal stresses may result;
- In statically undetermined structures, expansion of aluminium may lead to significant changes in the load distribution (Eberwien [14]);

Kammer [18] and Brandes [10] give test results on thermal expansion. The resulting coefficient of linear thermal expansion of pure aluminium varies linearly from $22{,}8 \cdot 10^{-6}$ at ambient temperature to $27{,}4 \cdot 10^{-6}$ at 500 °C. The coefficient varies little with the alloy.
The thermal expansion of aluminium is approximately 1,9 times higher than that of steel. As the modulus of elasticity of aluminium is only one third of the modulus of elasticity of steel (see section

3.3), thermal stresses in the elastic range in aluminium are lower than in case of steel with equal temperature increments (approximately 2/3 of steel).

3.3 Strength, stiffness and ductility at elevated temperature

Mild steel has a clearly defined yield point at room temperature, but shows inelastic mechanical behaviour at elevated temperature. Aluminium alloys have inelastic mechanical properties both at room and elevated temperature. At room temperature, the Ramberg-Osgood relation is mostly used to describe the stress-strain relation, see e.g. Mazzolani [28]. The stress at an irreversible plastic strain of 0,2% (f_o) is usually applied as the yield strength. This section gives an overview of the development of the mechanical properties at elevated temperature.

3.3.1 0,2 % proof stress and tensile strength

With increasing temperature, the strength of metals generally decreases (Koser [22]).
Voorhees and Freeman [32] and Kaufman [20] reported tensile tests on various aluminium alloys after various exposure times. The alloys incorporated in these reports are limited to those frequently applied in the USA. Tensile tests on alloy 6082, which is applied in many structures in Europe, are reported in Hepples and Wale [16], Broli and Mollersen [11], Amdahl, Eberg and Langhelle [8], Kleive and Gustavsen [21], Langhelle [25] and Bergli and Moe [9]. The strength at room temperature and at elevated temperature depends on the alloy and the temper. For most alloys and tempers, the 0,2% proof stress already decreases significantly at a temperature of 150 °C. The 0,2% proof stress at a temperature of 350 °C is on average reduced to 20 %of the strength at room temperature after an exposure period of 30 minutes. As a comparison, the yield stress of steel is not yet reduced at this temperature according to the data in EN 1993-1-2 [2].
Figure 4 shows the 0,2% proof stress of heat treatable alloy 6063 in tempers T42 and T6 after an exposure period of 0,5 hours. The strength of temper T42 increases at moderately elevated temperature, as this temperature speeds up the ageing process (see paragraph 3.1).

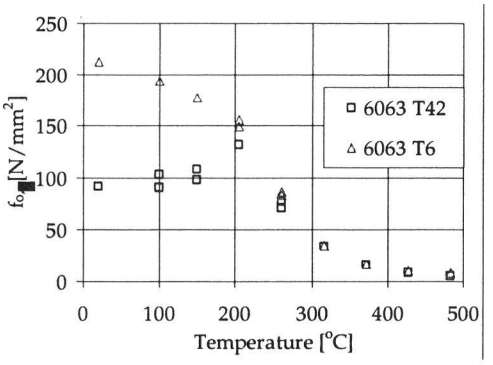

Figure 4: Tensile test results - 0,2% proof stress of alloy 6063 with various tempers

Figure 5 shows the 0,2% proof stress of the non-heat treatable alloy 5083 with tempers O and H113. The significant difference in strength at room temperature between these tempers vanishes at elevated temperature. The strengthening effect of the work hardening is rapidly lost and the same strength remains as for the untreated material. This was also found for other alloys and tempers.

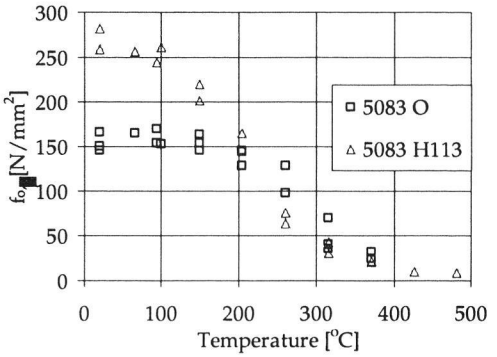

Figure 5: Tensile test results - 0,2% proof stress of alloy 5083 with various tempers

The tests data show that the difference between 0,2% proof stress and tensile strength decreases at increasing temperature, for all alloys and tempers. In case of non-heat treatable alloys, the strength does not vary for different thermal exposure periods. The strength of heat treatable alloys however depends on the thermal exposure period. According to data in Kaufman [20], the strength of 6xxx alloys at temperatures up to 425 °C after an exposure period of 0,5 hours reduces up to 80% of the strength at the same temperature after 0,1 hours.

Tensile tests at elevated temperature were only carried out on a limited number of alloys. When analysing the data however, the strength of different alloys in the same series and with the same temper shows an approximately equal decrease. As an example, figure 6 shows the 0,2% proof stress (left-hand picture) and the relative 0,2% proof stress (proof stress relative to that at room temperature, right-hand picture) of alloys in series 6xxx and temper T6, according to data by Kaufman [20]. The relative 0,2% proof stress corresponds reasonable for different alloys in this series, with this temper. When analysing data on other combinations of alloys and tempers, this seems to be the case for most combinations of alloy series and tempers.

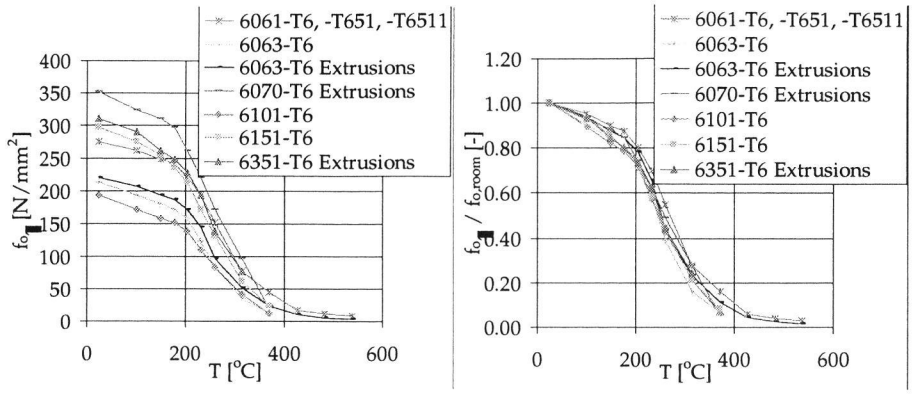

Figure 6: 0,2 % proof stress (left-hand) and relative 0,2% proof stress for alloy series 6xxx temper T6

3.3.2 Modulus of elasticity

The modulus of elasticity (E) can either be determined with an unloading-reloading cycle (adiabatic modulus of elasticity) or with the reflection of (sound) waves sent through the material (isothermal or dynamic modulus of elasticity). The first method was e.g. applied on alloys in series 5xxx and 6xxx in Kaufman [20], the second method was applied by Richter and Hanitzsch [29]. Results are shown in figure 7, together with the modulus of elasticity given in EN 1999-1-2 [3].

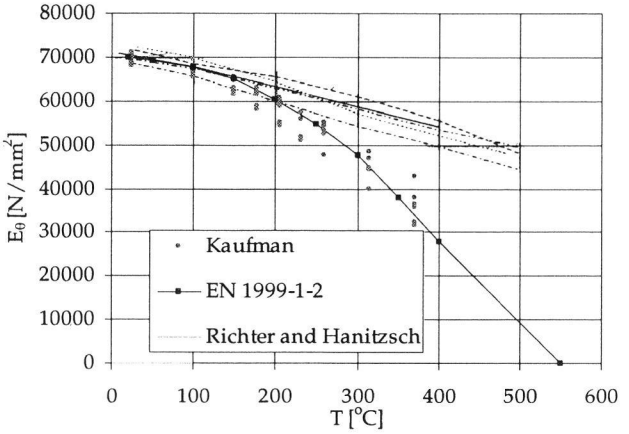

Figure 7: Adiabatic (Kaufman, 5xxx and 6xxx) and isothermal (Richter and Hanitzsch) modulus of elasticity

Figure 6 shows that the isothermal modulus of elasticity does not correspond with the adiabatic modulus of elasticity at elevated temperature. This is possibly due to viscoplastic behaviour, see section 3.4. Only a few data on the modulus of elasticity were found for temperatures exceeding 370 °C. For fire design, the adiabatic modulus of elasticity is of interest.

Except for naturally aged heat-treatable alloys (temper T4 and lower), the reduction in 0,2% proof stress at elevated temperature is larger than the reduction in modulus of elasticity. On the contrary,

in case of steel, the stiffness reduces faster than the strength for temperatures up to 900 °C, according to data in EN 1993-1-2 [2].

3.3.3 *Rupture strain*

For increasing temperatures, the rupture strain increases for most tempers until a temperature of approximately 400 °C. Exceptions are naturally aged heat-treatable alloys, for which ageing at moderately elevated temperature increases the strength, but reduces the rupture strain as they approach the artificially aged condition.
In case of temperatures exceeding 400 °C, data tabulated by Kaufman [20] show a decrease in rupture strain while Voorhees and Freeman [32] report an increase. The difference is attributed to the measurement technique not being straightforward. No extensive data was found in literature on the strain at the ultimate tensile strength.

3.4 *Viscoplastic behaviour (creep)*

Creep is time dependent distortion of material due to loading. Creep results in elongation of material and decrease in strength and stiffness. While creep of aluminium is neglected at ambient temperature in design standards, it may become significant at elevated temperature.
Creep deformations are divided in primary creep with decreasing creep rate, in secondary creep with constant creep rate and in tertiary creep with increasing creep rate (Kraus [23]). Creep rupture takes place at the end of the tertiary stage.

Voorhees and Freeman [32] and Kaufman [20] give elongation percentages after various exposure periods at constant elevated temperature and the time to rupture of various alloys and tempers at various stress levels. Kaspersen and Soras [19], Krokeide [24] and Broli and Mollersen [11] carried out creep tensile tests on alloy 6082 T6 at various temperatures with various stress levels. Their results are discussed in Eberg et al. [12] and in Langhelle [25]. Also Hepples and Wale [16] carried out creep tensile tests on alloy 6082 T6. Only Voorhees and Freeman [32] gave a limited amount of creep test results for temperatures exceeding 320 °C. The tests showed a strong increase of creep deformations and a decrease in the time to rupture for increasing stress level and temperature. According to data in Kaufman [20], the average creep rupture stress of various alloys for rupture after one hour is 79% and 66% of the tensile strength at temperatures of 204 and 316 °C, respectively.

Hepples and Wale [16] carried out creep tests to determine whether creep in the secondary stage influences the strength. The specimens of alloy 6082 were loaded with 30 % of the proof stress at ambient temperature. The thermal exposure period was 30 minutes up to two hours. They found no influence of this creep period on the strength. However, the strain after rupture was significantly

reduced. More tests with various stress levels should be carried out to determine whether this conclusion holds in general.

3.5 *Evaluation of structural material response*

The decrease in strength and stiffness at elevated temperature for most aluminium alloys and tempers is much larger than in case of steel. Creep cannot be neglected at elevated temperature. As an example, the material characteristics according to EN 1993-1-2 [2] and EN 1999-1-2 [3] of a square hollow section 50x50x2 are given in figure 8. The left-hand picture shows the yield strength and the right-hand picture the modulus of elasticity, relative to the properties at room temperature, of sections of steel and aluminium alloy 6063 T6 that are covered with soot. Note that the influence of creep periods is not taken into account in the material properties of EN 1999-1-2 [3], as it is assumed that the 0,2% proof stress is sufficiently conservative (Lundberg [27]).
As expected, both strength and stiffness of the aluminium sections reduce faster than that of steel sections with equal dimensions. It should be noted that both the aluminium and steel sections require protection in order to obtain the required fire-resistant period.

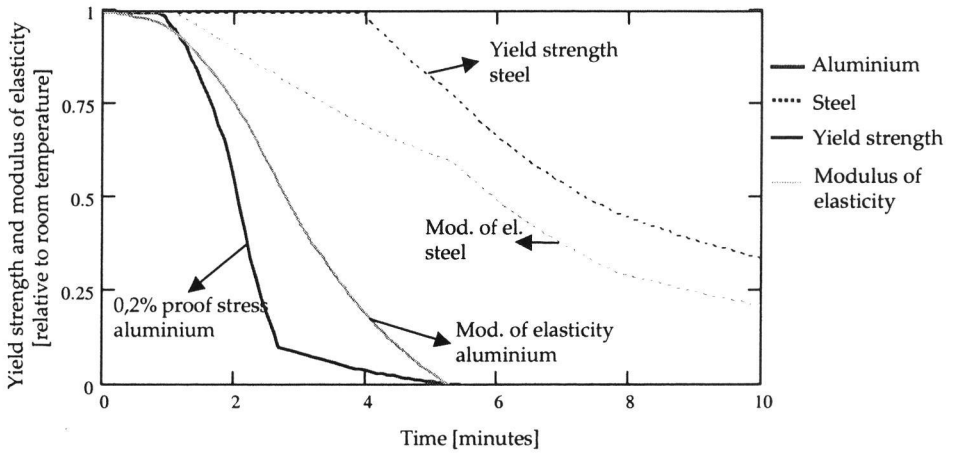

Figure 8: Mechanical properties of steel and aluminium square hollow section 50 x 50 x 2 exposed to a standard fire

The tensile and creep tests described in this chapter were carried out after an exposure period at a constant elevated temperature. In real fire exposed structures however, the temperature increases from room temperature to maximum temperature, while the load is in many cases assumed to remain constant. Tensile tests after a period with increasing temperature with constant load were not found in literature. It is recommended to obtain such data in future tests. With these tests, it should be determined whether creep is significant in real fire situations. Tests with the same heating

rate but not loaded during heating can be carried out in order to determine the reference strength; i.e. the strength without creep influence.

4 Mechanical response models for structures in EN 1999-1-2

Calculation methods for fire design of aluminium structures exposed to fire are the Norwegian standard NS 3478 [4] and the European standard EN 1999-1-2 [3]. The latter is the most recent standard and is discussed in this chapter. When available, the models are compared to test results on components.

4.1 Response models for entire structures

Where a global structural analysis is carried out, EN 1999-1-2 [3] prescribes that the relevant failure mode in fire exposure, the temperature-dependent material properties and member stiffness and effects of thermal expansions and deformations shall be taken into account. As EN 1999-1-2 [3] provides no simple calculation models for entire structures or parts of entire structures, advanced calculation models should be used. Advanced calculation models may be used in association with any heating curve, provided that the material properties are known for the relevant temperature range.

As the development and validation of advanced mechanical response models is complicated and time consuming for most structures, advanced models are usually not applied. On the other hand, these models may give the best approximation of the real structural behaviour during a fire. Besides, redistribution of forces can only be taken into account when the entire structure is evaluated. Advanced response models may therefore result in more economical structures.

4.2 Response models for individual members

When advanced models are not applied, EN 1999-1-2 [3] provides simple calculation models for the evaluation of structures exposed to fire. Simple calculation models can be applied when the structure is divided in separated members and each member is analysed individually. Some simplifications of the real mechanical response may be applied:

- The reactions at supports and internal forces and moments at boundaries of the considered part of the structure may be assumed to remain unchanged throughout the fire exposure.
- Only the effects of thermal deformations resulting from thermal gradients across the cross-section need to be considered. The effects of axial or in-plain expansion may be neglected.

These simplifications mean that load redistributions due to changes in stress-strain relations during fire and due to thermal deformations are being neglected. Also stresses resulting from restrained thermal expansion are not considered. In reality, these thermal stresses may influence the load bearing capacity significantly.

Notably, the thermal gradient in aluminium structures is generally negligible due to the high thermal conductivity, excluded sections that are exposed to some sides and protected at other sides.

4.2.1 Strength of the cross-section

In case of members in tension, it should be verified whether the design resistance of the gross cross-section, taking into account the material properties at elevated temperature, is larger than the normal force. EN 1999-1-2 [3] gives rules both for a uniformly distributed temperature and a non-uniformly distributed temperature. In case of non-uniform temperature distribution, the contribution of each part of the cross-section with a specific temperature is taken into account by using the 0,2% proof stress at that temperature. In case of welding, the strength of the heat affected zone should be determined multiplying the 0,2% proof stress of the parent material at elevated temperature with the reduction coefficient for the weld at room temperature.

4.2.2 Stability

The ratio between the 0,2% proof stress and the modulus of elasticity for aluminium alloys is high compared to steel. This makes aluminium sections (partly) in compression relatively sensitive to buckling. The following types of buckling are distinguished:

1. Global buckling of a member in compression (flexural, torsional or flexural-torsional);
2. Global buckling of a member in bending (lateral-torsional);
3. Local buckling.

Ad 1. In the Eurocodes for steel and aluminium structures, the buckling resistance is related to the relative slenderness (λ_{rel}), which depends on the square root between strength and stiffness, see equation (4). A relatively high value for the relative slenderness means that the section is relatively sensitive to buckling. The mathematical relation between the ultimate buckling resistance and the relative slenderness is called a buckling curve and takes into account influence of geometrical imperfections, residual stresses and inelastic material characteristics.

$$\lambda_{rel} = \sqrt{\frac{N_{pl}}{F_{cr}}} \sim \sqrt{\frac{f_o}{E}} \tag{3}$$

In fire design, the relative slenderness according to EN 1999-1-2 [3] should be determined with material properties at room temperature. As the ratio between strength and stiffness decreases at increasing temperature, the relative slenderness and thus the sensitivity to buckling may be overestimated at elevated temperature.

In addition, the buckling curve at room temperature should be applied to determine the buckling resistance with this relative slenderness. A study to whether this buckling curve is also appropriate at elevated temperature was not found.

In an experimental research on steel members in compression (Franssen et al. [15] and Talamona et al. [30]) it was concluded that a relative slenderness determined with material properties at elevated temperature gives a better correlation with the buckling resistance than using material properties at ambient temperature. A buckling curve for steel columns at elevated temperature was proposed. This buckling curve is less favourable than the buckling curves at room temperature, possibly caused by the fact that steel has a yield limit at room temperature, but inelastic material characteristics at elevated temperature. The method is applied in EN 1993-1-2 [2].

It is possible that the lateral deflection increases during buckling because of creep. EN 1999-1-2 [3] takes this into account by dividing the buckling resistance with a creep factor. This creep factor is given as 1,2, independent of the temperature and the time at elevated temperature. Thus:

$$N_{b,fi,t} = \frac{f_{o,\theta}}{f_{o,room}} \frac{N_b}{1,2} \tag{4}$$

With

Nb,fi,t = Buckling resistance at fire conditions

Nb = Buckling resistance at room temperature

Tests have been carried out on columns in compression of alloy 6082 with an additional bending moment (Langhelle [25], Langhelle et al. [26] and Eberg et al. [13]). 14 tests were carried out with constant load and a temperature linearly increasing in time. The critical temperature of tests with a relatively slow heating rate (so that the resistance was reached after approximately one hour) was approximately equal to the critical temperature of tests with a fast heating rate (resistance reached after 20-25 minutes). This may indicate that creep has no influence on the buckling resistance for the parameter field researched. Research is necessary to determine whether this conclusion holds for other alloys, load levels and a fire exposure period up to two hours.

Ad 2. The calculation model for buckling resistance of members subjected to lateral-torsional buckling in EN 1999-1-2 [3] is basically equal to that of members in compression, i.e. the slenderness should be determined with material properties at room temperature and the buckling curves for room temperature should be applied. However, no creep factor is taken into account in the calculation model for the buckling resistance for members in bending.

Ad 3. Research on local buckling at elevated temperature (see figure 9) has not yet been carried out. Therefore, no calculation model is implemented in EN 1999-1-2 [3] for local buckling. Calculation models for local buckling of steel structures are also not available in EN 1993-1-2 [2]. Local buckling is however specifically important for aluminium structures, because of the high ratio between strength and stiffness and because the extrusion process opens the possibility to design members of

arbitrary shapes with thin wall thickness. However, due to the decreasing ratio between the 0,2% proof stress and the modulus of elasticity at elevated temperatures, it is expected that the sensitivity for local buckling decreases. This assumption was checked with some preliminary finite element models (figure 9).

Local buckling may 1. dominate the overall strength in case of compression or bending, may 2. interact with global buckling, and may 3. influence the rotational capacity (and thus influences the possibility for redistribution of forces). Therefore, the development of a model for local buckling is a first and essential step for design models for fire exposed aluminium structures.

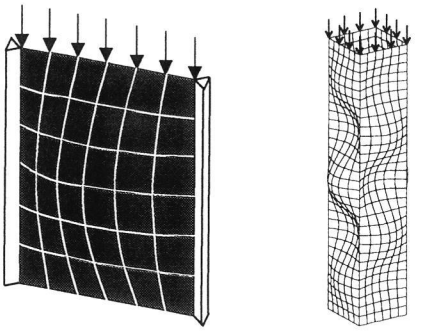

Figure 9: Examples of FEM models of local buckling of a plate (left hand) and of a section (right hand)

4.2.3 Connections

Connections in aluminium structures are welded, bolted or adhesive bonded. Fundamental research on the behaviour of aluminium connections exposed to fire was not found in literature. Simple calculation models for strength and stiffness of connections are not given in EN 1999-1-2. Instead, it is stated that the resistance of connections between members does not have to be checked provided that the thermal resistance of the fire protection of the connection is not less than the minimum value of the thermal resistance of the fire protection of any of the aluminium members joined by that connection.

No information is available on the stiffness of connections and the development of forces in the connections during fire.

4.3 Evaluation of mechanical response models

Only a limited number of fundamental studies was found on structural behaviour of fire exposed aluminium components. Most mechanical response models in EN 1999-1-2 are therefore either based on research on steel structures, or the same response models are applied as for room temperature. A mechanical response model for local buckling is not available and research on local buckling has neither been carried out on aluminium nor on steel structures.

No information was found regarding the influence of unequal thermal expansion of a partially insulated member on (local or global) buckling.

5 Conclusions and further work

The literature survey has led to the following conclusions:

- Physical properties are relatively independent of the alloy;
- Especially the high conductivity (2 to 4 times the conductivity of steel) and low density (one third of that of steel) cause aluminium alloys to heat quickly. Therefore, most aluminium structures need passive fire protection to meet standard fire resistance requirements.
- Thermal expansion of aluminium is approximately two times that of steel. However, the modulus of elasticity is only one third of that of steel. This means that thermal stresses when expansion is restrained are lower than in case of steel structures.
- Mechanical material properties at elevated temperature depend on the alloy and temper. In general, strength and stiffness of aluminium alloys are reduced significantly at moderately elevated temperatures. At a temperature of 350 °C, the strength is already reduced to 30%;
- The strengthening effects of tempering and work hardening is rapidly lost at moderate elevated temperatures of 150-250 °C. Beyond this temperature, there is hardly any difference between the strength of tempered and non-tempered aluminium of the same alloy;
- Except for naturally aged alloys, the modulus of elasticity reduces less fast than the strength at increasing temperature;
- It is not yet clear whether creep should be accounted for in mechanical response models;
- Mechanical response models of aluminium structures exposed to fire, applied in the recently developed standard EN 1999-1-2 [3], are not yet fully validated with tests or numerical research. Mechanical response models for local buckling do not exist.

Future research will concentrate on local buckling of sections exposed to fire. The influence of changes in material characteristics and creep influence on critical buckling load and ultimate resistance will be determined. Additional, it is aimed at determining the influence of unequal expansion on the buckling resistance in case of a partially insulated member.

Acknowledgement

This research was carried out under project number MC1.02147 in the framework of the Strategic Research programme of the Netherlands Institute for Metals Research in the Netherlands (www.nimr.nl).

References

[1] EN 1991-1-2, Eurocode 1: Actions on structures – Part 1-2: General actions – Actions on structures exposed to fire

[2] EN 1993-1-2, Eurocode 3: Design of steel structures – Part 1-2: General Rules – Structural fire design, September 2003

[3] EN 1999-1-2, Eurocode 9: Design of aluminium structures – Part 1-2: General Rules – Structural fire design, September 2003

[4] Norsk Standard NS 3478, Brannteknisk dimensjonering av bygningskonstruksjoner Beregning (Design for structural members for fire resistance), 1st edition, 1979

[5] TALAT, Training in Aluminium Application Technologies. CD version 2.0. European Aluminium Association

[6] SFPE Handbook of Fire Protection Engineering. Society of Fire Protection Engineers and National Fire Protection Association, USA 1988. ISBN 0-07-909388-4

[7] Altenpohl, D., Aluminium viewed from within, , ISBN 3-87017-138-3, Aluminium-Verlag Düsseldorf, 1982

[8] Amdahl, J., Eberg, E. and Langhelle, N.K., Experimental and theoretical investigation of aluminium tubes subjected to temperature loads. Sintef report, 1993

[9] Bergli G. and Moe, O. Mekaniske egenskaper ved kortvarige eleverte temperaturer for aluminiumlegeringen AA 6063 (T4 og T6). Graduating report at the division of Structural Engineering of NTNU Trontheim, 1994

[10] Brandes, A. Smithells Metals Reference Book. Butterworth & Co, ISBN 0-408-71053-5, 1993

[11] Broli, T. and Mollersen, S., Brannbelastede aluminium soyler. Graduating report at the division of Structural Engineering of NTNU Trontheim, 1985

[12] Eberg, E., Amdahl, J. and Langhelle, N.K., Experimental investigation of creep behaviour of aluminium at elevated temperatures, 1996

[13] Eberg, E. Langhelle N. and Amdahl, J. Experimental investigation of creep buckling behaviour of aluminium tubes subjected to temperature loads

[14] Eberwien, Entwicklung eines allgemeinen Verfahrens zur Berechnung von Versagenstemperaturen an Aluminiumkonstructionen des EC 9-1-2, 2003

[15] Franssen, J.M. Taloma, D. Kruppa, J. and Cajot, L.G. Stability of Steel Columns in Case of Fire: Experimental Evaluation, Journal of Structural Engineering, 1998, vol 124-2 pages 158-163

[16] Hepples, W. and Wale, D. High temperature tensile properties of 6082-T651. Alcan technical Assistance Report No. BTAR-93/024

[17] Holman, J.P. Heat Transfer. McGraw-Hill Publishing Company. 1990 ISBN 0-07-909388-4

[18] Kammer, C. Aluminium Taschenbuch 1. Grundlagen und Werkstoffe. Aluminium Verlag Düsseldorf 2002. 16. Auflag. ISBN 3-87017-274-6

[19] Kaspersen, R. and Soras, A. Krypeffekter i brannbelastede aluminiumskonstruksjoner. NTNU Trontheim, 1994

[20] Kaufman, J.G. Properties of aluminium alloys – Tensile, creep and Fatigue data at high and low temperatures, ASM international, 1999

[21] Kleive, M. and Gustavsen, L.K. Mekansike egenskaper ved kortvarige eleverte temperaturer for aluminiumlegering 6082-T6. Graduating report at the division of Structural Engineering of NTNU Trontheim, 1993

[22] Koser, J. Konstruieren mit aluminium, ISBN 3-87017-196-0, Aluminium-Verlag Düsseldorf, 1990

[23] Kraus, H. Creep analysis. ISBN 0-471-06255-3, Engineering Studies, The Hartford Graduate Center, 1980

[24] Krokeide, Brannbelastede konstruksjonskomponenter I aluminium, NTNU Trontheim, 1991

[25] Langhelle, N.K., Experimental validation and calibration of nonlinear finite element models for use in design of aluminium structures exposed to fire, MTA-report 1999:128, 1999

[26] Langhelle, N.K. Eberg, E. Amdahl, J. and Lundberg, S. Buckling tests of aluminium columns at elevated temperatures

[27] Lundberg, S. Design of aluminium alloy structures for fire resistance – influence of creep – Concluding remarks, Background document CEN/TC 250/SC 9/PT 4/N 73, 1995

[28] Mazzolani, F.M. Aluminum Alloy Structures, 2nd Ed. Chapman & Hall, UK 1985. ISBN 0-273-08653-7

[29] Richter, E.and Hanitzsch, E. Der Elastizitatsmodul und andere physikalische Eigenschaften von Aluminiumwerkstoffen, Teil 1

[30] Talamona, D. Franssen, J.M. Schleich, J.B. and Kruppa J. Stability of Steel Columns in Case of Fire: Numerical Modeling, Journal of Structural Engineering, 1997, vol 123-6 pages 713-720

[31] Twilt, L. Global investigation into the resultant emissivity of aluminium alloys, CEN/TC 250/SC 9/PT 4/N 70.

[32] Voorhees, H.R. and Freeman, J.W. Report on the elevated-temperature properties of aluminium and magnesium alloys, American Society of Testing Materials, STP No. 291, 1960

Shear and anchorage behaviour of fire exposed hollow core slabs

Joris Fellinger
TNO Centre for Fire Research, Delft, the Netherlands
Email: joris.fellinger@tno.nl, Phone: +31 15 276 3487

Jan Stark
Delft University of Technology, Fac. of Civil Engineering and Geosciences, Delft, the Netherlands

Joost Walraven
Delft University of Technology, Fac. of Civil Engineering and Geosciences, Delft, the Netherlands

The fire resistance of hollow core slabs is currently assessed considering flexural failure only. However, fire tests showed that shear or anchorage failure can also govern the load bearing behaviour. As the shear and anchorage capacity of these slabs rely on the tensile strength of the concrete, the load bearing capacity with respect to these failure modes decreases dramatically during fire due to the impact of thermal stresses. This paper presents a FE model for the shear and anchorage behaviour of fire exposed hollow core slabs, comprising new constitutive models for concrete and bond of prestressing strands at high temperatures. The constitutive models were calibrated with 60 new small scale tests carried out at elevated temperatures up to 600 °C. The FE model was validated on the basis of 25 full scale fire tests on hollow core slabs loaded in shear. Finally, a parameter study was carried out with the FE model. The results showed that the thermal expansion of concrete, the ductility of concrete in tension and the restraint against thermal expansion by the supports are the main influencing factors. It is recommended to control these factors in design in order to improve the safety level. This paper is an extended summary of the dissertation by the first author [10].

Key words: Fire resistance, shear failure anchorage failure, bond, prestressing strand, FE modelling.

1 Introduction

1.1 HC slabs

Hollow core (HC) slabs are made of pre-cast concrete with pre-tensioned strands. The slabs consist of pre-cast units of typically 1.2 m wide. The cross sectional depth depends on the intended span and ranges between 150-400 mm reaching spans up to 16 m. The number and shape of the hollow cores is adjusted to the depth of the slab. These slabs are very popular in offices and dwellings,

cores is adjusted to the depth of the slab. These slabs are very popular in offices and dwellings, thanks to the large span to depth ratio. This is a result of the reduction of weight, maintaining the effectiveness of the cross section, due to the hollow cores in combination with a relatively high strength of the concrete, typically C45 to C60.

The HC units are manufactured on long benches, typically 100-200 m in length. First, strands are tensioned along the bench. Subsequently, the concrete is cast automatically by a moulding and casting machine that is moving along the bench. After the concrete has reached sufficient strength, the external pre-stressing force is released and elements of desired lengths are sawn out.

Shear reinforcement or other mild reinforcement is never applied as it would obstruct the movement of the machine. Neither are anchors for the prestressing strands, because they would introduce large splitting stresses and their position should be known accurately before casting.

1.2 *Problem statement*

At ambient conditions, HC slabs are designed to be simply supported. Walraven and Mercx [20] determined four different failure modes, i.e. flexure, anchorage, shear tension and shear compression.

When HC slabs are exposed to fire, they have to maintain their load bearing and fire separating function for a minimum time as required by Building Regulations. Current design codes for fire design such as Eurocode 2 [16] take only flexural failure into account, while fire tests carried out in the past demonstrated that the other failure modes or combinations of failure modes can also dominate the behaviour. Because there is a lack of fundamental understanding of the shear and anchorage behaviour, an optimum design for both safety and economics can yet not be achieved.

Flexural failure of HC slabs under fire conditions can be assessed on the basis of the theory of plasticity and on the assumption that thermal strains can be neglected. As the production process does not allow for the inclusion of mild reinforcement, both the shear tension capacity and the anchorage capacity rely on the tensile strength of concrete. For such failure modes Eurocode 2 [16] states in Annex D: *....special consideration should be given where tensile stresses are caused by non-linear temperature distributions (e.g. voided slabs, thick beams, etc). A reduction in shear strength should be taken in accordance with these increased tensile stresses.*

However, a simple cross sectional analysis of the thermal stresses leads to the conclusion that within 20 minutes of fire exposure the thermal stresses equal the tensile strength, i.e. cracking occurs and according to the Eurocode there would be no shear strength left. But in most fire tests, no shear failure occurs at this time. So, there is a need for a better understanding of the impact of thermal stresses on the shear behaviour.

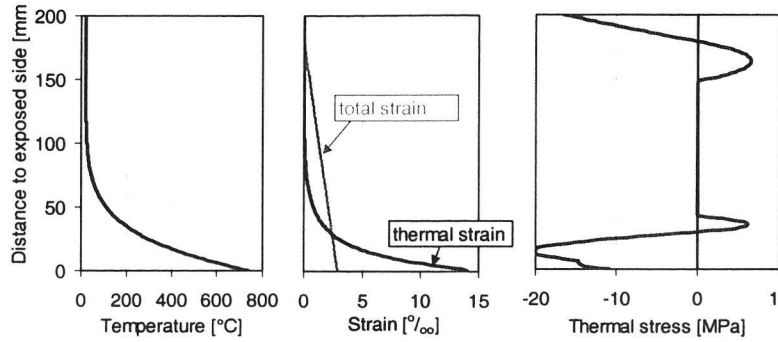

Figure 1 Calculated temperatures, strains and thermal stresses in a 200 mm deep HC slab after 15 minutes of standard fire exposure, calculated on the basis of gravel concrete thermal properties according to Eurocode 2 and assuming prestressing by 8 strands Ø9.3 mm with an initial prestress of 1050 MPa.

1.3 Objective

The objective of the study is to obtain a fundamental understanding of the shear and anchorage behaviour of fire exposed HC slabs and to develop numerical models to predict this behaviour. With the models, practical recommendations for design can be developed.

More specifically, it was postulated that for the assessment of shear and anchorage behaviour, the following phenomena should be taken into account:

- Incompatible thermal strains leading to thermal stresses
- Decomposition of strains in reversible and irreversible parts
- Support conditions that restrain the thermal expansion of the fire exposed slab
- Influence of the applied load on the deterioration of the load bearing capacity during fire
- Relation between the fire safety and the time to failure

The research is limited to HC slabs as defined in the European product standard [15], exposed to standard fire conditions [14] and simply supported on rigid supports like concrete walls. In addition, some attention is paid to the effects of restraint to thermal expansion by the supports.

1.4 Approach

Firstly, the load bearing behaviour at ambient conditions was evaluated. Theoretical formulations of the load bearing capacity with respect to the four failure modes were composed from different sources of literature and then compared with 257 tests at ambient conditions.
Secondly, the fire behaviour of HC slabs was assessed on the basis of 80 tests found in literature. It is noted that these tests generally served the commercial goal to demonstrate that a certain fire resistance could be achieved under realistic (and sometimes complex) boundary conditions rather

than the scientific goal to observe a failure mechanism under academic (and preferably simple) boundary conditions. With these tests, the failure modes under fire conditions were defined and it was tried to find relationships between various parameters and the observed behaviour.
From the inventory of existing fire tests, it was concluded that there was a need for further testing. Therefore, 25 full scale fire tests on HC slabs were carried out at the TNO Centre for Fire Research. The fire tests were carried out with the same test set-up with respect to the support conditions and the loading conditions as in the standard shear test as prescribed in the product standard [15].
The tests were also used to develop and validate new finite element (FE) models. Two two-dimensional models were developed. The first model is a model of the cross section. This was used to calculate the temperature distributions, the effect of incompatible thermal strains on the development of splitting cracks and the resulting confining action on the strand by the concrete around the strand. The second model is a model of the entire slab, including the support conditions and the loading. It contains a new plastic constitutive bond model for the interface element between the strands and the concrete. In this model, the bond yield strength depends on the confining action of the concrete cover around the strand as determined with the cross sectional model. Both FE models use a newly composed constitutive model for concrete, based on various literature sources [18],[17],[2],[1],[4], which allows for a dependency of the stress-strain relationship on both temperature and loading history during heating. It also includes the effect of transient creep.
Obviously, the new constitutive models needed calibration. Therefore, 60 small scale tests at elevated temperatures were carried out, on both the concrete properties and the bond properties of the pre-stressing strands. The main parameters were calibrated in a narrow range. With the calibrated values, the FE models were successfully validated against tests on the shear and anchorage behaviour of HC slabs at both ambient conditions and fire conditions. After the validation, a limited parameter study was carried out which is presented in paragraph 4.4.

2 Load bearing behaviour at ambient conditions

At ambient conditions, HC slabs are designed to be simply supported. Walraven and Mercx [20] determined four different failure modes, i.e. flexure, anchorage, shear tension and shear compression, see Figure 2.

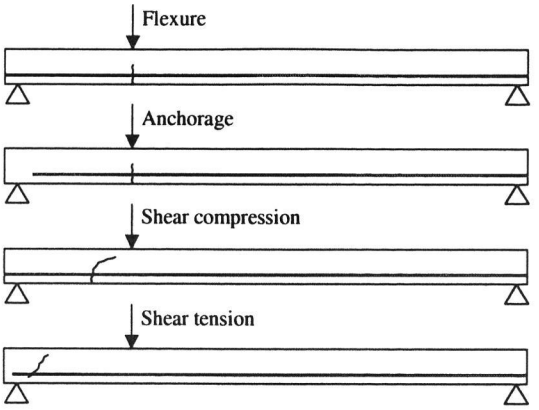

Figure 2 Failure modes for HC slabs at ambient conditions.

Flexural failure is the most common failure type and it is the preferred failure type as it is ductile and predictable. It is the result of a bending moment which first leads to the development of one or more flexural cracks, starting at the bottom side of the slab. The slab is designed in such a way that the strands can take over the tensile force that is released in the crack. A further increase of the bending moment will lead to yielding of the strands in one of the flexural cracks which is accompanied with large opening of this crack and large deflection. Ultimately, the slab fails by rupture of the strands. The slab is designed in such a way that rupture of the strands prevails over crushing of the concrete in the compression zone.

Anchorage failure can also occur, particularly when the load causes a large bending moment close to the end of the HC slab, near the support. Within this distance from the end of the slab, the so-called development length, the full tensile force required to lead to yielding and rupture of the strands can not be developed due to a lack of bond strength between the strands and the concrete over the embedment length. As a result, the slab collapses as the strands are pulled out. If the flexural crack occurs within a certain distance from the end of the slab, the so-called critical length, the strands will be pulled out immediately at the initiation of a flexural crack. If the flexural crack occurs outside the critical length but within the development length, the strands are not directly pulled out after the formation of the flexural crack, but after some further increase of the bending moment. Rupture of the strands will not occur. After a flexural crack has formed, an additional tensile force arises in the strand due to a change in the load bearing mechanism with respect to the shear force. Immediate pull-out at the onset of cracking has a brittle character whereas pull-out after a further increase of the load shows more ductility. The actual behaviour depends on the loading scheme. If a point load is applied near the support, the brittle mode will dominate, while the ductile mode will dominate for point loads further away from the support.

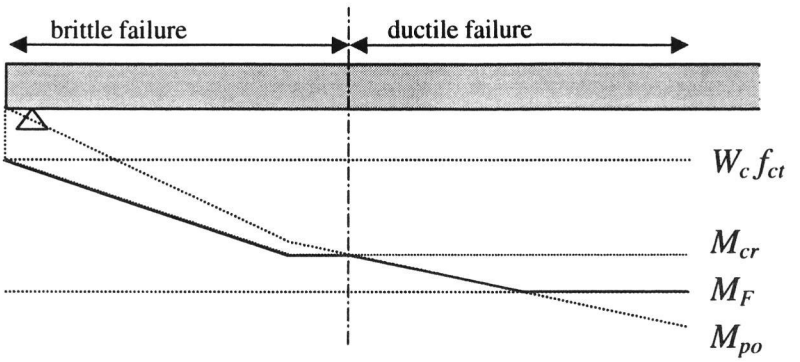

Figure 3 Development of the load bearing capacity against bending moment for flexural failure M_F and anchorage failure by pull-out of the strands M_{po} or the initiation of the crack M_{cr}. The continuous line indicates the ultimate capacity, W_c is the section modulus of the slab and f_{ct} the tensile strength of concrete.

Shear failure can occur in a cracked cross section, which is called shear compression failure, or near the support in an un-cracked cross section, the so-called shear tension failure. Shear compression failure is limited by the capacity to transfer shear by the concrete in the compression zone. This capacity is enhanced by the pre-stress, by the dowel action of the strands and by the rough crack surface, which is kept relatively closed by the strands. Shear tension failure occurs near the support, where flexural cracks can barely develop as the bending moment is almost zero. The shear stresses lead to a principal tensile stress in the webs which reaches a maximum just outside the zone where the support reaction affects the stress state. When these tensile stresses lead to cracking, no redistribution of stresses is possible as the embedment length of the strands with respect to these cracks is far too short and immediately brittle failure occurs.

It was proven that these four failure modes can be described sufficiently accurate by analytical formulations as given in Eurocode 2 [16] and the Model Code [12]. These formulations were validated by an extended comparison with the load bearing capacity obtained from 257 tests on HC slabs at ambient conditions, carried out in various laboratories over the world. Therefore the analytical formulations could be used to derive the degree of utilisation with respect to each failure mode for HC slabs in fire tests found in literature.

3 Fire conditions

3.1 Theoretical background

Under fire conditions, the load bearing capacity decreases due to the degradation of the material's mechanical properties at elevated temperatures and due to damage caused by thermal stresses.

Thermal stresses are caused by a thermal strain field that is incompatible. Strain fields must satisfy compatibility requirements resulting from the fact that six strain components (ε_{xx}, ε_{yy}, ε_{zz}, ε_{xy}, ε_{yz}, ε_{zx}) are obtained from three displacements (u_x, u_y, u_z). When a two-dimensional plane is considered, the compatibility requirement is given as:

$$\frac{d^2\varepsilon_{xx}}{du_z^{\,2}} + \frac{d^2\varepsilon_{zz}}{du_x^{\,2}} - 2 \cdot \frac{d^2\varepsilon_{xz}}{du_x \cdot du_z} = 0 \qquad \text{Eq. 1}$$

Thus, strains in the axial direction (ε_{xx}) that vary at a higher than linear degree along the depth of the slab (z- direction) must be accompanied by vertical or shear strains in order to satisfy the compatibility requirement.

For structural members with a high span to depth ratio, the vertical strains will be small and shear strains will develop. If the shear stiffness is high, the compatibility requirement results in the fulfilment of Bernouilli's hypotheses that plane cross sections remain plane. This justifies the cross sectional calculation of the thermal stresses shown in Figure 1. In fire exposed concrete slabs, the thermal strains in the axial direction do vary non-linearly over the depth of the slab. As a result, mechanical strains have to develop to counteract these incompatible thermal strains, in order to result in a linear distribution over the depth of the slab of the total strain in the axial direction. This distribution can be calculated on the basis of the requirement that the resulting displacements and rotations must satisfy the kinematic boundary conditions at the supports. Moreover, the mechanical strains lead to thermal stresses that have to be in equilibrium with the external loads. At the end of a simply supported structural member, no axial stresses can occur. Locally, cross sections are warped and shear strains develop to satisfy the compatibility requirement. These shear strains lead to shear stresses that lead to a gradual increase in the axial direction of the thermal stresses. So, the shear stiffness determines the length over which the axial thermal stresses are built up.

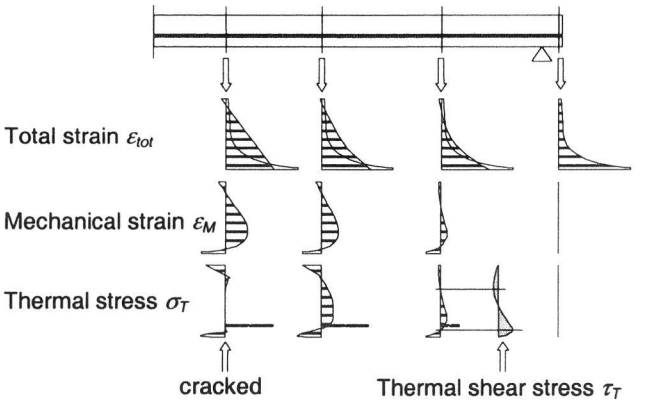

Figure 4 Development of thermal stresses near the end of a simply supported slab.

3.2 *Fire tests obtained from literature*

In literature, 80 fire tests on HC slabs have been found. It appeared that some kind of shear or anchorage failure dominated the load bearing behaviour in about 25 % of the tests, see Figure 5. These failures were in most cases premature, i.e. occurred before the required fire resistance time was reached. The distinction between shear tension, shear compression and anchorage failure could not be made, partly because these tests were poorly reported as all these tests were meant to demonstrate a satisfactory fire resistance rather than to obtain a scientific understanding of the failure behaviour.

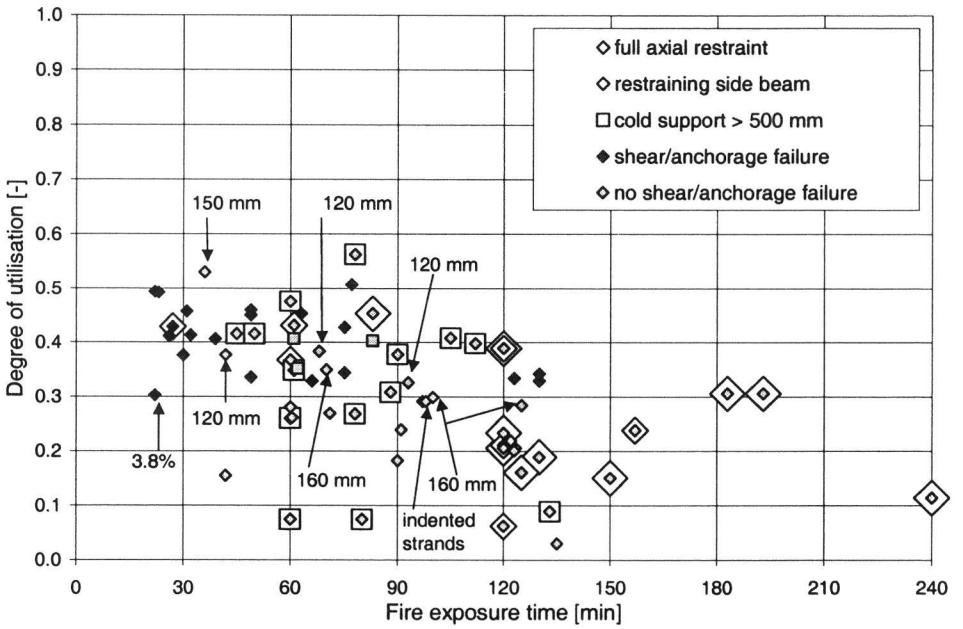

Figure 5 Fire resistance time versus the degree of utilisation with respect to anchorage loading. i.e. the ratio between the anchorage loading during fire and the anchorage capacity at room temperature with respect to the cross section with the highest anchorage loading. The axial restraint was either full or partial, realised by side beams. The degree of restraint is indicated with the size of the marker around the marker indicating the type of failure. The three specimens that did not fail while the anchorage loading was more than 30% and no isolation or restraint was applied are indicated with a grey box rather than a grey diamond. Other specimens that did not fail were either less deep than 200 mm or provided with axial restraint or an isolated support over at least 500 mm. One early failure at 22 minutes might be attributed to the relatively high moisture content of 3.8 %.

A study into the main influence parameters showed first and for all that supports that restrain the thermal expansion in the spanning direction improved the shear and anchorage behaviour significantly. This is just a confirmation of existing knowledge. Secondly, opposite to what might be expect, it was shown that an increase of the axis distance, i.e. the distance from the centre of the

strands to the exposed side, had rather a detrimental than a beneficial influence on the shear and anchorage behaviour. Apparently, the temperature of the strand is not an important indicator. Only if the end zone of the slab was isolated over 500 mm or more, shear and anchorage failure was avoided. Thirdly, shear and anchorage failure is less critical in thinner slabs as such a failure mode appeared only three times in slabs with a depth smaller than 200 mm. Those failures could be attributed to other factors, such as a very high shear loading. Generally, the shear and anchorage failure is more likely if the shear loading is higher. Except for three tests, all tests with a depth of 200 mm or more, without considerable axial restraint and without isolation of the end zone over at least 500 mm, failed if the degree of loading was more than 30 % relative to the actual anchorage capacity at ambient conditions. In these three tests the thermal expansion in the transverse direction was restrained at the support using either a steel belt or a heavily supporting beam that was properly connected to the slab. However, the transverse restraint was not always so effective. Finally, the age of the slab did not seem to play an important role, provided that the slab had an age of more than approximately one month and the moisture content was sufficiently low to avoid critical pore pressures.

3.3 *New fire tests*

As the existing fire test data did not provide an adequate basis for the understanding of the failure behaviour, 25 new fire tests were carried out. Most of these new tests (21) were conducted on double rib specimens sawn out of HC slab units, with the objective to observe the expected cracking in all webs due to thermal stresses and to measure the slip at the end of the strands during the fire exposure. The webs were visible thanks to the slender isolated steel plate that was used to close off the furnace, see Figure 6. The sawn end surface was accessible with a simple slip calliper.

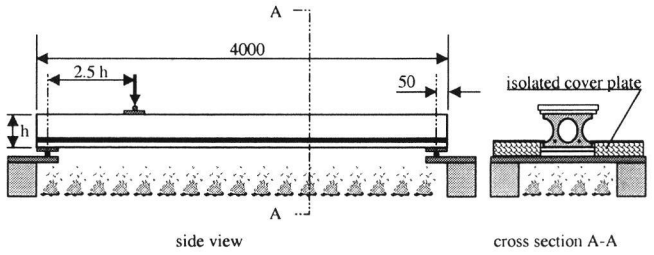

Figure 6 Test set-up for the new fire tests, loaded according to the standard shear test for HC slabs.

Some influencing parameters were evaluated: First the geometry was varied, using 4 different types of HC slabs, 200, 260, 265, and 400 mm deep, see Table 1. For the 200 mm deep slab, the axis distance of the strands and the production process were varied. For this type, coincidentally, the same geometry was produced in one plant using an extrusion process and in another plant using a slip form process. For the 260 mm deep slab, the load level was systematically varied with a shear

force between 11 and 23 % of the actual shear capacity at room temperature conditions. This capacity was for all fire test specimens obtained as the average capacity of three standard shear tests at room temperature. Finally, the support details were changed relative to the simply supported basic case of Figure 6. Three tests were carried out in which the thermal expansion in the spanning direction was restrained by a hydraulic actuator that simulated a spring with a stiffness of 50 kN/mm. The point of application was positioned at ¼·*h* from the exposed side for the specimens with a depth of *h* = 265 and 400 mm and ½·*h* for the 200 mm deep specimen. Three more tests on the 260 mm deep specimens were carried out with a reinforced end beam cast in one batch with a concrete filling of the central core over a length of 800 mm with a reinforcing bar of Ø 10 mm, in order to evaluate practical design recommendations [3].

Table 1 Overview of the fire tests on HC elements, see Figure 8 for cross sectional shapes of the slabs.

depth – # HC [mm]	Production process	axis dist. [mm]	type	Support detail [1]			load level	failure mode [2]			failure time	Remarks
				s	r	e	[%]	S	A	F	[min]	
200 - 7	slip form	40	ribs	s			21		A		96	*no slip measured*
	extrusion	40	ribs	s			16			F	125	V_u = 30 %
		44	ribs	s			18		A		125	V_u = 34 %
			ribs		r		18			F	159	V_u = 37 %
			unit	s			19			F	117	
260 - 5	slip form	40	ribs	s			23		A		48	
			ribs				17		A		45	*fluctuating load*
			ribs				11		A		123	V_u = 16 %
		[3]	ribs	s			23	S	A		55	
			ribs				20	S	A		56	*restarted after 8 min*
			ribs				17	S	A		114	
			ribs				14	S	A		123	*loading failed*
			ribs			e	23	S	A		49	
			ribs				20	S	A		50	
			ribs				17	S	A		99	
			unit	s			23	S	A		39,40,42	
265 - 5	extrusion	40	rib	s			23	S			35	
			rib		r		23	S			25	
			unit	s			23	S			33	
400 - 4	extrusion	[4]	rib	s			23	S			60	
			rib	s			30	S			24	*low quality core filling*
			unit	s			23	S			33	

[1] *(s) = simple supports, (r) = restraint in spanning direction, (e) = reinforced end beam*

[2] *(S) = shear failure, (A) = anchorage failure, (F) = flexural failure*

[3] *Strand position: 4x12.5–40 + 2x12.5-76 4, for the double ribs: 1x12.5-40 + 1x12.5-76*

[4] *Strand position: 6x9.3–40 + 2x9.3-73 + 5x12.5-40 + 3x12.5-88, for the double ribs: 4x9.3-40 + 1x12.5-40 + 1x12.5-88*

The other tests were carried out on complete single HC units. Three of these tests were conducted using identical units produced in one batch on the same prestressing bench. The fire tests appeared to be very reproducible with a consistent failure behaviour and consistent time to failure, i.e. failure times of 39, 40 and 42 minutes.

In all specimens, even in the restrained ones, thermal cracks developed in the webs on a regular distance over the entire span already within 14-16 minutes, see Figure 7. These cracks were first suggested by Prof. dr. ir. M. Fontana of ETH Zurich in an international technical meeting of ECCS-IPHA and now demonstrated by the author. Near the loading point, the cracks were slightly inclined, indicating some effect of the loading on the crack propagation. Moreover, splitting cracks developed around most strands, see Figure 8, which gives an overview of the observed crack patterns in all investigated types of HC slabs. In the 265 mm deep slabs, horizontal cracks developed through the smallest web section over almost the entire length. Also the slip of the strands increased rapidly directly from the start of the fire both at the loaded and unloaded end of the specimens, see §4.3, indicating that the slip is driven by the thermal expansion.

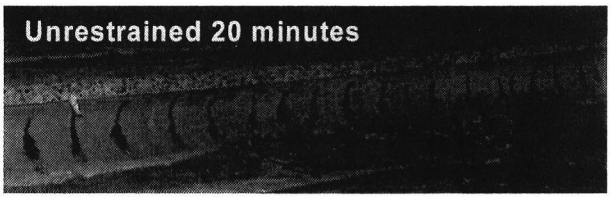

Figure 7 Thermal cracks in the web of a 200 mm deep slab after 20 minutes of fire exposure.

In case flexural failure dominated, the vertical crack in the web below the loading point grew into a flexural crack and opened until rupture of the strand occurred. In case anchorage failure dominated, the strand was pulled out. In case shear failure occurred, the horizontal cracks grew together with the vertical cracks and one large combined crack from the loading point to the nearest support opened up to failure. Near collapse, also significant slip of the strands developed. In case of combined shear and anchorage failure, horizontal splitting cracks through the web and vertical cracks grew together and opened. At the same time, the vertical crack below the loading point grew into a flexural crack. After a significant increase in slip of the strands, the slabs collapsed.

The impact of the shear load on the fire behaviour is a paradox. On the one hand, the crack development and slip development is hardly affected by it. On the other hand, the shear load has a large influence on the time to failure. Apparently, the damage, i.e. cracking and slip, caused by the incompatible thermal expansion caused a large and rapid decrease of the load bearing capacity in the first 30 minutes. Hereafter the further decrease is small. A too high shear load leads to early

failure whereas failure is postponed to 90 minutes and beyond when the shear load is sufficiently low.

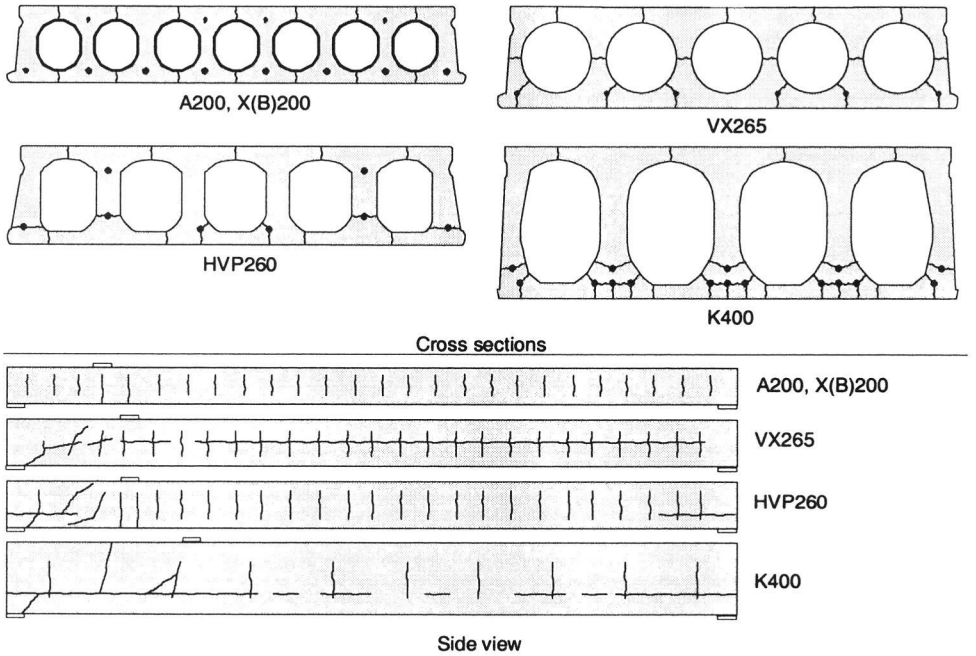

Figure 8 Sketch of the crack patterns for all slab geometries. The number in each type indication of the slabs indicates the depth of the slab.

Restraining the thermal expansion in the spanning direction did not prevent the development of vertical cracks although the length of the cracks was shorter. The use of the reinforced end beam together with the reinforced core filling did not improve the fire performance. The results were very similar to the tests without this measure. This was attributed to the lack of bond between the core filling and the slabs that was observed after the test. Consequently, the tensile thermal stresses in the web could not spread out over the core filling. Although the lack of bond might be attributed to the preparation of the test-specimen only, it is uncertain to what extent the bond can be guaranteed in practical applications.

4 Numerical modelling

4.1 Formulation

It was concluded from the test results that the splitting cracks, the vertical cracks and the slip development had to be included in the model for a realistic prediction of the actual behaviour. As splitting cracks result from circumferential tensile stresses around the strands in the cross section

and vertical cracks result from tensile stresses in the spanning direction, a 3D model was required. However, in combination with the mesh refinement required to model the crack propagation near the crack tips, such a 3D model appeared to be beyond current computer capabilities. Therefore two separate plane stress models were developed in the FE package DIANA, one cross sectional model and a model of the entire slab including a bond-slip interface between the concrete and the strands, see Figure 9.

The cross sectional model was used for the determination of the temperature distribution during the fire assuming heating from the bottom side and taking into account radiative and convective heat transfer in the hollow cores. The conductivity and heat capacity of concrete and steel were obtained from the draft version of Eurocode 2 [9]as extensive research in the past showed that these values were satisfactory [5]. For the model of the entire slab, the temperatures were averaged over the width of the slab.

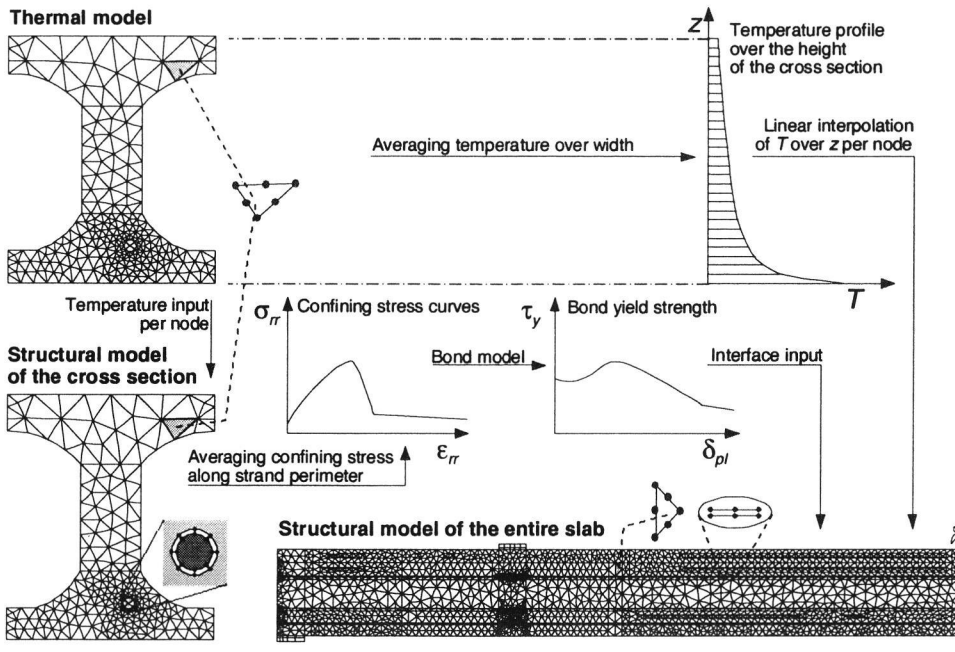

Figure 9 Overview of the modelling approach.

Both structural models contained a new constitutive model for concrete, decomposing the strain increments into seven strain components, i.e. the thermal strain ε_T, shrinkage strain ε_s, elastic strain ε_{el}, plastic strain ε_{pl}, crack strain ε_{cr}, transient creep strain ε_{tr} and normal creep strain ε_{crp}:

$$\Delta\varepsilon = \Delta\varepsilon_T + \Delta\varepsilon_s + \Delta\varepsilon_{el} + \Delta\varepsilon_{pl} + \Delta\varepsilon_{cr} + \Delta\varepsilon_{tr} + \Delta\varepsilon_{crp} \qquad \text{eq. 2}$$

The thermal strain was taken from Eurocode 2 [16]. The shrinkage strain and normal creep strain were introduced to be able to predict the transfer of the prestress at the time of the release of the prestress in the production plant as well as possible. The formulations were approximated on the basis of the *fib* Bulletins [11]. The transient creep formulation was obtained from Anderberg and Thelandersson [2] which is standard available in the software used [7]. The elastic, plastic and crack strain were calculated using the Rankine – Drucker Prager yield model [7]. The softening branches in compression and tension were both based on fracture energy, allowing for localisation of deformations. The stress-strain relations in compression and tension depended on temperature and on the stress level during heating for compression. For the compression regime, these relations were based on an approximation of the results obtained from literature[18], [1], [17]. For the tensile regime they were based on the calibration tests described in §4.2.

The model of the entire slab contained a newly developed constitutive model for the bond interface between the strands and the concrete embedment. It is an extension of the model for bond at room temperature developed by Den Uijl [19] with an elastic-plastic formulation and the effects of elevated temperature taken into account. The model decomposes the slip of the strand δ into an elastic part δ_{el} and a plastic part δ_{pl}, see Figure 10. The model assumes that the plastic part of the slip and a change in the steel strain ε_p of the strand lead to a fictitious radial expansion of the strand ε_{rr}. For various discrete time intervals (t_1, t_2,...) after casting of the slab, during curing and during fire exposure, the confining action of the concrete cover around the strand as a response to a fictitious radial expansion of the strand was calculated with the cross sectional model in terms of a confining stress σ_{rr}. The calculation included the effect of the non-linear temperature and thermal strain distribution and the development of splitting cracks. Through an adhesion-friction analogy, the bond yield strength τ_{pl} was related to the confining stress as calculated with the cross sectional model after averaging over the perimeter of the strand.

Due to the development of splitting cracks, the confining action depends on the history of radial expansion by releasing the prestress, loading and thermal effects. Cross sections near the end of the slab experience a completely different history than cross sections near mid span. This is because the release of the prestress only results in a slip and change of the steel strain in cross sections near the end of the slab. To overcome this difference, each model of the entire slab was fed with confining stress curves that were calculated at 0, 5, 15, 30, 60 and 120 minutes of fire exposure for both a cross section without any initial radial expansion during the release of the prestress and for the cross section at the end of the slab with the maximum initial radial expansion during the release of the prestress. For cross sections with an intermediate initial radial expansion, the yield strength was obtained through linear interpolation.

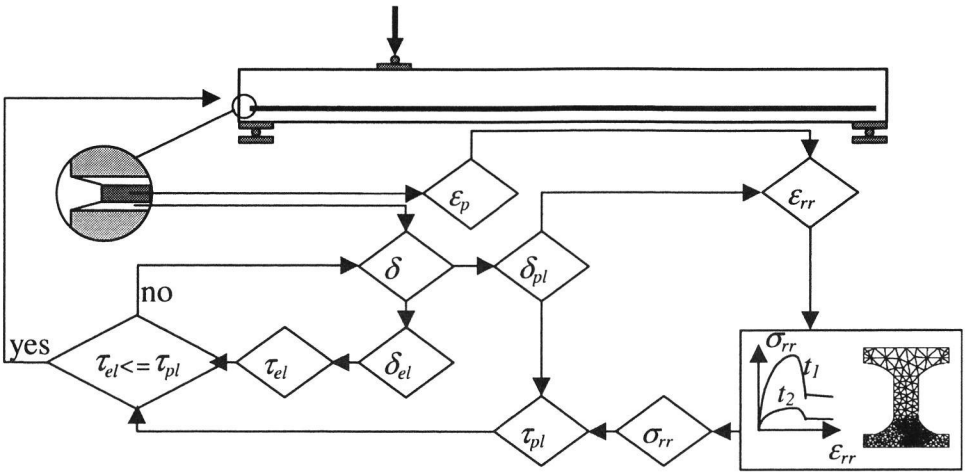

Figure 10 Overview of the constitutive bond model.

4.2 *Calibration*

The new constitutive models for concrete and the bond interface required calibration. For that purpose, a new test set up was developed, see Figure 11. The tensile strength and the fracture energy after cracking were determined for concrete at elevated temperatures of 20, 80, 150, 400 and 600 °C, using Brazilian splitting tests and pull-through tests respectively. The bond model parameters were determined with pull-out tests on strands embedded in small scale concrete cylinders at the same temperatures. In order to separate the contribution to the radial expansion of the strand by the slip and the change of the steel strain, pull-out tests were carried out with free and restrained passive end of the strand, see Figure 12. Each test was executed three times, resulting in a total of 60 tests.

First, the splitting force was measured in the Brazilian splitting tensile test. The tensile strength of concrete was deduced not only using a standard relation [13] between the splitting force and the tensile strength but also through inverse modelling using the FE model of the splitting test, in order to determine the effect of the non-linear stress-strain behaviour on the predicted splitting force. The non-linear stress-strain curve was obtained from Breunese [4].

Using again an inverse modelling technique, the fracture energy was calibrated at elevated temperatures. The confining stress as a function of the radial expansion was measured in the pull-through test. In this test, a conical bar is pulled through a slim concrete cylinder in which a conical central hole is cast. This results in a radial loading on the cylinder, leading to a curve of the pulling force versus the displacement similar to the confining stress curve as indicated in Figure 9. The pulling force was related to the confining stress through a friction coefficient which was fixed by

matching the peak values of the simulated confining stress curves to the peak value in the measured pulling force. With the confining stress curve and the tensile strength obtained in the splitting tests, the fracture energy of the concrete could be determined.

Finally, the friction coefficient of the embedded strands was determined on the basis of the pull-out tests using both the obtained tensile strength and the fracture energy. The other bond parameters could also be calibrated using the pull-out tests, but with less accuracy.

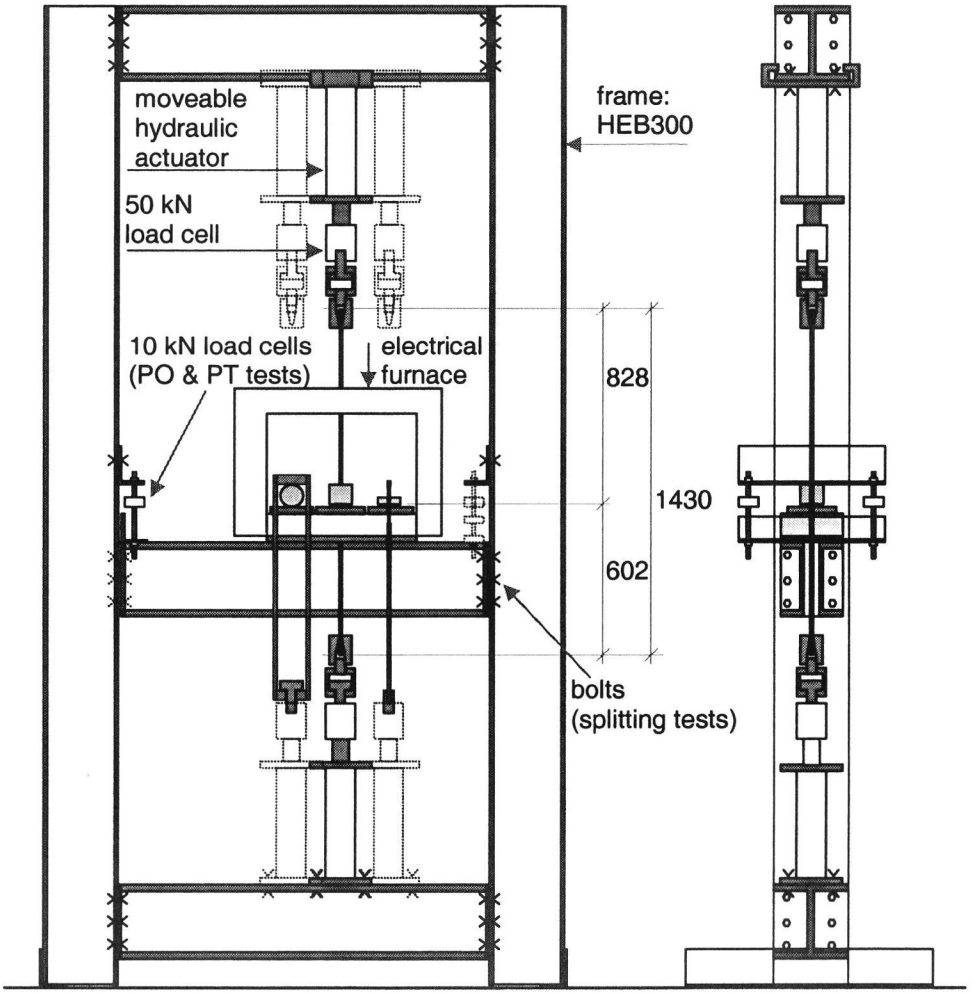

Figure 11 Newly developed test set up for the conduction of the calibration tests at elevated temperatures: splitting tensile tests (left specimen), pull-out (PO) tests (middle specimen) and pull-through (PT) tests (right specimen). In reality, opposite to what the figure suggests, only three identical specimen were installed in the furnace at the same time., since each type of test was carried out three times.

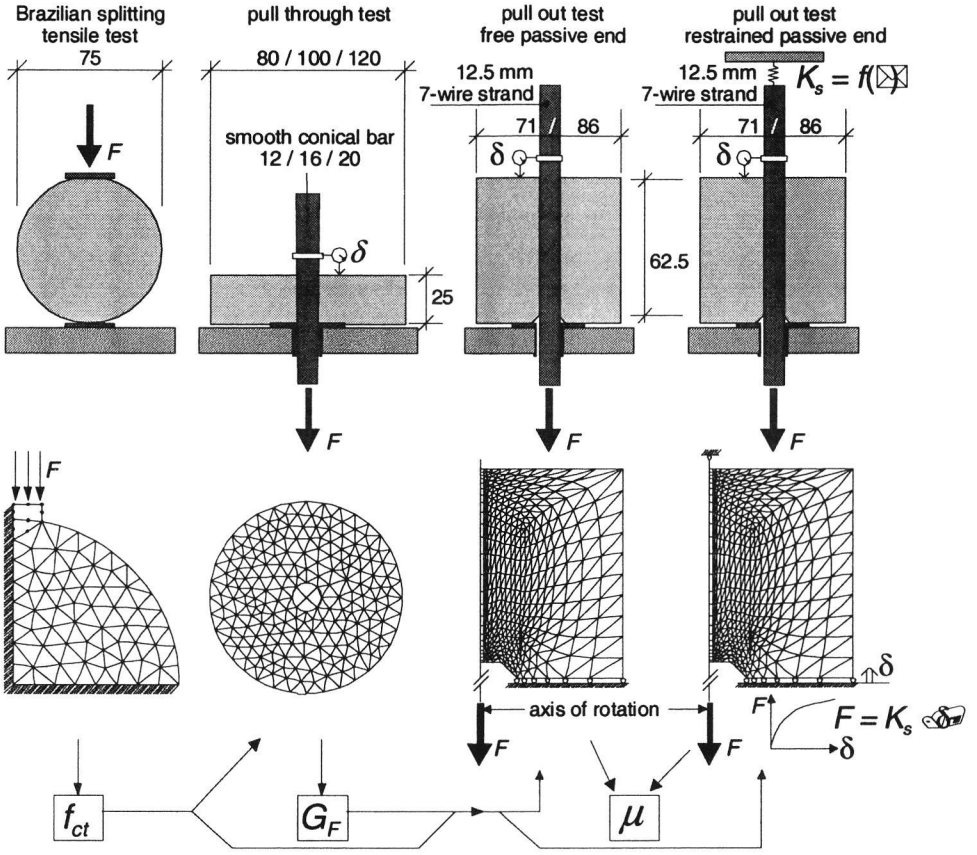

Figure 12 Overview of the types of specimen used in the calibration tests.

4.3 *Validation*

The FE models were validated against the fire tests described in §3.3 using the calibrated material's properties. First, anchorage failure was simulated with the model of the entire slab for a 260 mm deep slab at room temperature, see Figure 13. A flexural crack is initiated at a loading of 109 kN at a distance of 690 mm from the slab end. Then, the load falls back and slip starts. At a load of 125 kN the maximum shear load is reached and the strand is pulled out. It is noted that the yield strength of the prestressing steel was assumed to be 2000 MPa, so no rupture of the strand occurred. Anchorage failure was properly calculated. In the tests, the slab failed at a load of 99 kN. The discrepancy between the measured and calculated shear load is attributed to the variations in the bond model parameters.

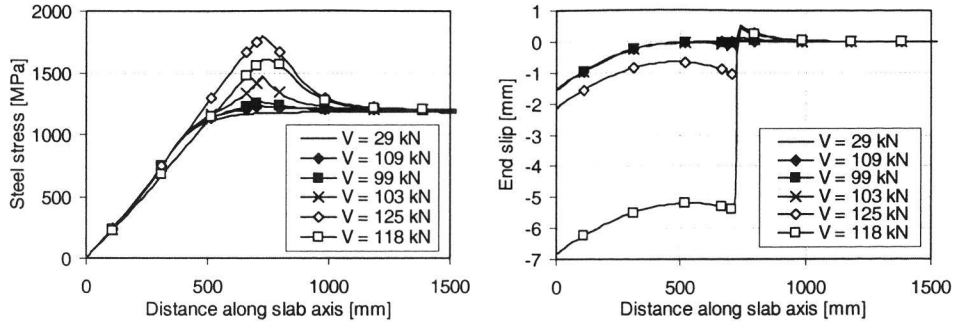

Figure 13 Development of steel stress (left) and slip (right) along the strand at various stages of shear loading.

Both the splitting cracks and the vertical cracks could well be simulated by the model, see Figure 14. The horizontal cracks in the 265 mm deep slab at the smallest section of the web were properly simulated by the cross sectional model. The bottom flange tends to rotate due to the thermal gradient while the upper flange remains straight, resulting in a bending moment around the spanning direction, leading to tensile stresses in the web and finally cracking. If the upper flange would be thinner, the upper flange would crack rather than the web, see Figure 14.

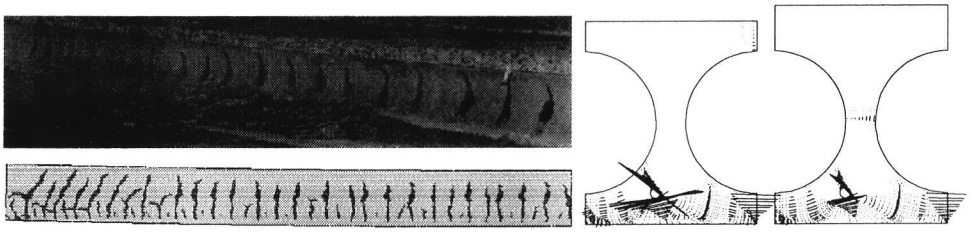

Figure 14 Comparison between experimental and simulated crack pattern in a 200 mm deep slab after 20 minutes (left) and horizontal cracking in the smallest section of the web of a 265 mm deep slab, depending on the thickness of the upper flange. Besides, large splitting cracks were calculated around the strand.

Also the simulated slip development of the strands is in acceptable agreement with the experimental results, see Figure 15. The figure shows that the slip development in the early stage of the fire is almost independent of the shear load, whereas the time to failure strongly depends on the shear load. The model follows the slip development rather well, although the time to failure is not calculated correctly. The difference in the time to failure is attributed to the sensitivity of the failure time to various influencing parameters, see next paragraph.

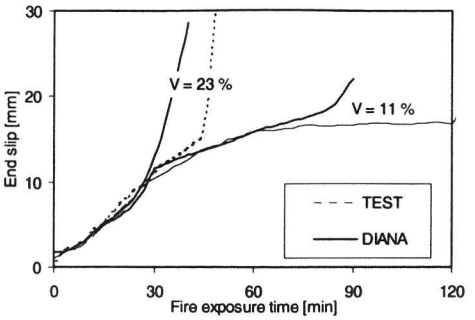

Figure 15 Comparison of the slip between the simulations with the FE model and two fire tests on double rib specimens of 260 mm depth, one test with 11 % and one test with 23 % shear load, relative to the actual capacity at room temperature.

4.4 *Evaluation*

With the validated models, a sensitivity study was carried out. The tensile strength, the fracture energy in tension and compression and the thermal expansion of the concrete were varied. It was demonstrated that the behaviour was almost identical for a mean tensile strength of 5 and 6 MPa. Also the fracture energy of the concrete in compression hardly affected the behaviour in terms of slip and crack development or time to failure.

However, the fracture energy of the concrete in tension and the thermal expansion have a strong influence on the fire behaviour, see fig. Figure 16. The type of aggregate determines largely the fracture energy [6] and the thermal expansion, as for instance is considered in the Eurocode [16]. If a less expanding aggregate is applied, like a calcareous concrete, the slip development and crack development lags behind concretes containing more expanding aggregates like siliceous aggregate or a mix of siliceous and calcareous aggregates which was used in Figure 16.

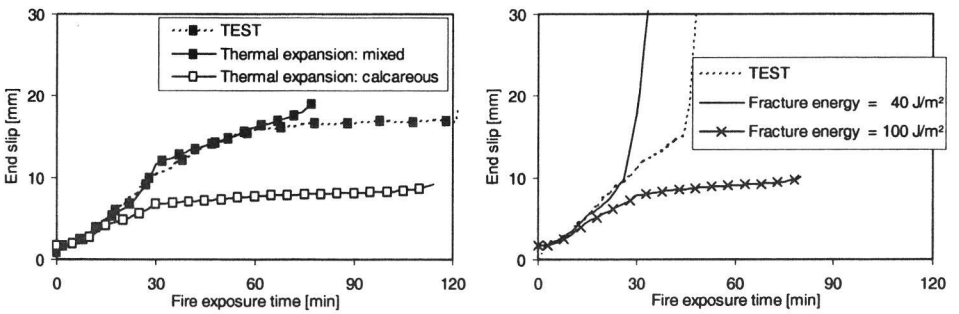

Figure 16 Effect on the slip development and the time to failure of the thermal expansion of concrete (left) and the fracture energy of concrete in tension (right) for a 260 mm deep double rib specimen.

Finally, the effect of the loading history on the load bearing capacity will be discussed Calculations in which the load was kept constant until failure were compared with calculations in which no load was applied during heating and the load was increased up to failure at discrete time intervals, see Figure 17. It shows that the decrease of the load bearing capacity is very large in the early stage of the fire. But subsequently, the further decrease is small. It also shows that the decrease is almost irrespective to the applied load during fire.

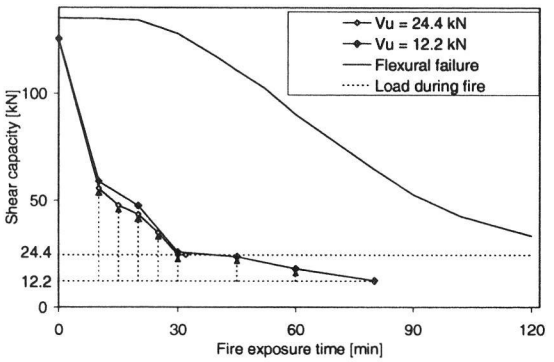

Figure 17 Decrease of the load bearing capacity during fire exposure as calculated with the FE models for two load levels during fire.

With these calculations it was found that either the brittle or the ductile anchorage failure mode could govern the behaviour. At room temperature, the pull-out resistance of the strands was sufficient to take over the tensile stresses that are released at the initiation of a flexural crack., i.e. when the cracking moment resistance was reached. However, during the early stage of fire, the pull out resistance decreases more due to the splitting cracks than the cracking moment resistance due to the vertical cracks in the webs. As a result, the cracking moment resistance was limited by the anchorage capacity from 10 up to 30 to 60 minutes, leading to brittle failure. Hereafter the pull-out resistance is larger than the cracking moment resistance and anchorage failure is ductile again.

The difference in load bearing capacity after 30 minutes and 120 minutes is small when compared to the decrease of the flexural capacity., which is shown as well in figure 16. The decrease of the capacity to bear shear forces in the standard shear test limited by the flexural capacity is given. As a consequence, a HC slab designed for 120 minutes fire resistance has almost the same shear capacity as a HC slab designed for 60 minutes, whereas the flexural resistance will significantly differ. So, a fire resistance requirement of 120 minutes instead of 60 minutes hardly increases the safety level.

5 Conclusions and Recommendation

Current design codes like the new Eurocode 2 do not adequately take into account the shear and anchorage failure of fire exposed HC slabs. On the basis of 25 new fire tests and an in-depth investigation into existing fire test data on HC slabs, is was demonstrated that the shear and anchorage behaviour can lead to premature failure. Therefore, these failure modes should be considered in the fire design of HC slabs.

Incompatible thermal expansion leads to structural damage like cracking and slip of strands within 15 minutes of standard fire exposure. As a result, the shear and anchorage capacity strongly decrease in the early stage of fire, eventually leading to collapse, depending on the load level. As the decrease of the load bearing capacity is small after an early drop in the first 30 minutes of fire exposure, it is recommended to avoid shear and anchorage failure completely rather than to try to meet the required fire resistance time more precisely. In doing so, a desirable ductile failure will occur due to flexure. The shear and anchorage failure can be avoided by limiting the allowable shear load on the HC slab during fire. This maximum load can be determined for each HC slab on the market using the FE models presented in this paper.

The important influencing parameter is the type of aggregate. The type of aggregate determines the fracture energy of concrete and the thermal expansion of concrete. By monitoring and controlling these parameters in the design and production process, the allowable shear load can be maximised.

Furthermore, support conditions that restrain the thermal expansion overshadow other aspects. The amount of restraint that is needed to increase the allowable shear load to a desired level can also be determined with the FE models. However, the available restraint in a practical building is unknown and can yet not be guaranteed as it is very sensitive to the way the HC units are connected on site to the adjacent parts of the structure. Therefore it is recommended not to rely on such a beneficial effect while it can not be assured in the design.

Finally, it is recommended to use the FE models to calculate for each type of HC slab on the market the maximum allowable shear load for which shear and anchorage failure is avoided. This results in a modification of the well known load-span interaction diagrams for these slabs. Currently, discussions between the first author and the national authorities and HC industry are going on to implement such an approach into Dutch regulations. In doing so, no complex fire analyses need to be carried out in the design stage anymore, but a simple check of the load-span interaction diagram suffices to ensure an adequate safety level.

Acknowledgement

The authors wish to thank the Dutch technology foundation STW for it's financial support. Also the financial contributions by the concrete industry through the Union of Producers of Concrete Products in the Netherlands BFBN (*Bond van Fabrikanten van Betonproducten in Nederland)* and the steel industry through Building with Steel (*Bouwen met Staal)* is gratefully acknowledged. Finally, the authors wish to thank TNO Building and Construction Research for the facilitation of the research over the years by means of their experimental and computational infrastructure.

References

[1] Abrams, M.S. (1971), 'Compressive strength of concrete at temperatures to 1600 F' *in Temperature and Concrete*, ACI Special Publications SP25, Detroit, USA, pp 33-58

[2] Anderberg, Y, S. Thelandersson (1976), 'Stress and deformation characteristics of concrete at high temperatures, Part 2: Experimental investigation and material behaviour model', Lund: Lund University of Technology, Division of Structural Mechanics and Concrete Construction, Bull. 54

[3] Brekelmans, J.W.P.M., J.H.H. Fellinger, B.W.E.M. van Hove (1999), 'Aanbevelingen voor het ontwerp, de vervaardiging en toetsing van vloeren bestaande uit kanaalplaten met geïntegreerde stalen liggers', CUR-BmS rapport, Gouda, the Netherlands (*in Dutch*)

[4] Breunese,A.J. (2001) 'Tensile properties of concrete during fire', Rijswijk, TU Delft – TNO Centre for Fire Research report 2001-CVB-R04634

[5] Both, C. (1998), ''The fire resistance of composite steel concrete slabs', Dissertation TU Delft, Delft: Delft University Press

[6] Darwin, D., S. Barham, R. Kozul, S. Luan (2001), 'Fracture energy of high strength concrete', in *ACI Material's Journal*, Vol 98, Sep./Oct., pp 410-417

[7] DIANA (2003), 'DIANA Finite element analysis, user's manual, release 8.1', Delft: TNO

[8] ECCS Publication 103 (1998), 'Guidelines for the application of prestressed hollow core slabs supported on built-in beams', Brussels: ECCS

[9] ENV1992-1-2 (1995), 'Eurocode 2: Design of concrete structures, Part 1.2: General rules, structural fire design', Brussels: CEN

[10] Fellinger, J.H.H. (2004), 'Shear and anchorage behaviour of fire exposed hollow core slabs', Dissertation TU Delft, Delft: Delft University Press

[11] FIB (1999), 'Structural concrete, textbook on behaviour, design and performance', *fib* manual bulletin 1, Lausanne: FIB.

[12] Model Code 1990 (1991), 'Design code for concrete structures', Trowbridge: Thomas Telford

[13] NEN 5959 (1997), 'Beton en mortel – Bepaling van de splijttreksterkte van proefstukken', Delft: NEN (*in Dutch*)

[14] ISO 834-1 (1999), 'Fire resistance tests, elements for building construction – Part 1: General requirements', Geneva: ISO

[15] prEN1168-1 (1997), 'Pre-cast concrete products - Hollow core slabs for floors – Part 1, Pre-stressed slabs', Brussels: CEN

[16] prEN1992-1-2 (2002), 'Eurocode 2: Design of concrete structures, Part 1.2 General rules, Structural fire design', Brussels: CEN

[17] Purkiss, J.A., A. Bali (1988), 'The transient behaviour of concrete at temperatures up to 800 °C', in *Proceedings of the 10th Ibausil Weimar 1988, Hochschule für Architectur und Bauwesen*, Weimar, pp. 234-239

[18] Schneider, U. (1988), 'Concrete at high temperature – A general review', in *Fire Safety Journal*, Vol. 13, pp 55-68

[19] den Uijl, J.A. (1998), 'Bond modelling of prestressing strand', in *ACI Special Publication 180*, Michigan USA, pp 145-169

[20] Walraven, J.C., P. Mercx (1983), 'The bearing capacity of prestressed hollow core slabs', in *Heron* Vol. 28 – No. 3

Numerical modelling and experimental assessment of concrete spalling in fire

Manuchehr Shamalta
TNO Centre for Fire Research, Delft, the Netherlands
Email: manuchehr.shamalta@tno.nl, Phone: +31 15 276 3285

Arnoud Breunese
TNO Centre for Fire Research, Delft, the Netherlands

Willy Peelen
TNO Civil Infrastructure, Delft, the Netherlands

Joris Fellinger
TNO Centre for Fire Research, Delft, the Netherlands

In this paper, the phenomenon of spalling of concrete in fire has been studied using a numerical model. Spalling is the violent or non-violent breaking off of layers or pieces of concrete when it is exposed to high temperatures as experienced in fires. The types and mechanisms of spalling have been explained. A numerical model has been developed, which takes into account main characteristics of the real phenomenon. To improve the stability, robustness and calculation time of the model analysis, the transport phenomenon and the mechanical behaviour have been coupled in a staggered way. The system of differential equations describing the transport phenomenon has been implemented in FEMLAB, an interactive environment to model single and coupled phenomenon based on partial differential equations. A one-dimensional example has been studied. It has been shown that the results are physically reasonable but still validation of the results needs to be done. These results will be validated against the experimental measurements and the results obtained by other recently developed models predicting the concrete spalling.

Keywords: concrete spalling, fire, high temperatures, porous medium, numerical modelling, staggered analysis

1 Introduction

A series of fires in road and rail tunnels have occurred across Europe over the past decade, causing a serious loss of life and significant structural damage. It was in the first place the human casualties

and second the structural damage and as consequence the financial loss in the Mont Blanc tunnel, Tauern tunnel, Kaprun tunnel, Gotthard tunnel, Great Belt tunnel (during construction) and Channel tunnel (soon after commissioning) fires that have provided the impetus to take the fire safety more seriously. These unforgettable disasters seize the public attention, the European authorities attention and as consequence the engineers attention to focus on the fir safety.
As far as the fire safety is concerned the main structure shouldn't collapse until both rescue workers and users are safe. To this end it is important to know about the behaviour of the construction exposed to fire. The use of incombustible materials does not guarantee the safety of a structure. Steel, for instance, quickly loses its strength when heated and its yield strength decreases significantly as it absorbs heat, endangering the stability of the structure. Also reinforced concrete is not immune to fire. Concrete is the most widely used construction material on earth and has proved to be very durable under most conditions. Despite the fact that concrete has the advantages of durability in comparison to other construction materials, massiveness and in-combustibility related to fire safety, it can also undergo serious damages under fire conditions. Concrete may spall under elevated temperatures, exposing the steel reinforcement and weakening structural members. Spalling of concrete is currently a hot issue in civil engineering and it is indicated as the major cause for non-recoverable damage in structures subjected to fire. Figure 1 shows the construction damage that occurred due to the fire inside the Channel tunnel. The concrete was completely destroyed and vanished leaving only the bare steel reinforcement which lost it's strength and bent down in the intense heat. This fire caused huge finance damage but fortunately no lives were lost.

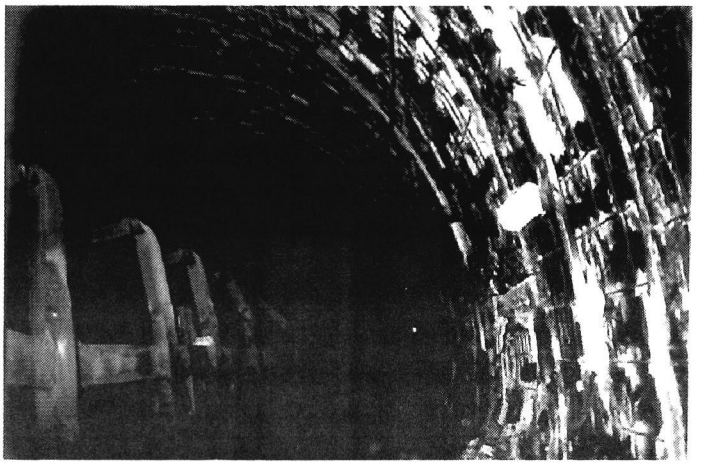

Figure 1: Fire damage in Channel tunnel

Spalling of concrete is the violent or non-violent breaking off of layers or pieces of concrete from the surface of a structural element when it is exposed to high temperatures as expected in fires. Spalling

of concrete has serious consequences. Loss of section (i.e. reduction of the cross-sectional area of the concrete so that it is no longer able to sustain the stresses) and loss of protection to steel reinforcement (reinforcement reaching excessive temperatures) lead to a decrease of the structural load bearing capacity and ultimately failure.

In this paper, a model is employed to describe the phenomenon of spalling of concrete due to high temperatures. The concrete is modelled as a three-phase porous medium with constituents in the solid phase (solid matrix and chemically bound water), the liquid phase (capillary or free water and physically adsorbed water) and the gas phase (dry air and water vapour). This model also takes into account the phase changes of water.

The governing differential equations describing the equilibrium of the flow of mass, energy and momentum have been obtained based on the mixture theory by fully integration of the energy and mass conservation equations. Four primary state variables, i.e. gas pressure p_g, capillary pressure p_c, temperature T and displacement vector of the solid matrix $\mathbf{u}$, were chosen to describe the state of concrete at high temperatures. After introducing the constitutive relationships and the thermodynamic state relationship a system of differential equation of four coupled partially differential equations was found. Three of them (p_g, p_c and T) describe the transport phenomenon and the fourth one ($\mathbf{u}$) describes the mechanical behaviour of the system. This paper describes the fully coupled system. However, for the implementation of the model, the transport phenomenon and the mechanical behaviour are coupled in a staggered way. It means that the effect of the transport parameters on the mechanical behaviour is considered but the influence of the mechanical behaviour on the transport phenomena is assumed to be negligible. Staggered analysis of this system has several advantages. First of all the analysis will be more stabile and robust. Second, the calculation time will be decreased by choosing different discretisations in time and space to calculate the transport parameters than that to calculate the displacements.

The differential equations describing the transport phenomenon was solved using the computer programme FEMLAB. A one-dimensional example was studied. In the frame of this example the temperature and pressures were calculated inside an concrete wall exposed to fire at one side. The results were plotted for different saturation degrees of the concrete.

Next development within the framework of this project is to validate these results. The validation will be done firstly using experimental results and secondly by comparison with the results obtained by another recently developed numerical model [3] describing the phenomenon spalling of concrete.

2 Mechanisms which lead to spalling

Spalling can be grouped into five categories violent spalling, sloughing-off, corner spalling, explosive spalling and post-cooling spalling [1].

Many material (e.g. aggregate type), geometric (e.g. section shape and size), productional (e.g. casting process) and environmental (e.g. heating rate) factors have been identified from experiments as influencing spalling of concrete in fire. The main factors influencing spalling are the heating rate, permeability of the material, initial pore saturation level and the level of external applied load. High strength concrete is more likely to explosively spall than normal strength concrete despite its higher tensile strength. This is because of the lower ductility and the greater pore pressures that build up during heating owing to the material's lower permeability. Other factors such as the cross sectional size and shape, heating profile, concrete age, aggregate size and type, the presence of cracking and reinforcement also play a role.

Each kind of concrete spalling is caused by a specific combination of physical or chemical mechanisms. These are as follows:

- Pore pressure rises due to expanding and evaporating water at elevated temperatures;
- Compression of the heated surface due to a thermal gradient in the cross section;
- Internal cracking due to difference in thermal expansion between aggregate and cement paste;
- Cracking due to difference in thermal expansion/deformation between concrete and reinforcement bars;
- Strength loss due to chemical transitions during heating.

Violent spalling which is separation of small or large pieces of concrete from the cross section, is caused by pore pressure, thermal gradients and internal cracking. Sloughing-off spalling is caused by strength loss due to internal cracking and chemical deterioration of the cement paste. Corner spalling is caused by cracks due to the different thermal deformation of concrete and reinforcement bar at the corner of concrete. Explosive spalling is the result of the combination of the pore pressure and thermal gradients in the cross-section. Post-cooling spalling occurs after the fire is over and caused by internal cracking due to different thermal expansion of aggregate and loss of strength due to chemical transitions.

3 Numerical approach

3.1 General overview

To study the phenomenon concrete spalling in fire a fully coupled multi-phase hydro-thermal-mechanical model is considered, which takes into account the main characteristics of this problem. Within this model the concrete is considered to be a three phase porous medium based on mixture theory or averaging theory. This theory offers possibilities for a better understanding of the microscopic situation and its relation to the macroscopic level.

The three considered phases within this model are solid phase, liquid phase and gas phase. The solid phase consists of solid matrix and chemically bound water. The liquid phase consists of capillary or free water and physically adsorbed water. Physically adsorbed water is present in the hole range of water contents of the medium, while, the capillary or free water appears when water content exceeds the so-called solid saturation point S_{ssp} [6]. The gas phase is a mixture of dry air and water vapour.

Transitions that take place between the three abovementioned phases can be physical or chemical in nature and are thermodynamically not fully reversible. In cement based concrete these phase changes are dehydration/hydration of chemically bound water, evaporation/condensation of free water and desorption/adsorption of physically adsorbed water. Other phase changes such as the decarbonation/carbonation and α-β inversion/ β- α inversion (α-β transformation of quartz at 573 °C) were not incorporated within this model. It has also been assumed that the phase changes happen only between water vapour and the other three, i.e. there is no direct mutual exchange between chemically bound water, physically adsorbed water and capillary water. Figure 2 shows schematically the phase changes of water implemented in model.

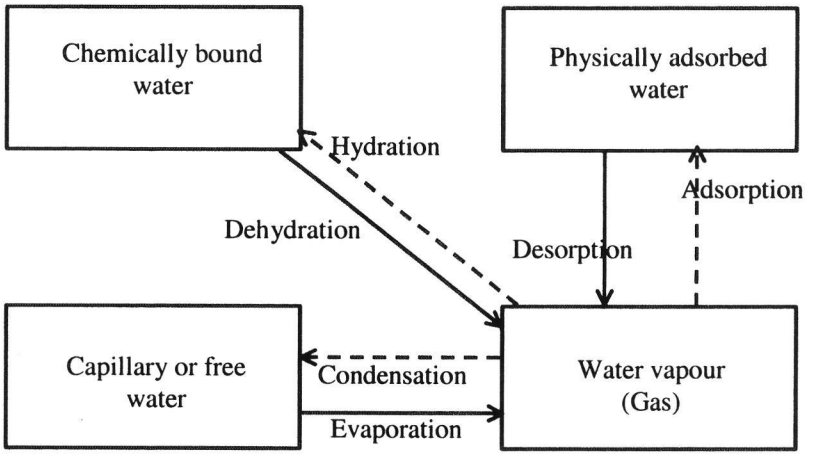

Figure 2: Phase changes of water; solid arrows indicate energy consumption, dashed arrows indicate energy release

One can see in this figure that dehydration is the phase change of chemically bound water to water vapour which is an energy consuming chemical process. This process produces a reduction in the solid skeleton mass of the cement paste. Hydration, which is a reverse process of dehydration, takes place at room temperature and the process increases with temperature in the presence of moisture up to 80 °C or more resulting in an increase in the mass of solid skeleton. Above this temperature, dehydration is a gradual process up to 850 °C [7]. Evaporation is the process by which water gains

energy to change from the capillary or free water to the gas phase. In contrary, condensation is the process whereby water vapour is returned to the liquid phase. Desorption is the evaporation of water molecules from the surface of the solid, gaining energy, while, adsorption is the binding of the water molecules to the surface of the solid. Evaporation of water increases with temperature particularly above approximately 80 °C depending on the pressure. The loss of the capillary water does not significantly influence the mechanical property of the cement paste but the loss of physically adsorbed water has a major influence on the mechanical properties. Beyond the triple point of water (374.14 °C) no difference exists anymore between capillary water and water vapour. Also the capillary pressure vanishes.

The basic equations used in this model fall under three main categories: a) constitutive relationship of concrete describing the real behaviour of the material derived directly from experiments, b) thermodynamic state equations allowing the treatment of dry air and moist air as ideal gases (Clapeyron's law) as well as equilibrium relations for capillary menisci (Kelvin's law) and gas phases (Dalton's law) c) general laws of conservation which must be obeyed in space and time including the first principle of thermodynamics (enthalpy conservation). Before these equations are discussed, first the definition of the material time derivative is given.

3.2 *Material time derivative*

The material time derivative of any differentiable function $f_\pi(x,t)$, given in its spatial description and referring to a moving particle of the π phase of a material, is

$$\frac{D_\pi f_\pi}{Dt} = \frac{\partial f_\pi}{\partial t} + \nabla f_\pi \cdot \mathbf{v}_\pi , \tag{1}$$

with $\mathbf{v}_\pi$ the mass velocity of the π phase. If subscript α is used it gives

$$\frac{D_\alpha f_\pi}{Dt} = \frac{\partial f_\pi}{\partial t} + \nabla f_\pi \cdot \mathbf{v}_\alpha . \tag{2}$$

Subtraction of these derivatives yields to the following relation:

$$\frac{D_\alpha f_\pi}{Dt} = \frac{D_\pi f_\pi}{Dt} + \nabla f_\pi \cdot \mathbf{v}_{\alpha\pi} , \tag{3}$$

where $\mathbf{v}_{\alpha\pi}=-\mathbf{v}_{\pi\alpha}=\mathbf{v}_\alpha-\mathbf{v}_\pi$, known as diffusion velocity, is the velocity of the α phase with respect to the π phase. In these relations Δ is the gradient operator defined as $=\{\partial/\partial x, \partial/\partial y, \partial/\partial z\}^T$.

3.3 *Constitutive relationship and thermodynamic state relationships*

In this model we assume the moist air as a mixture of two ideal gases, i.e. dry air and water vapour. The equations of state of a perfect gas, applied to dry air (ga), vapour (gw) and moist air (g) are

$$p_{ga} = \rho_{ga}\frac{RT}{M_a},\ p_{gw} = \rho_{gw}\frac{RT}{M_w},\ \rho_g = \rho_{ga} + \rho_{gw},\ p_g = p_{ga} + p_{gw},$$

$$\frac{1}{M_g} = \frac{\rho_{gw}}{\rho_g}\frac{1}{M_{gw}} + \frac{\rho_{ga}}{\rho_g}\frac{1}{M_{ga}} \tag{4}$$

where M_π, ρ_π and p_π are the molar mass, the density and pressure of constituent π, respectively, and R is the universal gas constant. The degree of saturation of constituent π is defined as the ratio of the volume of constituent π to the volume of the void. It follows immediately for the saturation degree of liquid water and the gas that

$$S_w + S_g = 1. \tag{5}$$

The degree of saturation with liquid water is an experimentally determined function of capillary pressure p_c and temperature T. This function is usually presented in the form of the sorption isotherms [2,3].

The capillary pressure is defined as the pressure difference between the gas phase and the liquid phase, which can be find through the Laplace equation from the pore radius r and the surface tension σ

$$p_c = p_g - p_w = \frac{2\sigma}{r}, \tag{6}$$

and the pressure in the solid phase is

$$p_s = p_w S_w + p_g S_g = p_g - p_c S_w. \tag{7}$$

where S_π is the saturation degree of the constituent π.

For the density of water many experiments were carried out in the past. The values were approximated by a linearization in temperature and pressure:

$$\rho_w = \rho_{wo}\exp\left(-\beta_w\left(T - T_o\right) + C_w\left(p_w - p_{wo}\right)\right), \tag{8}$$

where ρ_{wo} is the water density at the reference temperature T_o and pressure p_{wo}, β_w is the thermal expansion coefficient and C_w is the compressibility coefficient.

For the relationship between the relative humidity (RH) and the capillary pressure in the pores, the Kelvin-Laplace law is assumed to be valid

$$RH = \frac{p_{gw}(T)}{p_{gws}(T)} = \exp\left(\frac{p_c M_w}{\rho_w RT}\right), \tag{9}$$

with $p_{gws}(T)$ the water vapour saturation pressure which can be calculated using the Clausous-Clapeyron equation,

$$p_{gws}(T) = p_{gwso} \exp\left(-\frac{M_w \Delta H_{gw}}{R} \left(\frac{1}{T} - \frac{1}{T_o} \right) \right), \tag{10}$$

where p_{gwso} is the water vapour pressure at reference temperature T_o and ΔH_{gw} is the specific enthalpy of evaporation.

Darcy's law is assumed valid for transport of both water and gas in slow phenomenon.

$$\mathbf{v}_{\pi s} = \frac{k_{r\pi} \boldsymbol{\kappa}}{n S_\pi \mu_\pi} \left(-\nabla p_\pi + \rho_\pi \mathbf{g} \right). \tag{11}$$

In this relation $\boldsymbol{\kappa}$ is the permeability tensor of the medium, μ_π is the dynamic viscosity of the constituent π, n is the porosity and $k_{r\pi}$ is the relative permeability. The porosity n is defined as the ratio of the volume of the void to the total volume of the medium

Diffusive-dispersive mass flux $\mathbf{J}_{\pi\alpha}$ is governed by Fick's law

$$\mathbf{J}_{\pi\alpha} = n S_\pi \rho_\alpha \mathbf{v}_{\pi\alpha} = -\rho_\alpha \mathbf{D}_{\pi\alpha} \nabla \left(\frac{\rho_\pi}{\rho_\alpha} \right), \tag{12}$$

where $\mathbf{D}_{\pi\alpha}$ is effective dispersion tensor, π is the diffusion phase and α is the phase in which diffusion takes place (α=w,g).

A constitutive assumption for the heat flux is the generalised version of Fourier's law, $\mathbf{q}$=-$\boldsymbol{\lambda}_{eff}\Delta T$, with $\boldsymbol{\lambda}_{eff}$ the effective thermal conductivity tensor and $\mathbf{q}$ the heat flux of the multiphase medium, the sum of the partial heat fluxes $\mathbf{q}_\pi$. For porous media the following linear relationship may be used [8]:

$$\lambda_{eff} = \lambda_{dry} \left(1 + 4 \frac{n S_w \rho_w}{(1-n)\rho_s} \right). \tag{13}$$

3.4 *Governing equations*

To find the governing equations we need to fully integrate the conservation equations of the three quantities, mass, energy and momentum (force balance). These conservation equations can be derived using the general conservation equation. For a generic conserved variable ψ (e.g. like mass, momentum and energy) the general conservation equation may be written as

$$\frac{\partial \psi}{\partial t} + \nabla \cdot \left(\mathbf{f} + \psi \mathbf{v} \right) - H = 0, \tag{14}$$

with $\mathbf{f}$ the flux of ψ in the absence of the fluid transport, $\psi\mathbf{v}$ the transport flux and H the source or sink of ψ. Given equation (14) for the conservation of anything and specifying the subscript s for solid, w for liquid phase and g for the gas phase (dry air plus vapour), it is now straightforward to consider the conservation equations.

To derive the conservation equation of solid mass we just substitute $\psi = (1-n)\rho_s$ (density is amount of mass per unit volume), $\mathbf{f} = \mathbf{0}$ (mass flux can only change due to transport) and $H = -\partial (m_{dehydr})/\partial t$ (solid mass can change by dehydration/hydration process) into equation (14) to get

$$\frac{\partial\left((1-n)\rho_s\right)}{\partial t} + \nabla\cdot\left((1-n)\rho_s \mathbf{v}_s\right) = -\dot{m}_{dehydr}\,. \tag{15}$$

The mass conservation equations of liquid water, vapour water and dry air can be derived in the same way as equation (15) by substitution $H = -\partial (m_l)/\partial t$ for liquid water (mass of liquid water can be change by eider evaporation/condensation or desorption/adsorption processes), $H = \partial (m_{dehydr} + m_l)/\partial t$ for vapour water (mass of vapour water can be change by dehydration/hydration, evaporation/condensation and desorption/adsorption processes) and $H = 0$ (dry air can not be crated or destroyed) for dry air into (14). Hence, one may find for mass balance equation of liquid water

$$\frac{\partial\left(nS_w\rho_w\right)}{\partial t} + \nabla\cdot\left(nS_w\rho_w \mathbf{v}_w\right) = -\dot{m}_l\,, \tag{16}$$

for mass balance equation of vapour water

$$\frac{\partial\left(nS_g\rho_{gw}\right)}{\partial t} + \nabla\cdot\left(nS_g\rho_{gw} \mathbf{v}_{gw}\right) = \dot{m}_{dehydr} + \dot{m}_l\,, \tag{17}$$

and for mass balance equation of dry air

$$\frac{\partial\left(nS_g\rho_{ga}\right)}{\partial t} + \nabla\cdot\left(nS_g\rho_{ga} \mathbf{v}_{ga}\right) = 0\,. \tag{18}$$

The amount of heat (energy) per unit volume is $\psi = (\rho C_p)_{eff} T$ where C_p is the specific heat, T is the temperature and $(\rho C_p)_{eff}$ is the effective thermal capacity of partially saturated concrete. The heat flux has two components due to conduction and transport. In the absence of transport the heat flux is $\mathbf{f} = -\lambda_{eff}\nabla T$ where λ_{eff} is the effective thermal conductivity of partially saturated concrete. Finally, heat can be released/absorbed during dehydration/hydration, evaporation/condensation and desorption/adsorption. The of energy related to the phase changes is equal to the change in the enthalpy, ΔH. Thus the heat released/absorbed during abovementioned processes may be calculated as $H = \Delta H_{dehydr}\partial(m_{dehydr})/\partial t + \Delta H_l \partial (m_l)/\partial t$. Hence, the energy conservation equation may be written as follows:

$$\left(\rho C_p\right)_{eff}\frac{\partial T}{\partial t} + \left(\rho_w C_{pw}\mathbf{v}_w + \rho_g C_{pg}\mathbf{v}_g\right)\cdot\nabla T - \nabla\cdot\left(\lambda_{eff}\nabla T\right) = \dot{m}_{dehydr}\Delta H_{dehydr} + \dot{m}_l \Delta H_l\,. \tag{19}$$

In these equations $l = desorp$ if $S \le S_{ssp}$ and $l = evap$ if $S > S_{ssp}$.

Conservation of linear momentum or force balance can be derived in exactly the same way, however momentum is a vector field. In general momentum is $m\mathbf{v}$, therefore the amount of momentum per unit volume is $\psi = (1-n)\rho_s\mathbf{v}_s$ for solid phase, $\psi = nS_w\rho_w\mathbf{v}_l$ for liquid water phase, $\psi = nS_g\rho_{gw}\mathbf{v}_{gw}$ for vapour water phase and $\psi = nS_g\rho_{ga}\mathbf{v}_{ga}$ for dry air phase. The momentum can be changed by forces. As stress is simply force per unit area, the stress can also be thought of as a flux of the force potential, i.e. $\mathbf{f}=-(1-n)\boldsymbol{\sigma}_s$ for solid phase, $\mathbf{f}=-nS_w\boldsymbol{\sigma}_w$ for liquid water phase, $\mathbf{f}=-nS_g\boldsymbol{\sigma}_{gw}$ for vapour water phase and $\mathbf{f}=-nS_g\boldsymbol{\sigma}_{ga}$ for dry air phase. The other forces are body forces such as gravity and internal forces. Neglecting the internal forces and considering the change of linear momentum due to dehydration/hydration, evaporation/condensation and desorption/adsorption processes, thus $H=(1-n)\rho_s\mathbf{g}-[\partial(m_{dehydr})/\partial t]\mathbf{v}_s$ for solid phase, $H=nS_w\rho_w\mathbf{g}-[\partial(m_l)/\partial t]\mathbf{v}_w$ for liquid water phase, $H=nS_g\rho_{gw}\mathbf{g}+[\partial(m_{dehydr})/\partial t+\partial(m_l)/\partial t]\mathbf{v}_{gw}$ for vapour water phase and $H=nS_g\rho_{ga}\mathbf{g}$ for dry air phase where $\mathbf{g}$ is the net acceleration. Substituting into (14) yields

$$\frac{\partial\left((1-n)\rho_s\mathbf{v}_s\right)}{\partial t}+\nabla\cdot\left((1-n)\rho_s\mathbf{v}_s\otimes\mathbf{v}_s\right) -\nabla\cdot\left((1-n)\boldsymbol{\sigma}_s\right)-(1-n)\rho_s\mathbf{g}+\dot{m}_{dehydr}\mathbf{v}_s=0, \tag{20}$$

$$\frac{\partial\left(nS_w\rho_w\mathbf{v}_l\right)}{\partial t}+\nabla\cdot\left(nS_w\rho_w\mathbf{v}_w\otimes\mathbf{v}_w\right)-\nabla\cdot\left(nS_w\boldsymbol{\sigma}_w\right) -nS_w\rho_w\mathbf{g}+\dot{m}_l\mathbf{v}_w=0, \tag{21}$$

$$\frac{\partial\left(nS_g\rho_{gw}\mathbf{v}_{gw}\right)}{\partial t}+\nabla\cdot\left(nS_g\rho_{gw}\mathbf{v}_{gw}\otimes\mathbf{v}_{gw}\right)-\nabla\cdot\left(nS_g\boldsymbol{\sigma}_{gw}\right) -nS_g\rho_{gw}\mathbf{g}-\left(\dot{m}_{dehydr}+\dot{m}_l\right)\mathbf{v}_{gw}=0, \tag{22}$$

$$\frac{\partial\left(nS_g\rho_{ga}\mathbf{v}_{ga}\right)}{\partial t}+\nabla\cdot\left(nS_g\rho_{ga}\mathbf{v}_{ga}\otimes\mathbf{v}_{ga}\right)-\nabla\cdot\left(nS_g\boldsymbol{\sigma}_{ga}\right)-nS_g\rho_{ga}\mathbf{g}=0, \tag{23}$$

for solid, liquid water, vapour water and dry air phase, respectively. Expanding the first and second terms of equations (20)-(23) and summation of these equations and by substitution of equations (15) -(18) into the result yield to the following conservation of momentum

$$\nabla\cdot\boldsymbol{\sigma}+\rho\mathbf{g}=(1-n)\rho_s\left(\frac{\partial\mathbf{v}_s}{\partial t}+\mathbf{v}_s\nabla\cdot\left(\mathbf{v}_s\right)\right)+nS_w\rho_w\left(\frac{\partial\mathbf{v}_w}{\partial t}+\mathbf{v}_w\nabla\cdot\left(\mathbf{v}_w\right)\right) +nS_g\rho_{gw}\left(\frac{\partial\mathbf{v}_{gw}}{\partial t}+\mathbf{v}_{gw}\nabla\cdot\left(\mathbf{v}_{gw}\right)\right)+nS_g\rho_{ga}\left(\frac{\partial\mathbf{v}_{ga}}{\partial t}+\mathbf{v}_{ga}\nabla\cdot\left(\mathbf{v}_{ga}\right)\right), \tag{24}$$

where ρ is the average density of the multiphase medium, given by $\rho=(1-n)\rho_s+nS_w\rho_w+ nS_g\rho_g$ and $\boldsymbol{\sigma}$ the total stress of the multiphase medium, expressed by $\boldsymbol{\sigma}=(1-n)\boldsymbol{\sigma}_s+nS_w\boldsymbol{\sigma}_w+nS_g\boldsymbol{\sigma}_g$. In which $\boldsymbol{\sigma}_s$, $\boldsymbol{\sigma}_w$ and $\boldsymbol{\sigma}_g$ are the intrinsic stresses and can be calculated by:

$$\boldsymbol{\sigma}_s = \boldsymbol{\sigma}' - \alpha \mathbf{I} p_s,\ \boldsymbol{\sigma}_w = \mathbf{I} p_w,\ \boldsymbol{\sigma}_g = \mathbf{I} p_g, \tag{25}$$

with I the identity tensor, $\boldsymbol{\sigma}'=\mathbf{D}_e\boldsymbol{\varepsilon}$ the effective stress and $\alpha=1-(K_s/K_M)$ is the Biot's constant with K_s and K_M the bulk moduli of solid and porous medium, matrix $\mathbf{D}_e$ is the stiffness matrix and $\boldsymbol{\varepsilon}=\mathbf{L}\mathbf{u}$ the stress tensor, where L is the differential operator defined as follows:

$$\mathbf{L} = \begin{bmatrix} \frac{\partial}{\partial x} & 0 & 0 & \frac{\partial}{\partial y} & 0 & \frac{\partial}{\partial z} \\ 0 & \frac{\partial}{\partial y} & 0 & \frac{\partial}{\partial x} & \frac{\partial}{\partial z} & 0 \\ 0 & 0 & \frac{\partial}{\partial z} & 0 & \frac{\partial}{\partial y} & \frac{\partial}{\partial x} \end{bmatrix}^{\mathrm{T}} \tag{26}$$

Under the assumptions of small-strain theory and isothermal equilibrium and with neglecting the influence of the acceleration term $\partial\mathbf{v}/\partial t$ and the convector terms $\mathbf{v}(\nabla.\mathbf{v})$, results for conservation of momentum

$$\nabla \cdot \boldsymbol{\sigma} + \rho \mathbf{g} = \mathbf{0}. \tag{27}$$

The conservation of angular momentum leads to the observation that the stress tensor is symmetrical.

3.5 *Formulation of system of equations*

Applying the material time derivatives (1)-(3) and expansion of the divergence terms in conservation equations (15)-(18) one may find for solid mass conservation equation

$$\frac{(1-n)}{\rho_s}\frac{D_s\rho_s}{Dt} - \frac{D_s n}{Dt} + (1-n)\nabla \cdot \mathbf{v}_s = -\frac{\dot{m}_{dehydr}}{\rho_s}, \tag{28}$$

for mass balance equation for liquid water

$$\frac{D_s n}{Dt} + \frac{n}{S_w}\frac{D_s S_w}{Dt} + \frac{n}{\rho_w}\frac{D_s \rho_w}{Dt} + \frac{1}{S_w\rho_w}\nabla \cdot (nS_w\rho_w\mathbf{v}_{ws}) + n\nabla \cdot \mathbf{v}_s = \frac{-\dot{m}_l}{S_w\rho_w}, \tag{29}$$

for mass balance equation for vapour water

$$\frac{D_s n}{Dt}+\frac{n}{S_g}\frac{D_s S_g}{Dt}+\frac{n}{\rho_{gw}}\frac{D_s \rho_{gw}}{Dt}+\frac{1}{S_g\rho_{gw}}\nabla\cdot\left(nS_g\rho_{gw}\mathbf{v}_{gs}\right)$$
$$+\frac{1}{S_g\rho_{gw}}\nabla\cdot\left(nS_g\rho_{gw}\mathbf{v}_{gwg}\right)+n\nabla\cdot\mathbf{v}_s=\frac{\dot{m}_{dehydr}+\dot{m}_l}{S_g\rho_{gw}}, \tag{30}$$

for mass balance equation for dry air

$$\frac{D_s n}{Dt}+\frac{n}{S_g}\frac{D_s S_g}{Dt}+\frac{n}{\rho_{ga}}\frac{D_s \rho_{ga}}{Dt}+\frac{1}{S_g\rho_{ga}}\nabla\cdot\left(nS_g\rho_{ga}\mathbf{v}_{gs}\right)$$
$$+\frac{1}{S_g\rho_{ga}}\nabla\cdot\left(nS_g\rho_{ga}\mathbf{v}_{gag}\right)+n\nabla\cdot\mathbf{v}_s=0. \tag{31}$$

The first term in equation (28) that is related to the material time derivative of the solid density. The solid density ρ_s has been considered as function of solid pressure p_s, temperature T, the first invariant of effective stress tensor $\mathrm{tr}\boldsymbol{\sigma}'$ and the degree of cement dehydration Γ_{dehydr}. Thus its derivative with respect to time t leads to:

$$\frac{1}{\rho_s}\frac{D_s\rho_s}{Dt}=\frac{1}{\rho_s}\left(\frac{\partial\rho_s}{\partial p_s}\frac{D_s p_s}{Dt}+\frac{\partial\rho_s}{\partial T}\frac{D_s T}{Dt}\right.$$
$$\left.+\frac{\partial\rho_s}{\partial\mathrm{tr}\boldsymbol{\sigma}'}\frac{D_s\mathrm{tr}\boldsymbol{\sigma}'}{Dt}+\frac{\partial\rho_s}{\partial\Gamma_{dehydr}}\frac{D_s\Gamma_{dehydr}}{Dt}\right). \tag{32}$$

However $\frac{1}{\rho_s}\frac{\partial\rho_s}{\partial p_s}=\frac{1}{K_s}$, $\frac{1}{\rho_s}\frac{\partial\rho_s}{\partial T}=-\beta_s$, $\frac{1}{\rho_s}\frac{\partial\rho_s}{\partial\mathrm{tr}\boldsymbol{\sigma}'}=\frac{1}{3(n-1)K_s}$ and

$\frac{D_s\Gamma_{dehydr}}{Dt}=-3(1-\alpha)K_s\left(\nabla\cdot\mathbf{v}_s+\frac{1}{K_s}\frac{D_s p_s}{Dt}-\beta_s\frac{D_s T}{Dt}\right)$ in which K_s is the bulk modulus of solid, β_s is the thermal expansion coefficient of solid and α is the Biot's constant. Substitution of these expressions into relation (32) gives

$$\frac{1}{\rho_s}\frac{D_s\rho_s}{Dt}=\frac{1}{1-n}\left(\frac{\alpha-n}{K_s}\frac{D_s p_s}{Dt}-(\alpha-n)\beta_s\frac{D_s T}{Dt}-(1-\alpha)\nabla\cdot\mathbf{v}_s\right.$$
$$\left.+\frac{1-n}{\rho_s}\frac{\partial\rho_s}{\partial\Gamma_{dehydr}}\frac{D_s\Gamma_{dehydr}}{Dt}\right). \tag{33}$$

Similarly, the third term in equation (29) that is related to the material time derivative of the water density can be obtained by assuming that ρ_w is a function of water pressure p_w and temperature T. Thus its derivative with respect to time t leads to:

$$\frac{1}{\rho_w}\frac{D_s\rho_w}{Dt}=\frac{1}{\rho_w}\left(\frac{\partial\rho_w}{\partial p_w}\frac{D_s p_w}{Dt}+\frac{\partial\rho_w}{\partial T}\frac{D_s T}{Dt}\right). \tag{34}$$

However $\frac{1}{\rho_w}\frac{\partial\rho_w}{\partial p_w}=\frac{1}{K_w}$ and $\frac{1}{\rho_w}\frac{\partial\rho_w}{\partial T}=-\beta_w$ in which K_w is the bulk modulus of water and β_w is the thermal expansion coefficient of water. Hence equation (34) can be rewritten as:

$$\frac{1}{\rho_w}\frac{D_s\rho_w}{Dt}=\frac{1}{K_w}\frac{D_s p_w}{Dt}-\beta_w\frac{D_s T}{Dt}. \tag{35}$$

Solving the material derivative of porosity n from the solid mass balance equation (28) and substitution into the equations (29)-(31) and by introducing the relations (6)-(5), (11), (12), (33) and (35) into the results yield for mass balance equation for liquid water

$$\begin{aligned}
&S_w\left(\frac{\alpha-n}{K_s}+\frac{n}{K_w}\right)\frac{D_s p_g}{Dt}-S_w\left(\frac{\alpha-n}{K_s}S_w+\frac{n}{K_w}\right)\frac{D_s p_c}{Dt}+\alpha S_w\nabla\cdot\mathbf{v}_s\\
&\quad-S_w\left((\alpha-n)\beta_s+n\beta_w\right)\frac{D_s T}{Dt}+\left(n-\frac{\alpha-n}{K_s}S_w p_c\right)\frac{D_s S_w}{Dt}\\
&\quad+\frac{1}{\rho_w}\nabla\cdot\left(nS_w\rho_w\mathbf{v}_{ws}\right)+S_w\frac{1-n}{\rho_s}\frac{\partial\rho_s}{\partial\Gamma_{dehydr}}\frac{D_s\Gamma_{dehydr}}{Dt}\\
&\quad=-S_w\frac{\dot{m}_{dehydr}}{\rho_s}-\frac{\dot{m}_l}{\rho_w},
\end{aligned} \tag{36}$$

for mass balance equation for vapour water

$$
\begin{aligned}
&S_g \frac{\alpha-n}{K_s}\frac{D_s p_g}{Dt} - S_g S_w \frac{\alpha-n}{K_s}\frac{D_s p_c}{Dt} + \alpha S_g \nabla\cdot\mathbf{v}_s \\
&\quad -(\alpha-n)\beta_s S_g \frac{D_s T}{Dt} - \left(n + p_c S_g \frac{\alpha-n}{K_s}\right)\frac{D_s S_w}{Dt} \\
&\quad + \frac{1}{\rho_{gw}}\nabla\cdot\left(nS_g\rho_{gw}\mathbf{v}_{gs}\right) + \frac{1}{\rho_{gw}}\nabla\cdot\left(nS_g\rho_{gw}\mathbf{v}_{gwg}\right) \\
&\quad + S_g \frac{n}{\rho_{gw}}\frac{D_s\rho_{gw}}{Dt} + S_g \frac{1-n}{\rho_s}\frac{\partial\rho_s}{\partial\Gamma_{dehydr}}\frac{D_s\Gamma_{dehydr}}{Dt} \\
&\quad = -S_g \frac{\dot{m}_{dehydr}}{\rho_s} + \frac{\dot{m}_{dehydr}+\dot{m}_l}{\rho_{gw}},
\end{aligned}
\tag{37}
$$

for mass balance equation for dry air

$$
\begin{aligned}
&S_g \frac{\alpha-n}{K_s}\frac{D_s p_g}{Dt} - S_g S_w \frac{\alpha-n}{K_s}\frac{D_s p_c}{Dt} + \alpha S_g \nabla\cdot\mathbf{v}_s \\
&\quad - S_g(\alpha-n)\beta_s \frac{D_s T}{Dt} - \left(n + p_c S_g \frac{\alpha-n}{K_s}\right)\frac{D_s S_w}{Dt} \\
&\quad + \frac{1}{\rho_{ga}}\nabla\cdot\left(\rho_{ga}\frac{k_{rg}\boldsymbol{\kappa}}{\mu_g}\left(-\nabla p_g + \rho_g\mathbf{g}\right)\right) + \frac{1}{\rho_{ga}}\nabla\cdot\left(nS_g\rho_{ga}\mathbf{v}_{gag}\right) \\
&\quad + S_g \frac{n}{\rho_{ga}}\frac{D_s\rho_{ga}}{Dt} + S_g \frac{1-n}{\rho_s}\frac{\partial\rho_s}{\partial\Gamma_{dehydr}}\frac{D_s\Gamma_{dehydr}}{Dt} = -S_g \frac{\dot{m}_{dehydr}}{\rho_s}.
\end{aligned}
\tag{38}
$$

Five partial differential equations (19), (27) and (36)-(38) form the system of differential equations of this problem. Choosing gas pressure p_g, capillary pressure p_c, temperature T and displacement vector of the solid matrix $\mathbf{u}$ as four primary state variables we need to eliminate one of equations. Solving the term $\partial(m_l)/\partial t$ from equation (36) and with substitution in other equations, as well as the following relationships:

$$
\nabla\cdot\mathbf{v}_s = \mathbf{I}\mathbf{L}\frac{\partial\mathbf{u}}{\partial t}, \tag{39}
$$

$$
\frac{\partial S_w}{\partial t} = \frac{\partial S_w}{\partial p_c}\frac{\partial p_c}{\partial t} + \frac{\partial S_w}{\partial T}\frac{\partial T}{\partial t}, \tag{40}
$$

$$
\frac{\partial}{\partial t}\left(\frac{M_w}{TR}p_{gw}\right) = \frac{M_w}{RT}\frac{\partial p_{gw}}{\partial p_c}\frac{\partial p_c}{\partial t} + \frac{M_w}{RT}\left(\frac{\partial p_{gw}}{\partial T} - \frac{p_{gw}}{T}\right)\frac{\partial T}{\partial t}, \tag{41}
$$

$$\frac{\partial}{\partial t}\left(\frac{M_a}{TR}p_{ga}\right)=\frac{M_a}{RT}\frac{\partial p_g}{\partial t}-\frac{M_a p_g}{RT^2}\frac{\partial T}{\partial t}-\frac{M_a}{RT}\frac{\partial p_{gw}}{\partial p_c}\frac{\partial p_c}{\partial t}+\frac{M_a}{R\theta}\left(\frac{p_{gw}}{T}-\frac{\partial p_{gw}}{\partial T}\right)\frac{\partial T}{\partial t}, \tag{42}$$

$$\nabla\left(\frac{p_{gw}}{p_g}\right)=\frac{1}{p_g}\frac{\partial p_{gw}}{\partial p_c}\nabla p_c-\frac{p_{gw}\nabla p_g}{\left(p_g\right)^2}, \tag{43}$$

and using the Galerkin's method (weighted residuals) one can finally obtain the governing equations written in matrix form as follows:

$$\mathbf{C}\frac{\partial \mathbf{x}}{\partial t}+\mathbf{K}\mathbf{x}=\mathbf{F}, \tag{44}$$

with $\mathbf{x}=\begin{Bmatrix}\mathbf{p}_g\\ \mathbf{p}_c\\ \mathbf{T}\\ \mathbf{u}\end{Bmatrix}$, $\mathbf{K}=\begin{bmatrix}\mathbf{K}_{gg} & \mathbf{K}_{gc} & \mathbf{K}_{gT} & \mathbf{0}\\ \mathbf{K}_{cg} & \mathbf{K}_{cc} & \mathbf{K}_{cT} & \mathbf{0}\\ \mathbf{K}_{Tg} & \mathbf{K}_{Tc} & \mathbf{K}_{TT} & \mathbf{0}\\ \mathbf{K}_{ug} & \mathbf{K}_{uc} & \mathbf{K}_{uT} & \mathbf{K}_{uu}\end{bmatrix}$,

$$\mathbf{C}=\begin{bmatrix}\mathbf{C}_{gg} & \mathbf{C}_{gc} & \mathbf{C}_{gT} & \mathbf{C}_{gu}\\ \mathbf{C}_{cg} & \mathbf{C}_{cc} & \mathbf{C}_{cT} & \mathbf{C}_{cu}\\ \mathbf{C}_{Tg} & \mathbf{C}_{Tc} & \mathbf{C}_{TT} & \mathbf{C}_{tu}\\ \mathbf{0} & \mathbf{0} & \mathbf{0} & \mathbf{0}\end{bmatrix} \text{ and } \mathbf{F}=\begin{Bmatrix}\mathbf{f}_g\\ \mathbf{f}_c\\ \mathbf{f}_T\\ \mathbf{f}_u\end{Bmatrix}.$$

The terms of the matrices **K**, **C** and **F** are presented in Appendix A.

4 Staggered analysis of the problem

The coupled system of differential equations (44) can be solved numerically using the generalized method also known as the generalized midpoint role. In the model the transport phenomenon are coupled with the mechanical behaviour in staggered way. It is stated that the coupling terms, $\mathbf{C}_{gu}$, $\mathbf{C}_{cu}$ and $\mathbf{C}_{Tu}$ have relatively small influence to the solutions and are negligible. Still the effect of mechanical properties can be taken into account on the transport phenomena by an update of the transport parameters such as the permeability on the basic of the results of the previous steps in terms of mechanical stresses, strains and internal state variables such as cracks. This kind of coupling or staggered approach bring about some advantages. First of all the numerical stability of the analysis will be improved. For instance the transport phenomenon can be calculated using different elements than the mechanical behaviour. Second and as consequence of the first advantage

the calculation time will be obviously decreased. Finally it will be possible to study the results easier and with more insight. The influence of parameters involved within this problem will be more obvious. The objective is to couple the results obtained solving the transport phenomenon to already available and most sophisticated mechanical FEM models.
Up to now, calculations were performed of the coupled transport phenomena. Coupling to the mechanical behaviour is foreseen for 2005-2006.

5 Analysis of the numerical results

The coupled system of differential equation (44) describing only the transport phenomenon was solved numerically using the computer programme FEMLAB, an interactive environment to model single and coupled phenomenon based on partial differential equations. As a first attempt, the approach by Majorana et al [8], setting C_w=0 was followed. A one-dimensional example has been solved which deals with a concrete wall of 40 cm thickness. The initial conditions applied in this example at time instant t=0 are p_g=p_{g0}, p_c=p_{c0}, T=T_0. The Dirichlet boundary conditions are p_g=p_{g0} on Γ_g, p_c=p_{c0} on Γ_c, T=T_0 on Γ_T, and the Neumann boundary conditions are for the water flux (free water and vapour water) q_w+q_{gw}=$\beta_c(\rho_{gw}$-$\rho_{gw\infty})$ on Γ_w, for the gas flux q_{ga}=0 on Γ_g, for the heat transfer q_T=$\alpha_c(T$-$T_\infty)$ on Γ_T. This wall has been subjected to transient heating from one side shown in Figure 3: (left). This Figure shows that temperature increases within very short time up to 1000 °C. at the other side the temperature is kept constant at T_0=20 °C. The main characteristic parameters of the material employed in the calculations are chosen from reference [6].

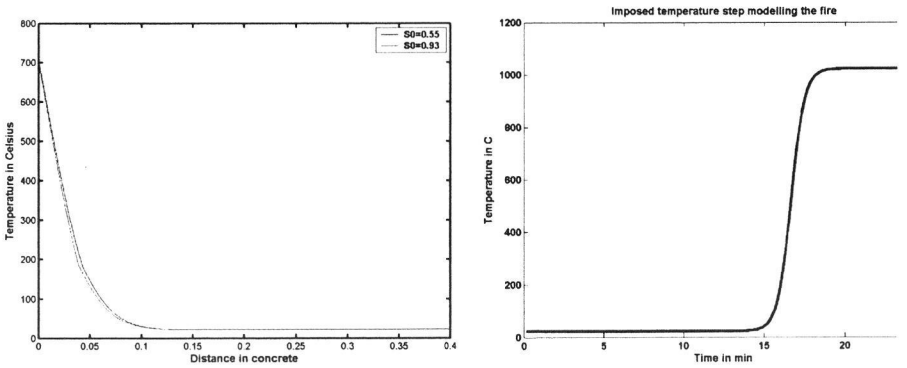

Figure 3: Imposed temperature (left) and temperature of the concrete wall after 26 minutes (right)

The problem is solved for two cases of different initial saturation degrees 55% and 93%. Figure 3: (right) shows the temperature in the concrete wall after about 26 minutes. This figure shows that during this time the initial temperature of the wall has changed with the minimum temperature as

initial temperature and the maximum temperature about 700 °C. One can see in this figure that the difference between the temperatures for two different initial saturation degrees is very small. That means that so far the initial saturation degree hasn't too much influence on the temperature.

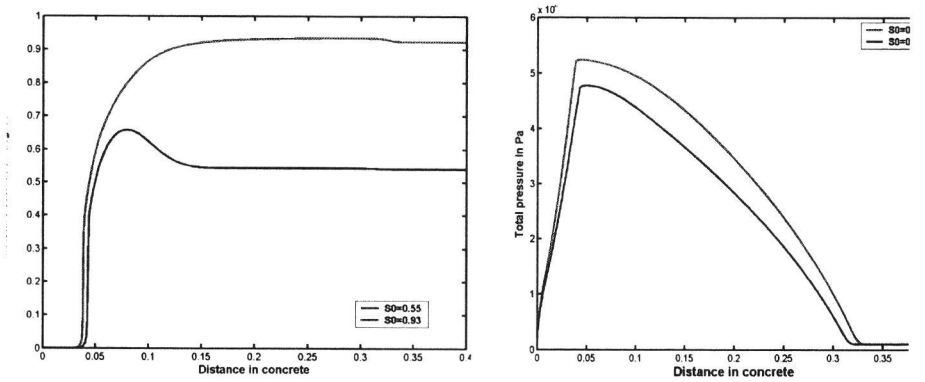

Figure 4: Saturation degree (left) and gas pressure in the concrete wall after 26 minutes (right)

The change of the saturation degree in the concrete wall is shown for both initial saturation degree in Figure 4: (left). This figure shows that the change of the saturation degree especially in the case of concrete with low initial saturation degree is considerable high. This change is even in contrast to temperature perceptible deep inside the concrete wall about 34 centimetre. One can see in Figure 4: (right) that the gas pressure is also changed as deep inside the wall as saturation degree.

6 Ongoing and future research

Validation of the model is the main part of this ongoing research. Previous to the validation, the material parameters will be improved and the staggered coupling of the transport phenomenon with the mechanical behaviour needs to be realised. In our ongoing and future work, we are focusing on the following challenges:

- Improving the material parameters and further implementation in FEMLAB;
- Coupling of the transport phenomenon calculated by FEMLAB with an FEM programme able to calculate the mechanical behaviour, for example DIANA;
- Comparison of the results of the final so-called staggered analysed system with the results of the other numerical programs such as HITECOSP [3], able to model the spalling of concrete;
- Validation of the results using the experimental results.

7 Conclusions

The phenomenon spalling of concrete at elevated temperatures was studied. Five manifestations of spalling of concrete were introduced. These are violent spalling, sloughing-off spalling, corner spalling, explosive spalling and post-cooling spalling. The mechanisms which lead to spalling have been explained. Pore pressure, thermal gradient, different thermal expansion between aggregate and cement paste, different thermal expansion between concrete and reinforcement bars and the change of the material properties due to temperature are the main factors influencing the spalling.
To analyse the phenomenon of concrete spalling a fully coupled multi-phase hydro-thermal-mechanical model was introduced, based on the existing Hitecosp model [3]. Concrete was modelled as a three-phase porous material at high temperature. The three phases within this model are solid phase, liquid phase and gas phase. Phase changes are taken into account.
The constitutive relationships and the thermodynamic state equations describing the real behaviour of concrete were discussed. The governing equations that describe the behaviour of concrete as a three-phase porous material at high temperatures are presented. These equations were found by full integration of the mass, energy and momentum balance equations. The final form of the governing equations, choosing gas pressure p_g, capillary pressure p_c, temperature T and displacement vector of the solid matrix $\mathbf{u}$ as primary state variables, were derived. The coupled system of differential equations describing only the transport phenomenon coupling three gas pressure p_g, capillary pressure p_c and temperature T were solved using FEMLAB. A one-dimensional example has been solved which deals with a concrete wall exposed to a fast temperature rise up to 1000 °C. The temperature, saturation degree and gas pressure in the concrete wall have been presented for two different initial saturation degrees. These results are physically reasonable. It shows that inside concrete the moisture content has a minor effect on the temperature distribution within the investigated range. The further steps of this research are firstly to improve the material parameters used within this model, second to couple this model to an FEM programme capable describing the mechanical behaviour and finally to validate the final results. The latest will be done using the experimental results and the results obtained by other recently developed models predicting the concrete spalling.

References

[1] Lewis, R.W., B. A. Schrefler, 'The Finite Element Method in the Static and Dynamic Deformation and Consolidation of Porous Media', Second Edition.

[2] Bazant, Z.P., W. Thonguthai (1978), 'Pore pressure and drying of concrete at high temperature', J. Engng. Mech. Div. ASCE, 104, 1059-1079

[3] Gawin, D., C. E. Majorana and B. A. Schreßer, (1996) 'Hygro- thermic and mechanical behaviour of concrete at high temperatures', in *Advances in Computational Mechanics*, Z. Wanxie, C. Gengdong and L. Xikui eds, Int. Academic Publishers, Beijing, pp. 221-242.

[4] Breunese, A.J., J.H.H. Fellinger (2003), 'Tensile properties of concrete during fire', ECI Conference Advances in Cement and Concrete IX, Copper Mountain, Colorado, 10-14 Agust.

[5] Khoury, G.A., C.E. Majorana (2001), 'Modelling of concrete spalling in fire', 15th AIMETA Congress of Theoretical and Applied Mechanics, Taormina, 26-29 September.

[6] Gawin, D., F. Pesavento, B.A. Schrefler, (2003) 'Modelling of hygro-thermal behaviour of concrete at high temperature with thermo-mechanical and mechanical material degradation", CMAME, 192, pp.1731-1771.

[7] Harmathy, T. Z. (1970), ' Thermal Properties of Concrete at Elevated Temperatures'. in *Journal Materials* (coden JMLSA), vol. 5, no. 1, American Society Testing Materials, pp. 47-74.

[8] Gawin, D., C. E. Majorana and B. A. Schreßer (1999), 'Numerical analysis of hygro-thermic and damage of concrete at high temperature', Mech. Cohes.-Frict. Mater. 4, pp. 37-74.

Appendix A: Terms of the matrices

The terms of the matrices **K**, **C** and **F** are

$$\mathbf{K}_{uT} = \int_{\Omega} \mathbf{B}^T \left(\mathbf{D}_e \mathbf{m}^T \left(\frac{\beta_s}{3} \right) \mathbf{N}_T \right) d\Omega \,,\; \mathbf{K}_{uu} = -\int_{\Omega} \mathbf{B}^T \mathbf{D}_e \mathbf{B} d\Omega \,,$$

$$\mathbf{f}_u = -\int_{\Omega} \mathbf{B}^T \left(\mathbf{D}_e \boldsymbol{\varepsilon}_0 \right) d\Omega - \int_{\Gamma_u^q} \mathbf{N}_u^T \bar{\mathbf{t}} d\Gamma_u^q - \int_{\Omega} \mathbf{N}_u^T \left[(1-n)\rho_s + nS_w \rho_w + nS_g \rho_g \right] \mathbf{g} d\Omega$$

$$, \mathbf{C}_{gg} = \int_{\Omega} \mathbf{N}_p^T S_g \left(\frac{\alpha - n}{K_s} \rho_{ga} + n \frac{M_a}{RT} \right) \mathbf{N}_p d\Omega \,,$$

$$\mathbf{C}_{gc} = \int_{\Omega} \mathbf{N}_p^T \left[-\frac{\alpha - n}{K_s} S_w S_g \rho_{ga} \mathbf{N}_p - \rho_{ga} \left(n + \frac{\alpha - n}{K_s} p_c S_g \right) \left(\frac{\partial S_w}{\partial p_c} \mathbf{N}_p \right) - n S_g \frac{M_a}{RT} \frac{\partial p_{gw}}{\partial p_c} \mathbf{N}_p \right] d\Omega$$

$$,$$

$$\mathbf{C}_{gT} = \int_{\Omega} \mathbf{N}_p^T \left[-\rho_{ga} \left(n + \frac{\alpha - n}{K_s} p_c S_g \right) \frac{\partial S_w}{\partial T} \mathbf{N}_T - \rho_{ga} \beta_s (\alpha - n) S_g \mathbf{N}_T \right] d\Omega$$

$$+ \int_{\Omega} \mathbf{N}_p^T \left[n S_g \frac{M_a}{RT} \left(\frac{p_{gw}}{T} - \frac{\partial p_{gw}}{\partial T} \right) \mathbf{N}_T - n S_g \frac{M_a p_g}{RT^2} \mathbf{N}_T \right] d\Omega$$

$$+ \int_{\Omega} \mathbf{N}_p^T \left[\frac{\rho_{ga} S_g}{\rho_s} \left((1-n) \frac{\partial \rho_s}{\partial \Gamma_{dehydr}} \frac{\partial \Gamma_{dehydr}}{\partial T} + \frac{\partial m_{dehydr}}{\partial T} \right) \mathbf{N}_T \right] d\Omega,$$

$$\mathbf{C}_{gu} = \int_{\Omega} \mathbf{N}_p^T \left[\alpha S_g \rho_{ga} \mathbf{m}^T \mathbf{L} \mathbf{N}_u \right] d\Omega \,,$$

$$\mathbf{K}_{gg} = \int_{\Omega} \left(\nabla \mathbf{N}_p \right)^T \left[\rho_{ga} \frac{\kappa k_{rg}}{\mu_g} \left(\nabla \mathbf{N}_p \right) \right] d\Omega + \int_{\Omega} \left(\nabla \mathbf{N}_p \right)^T \left[\rho_g \frac{M_a M_w}{M_g^2} \mathbf{D}_g \left(\frac{p_{gw}}{\left(p_g \right)^2} \nabla \mathbf{N}_p \right) \right] d\Omega$$

$$, \mathbf{K}_{gc} = -\int_{\Omega} \left(\nabla \mathbf{N}_p \right)^T \left[\rho_g \frac{M_a M_w}{M_g^2} \mathbf{D}_g \left(\frac{1}{p_g} \frac{\partial p_{gw}}{\partial p_c} \nabla \mathbf{N}_p \right) \right] d\Omega \,,$$

$$\mathbf{K}_{gT} = -\int_{\Omega} \left(\nabla \mathbf{N}_p \right)^T \left[\rho_g \frac{M_a M_w}{M_g^2} \mathbf{D}_g \left(\frac{1}{p_g} \frac{\partial p_{gw}}{\partial p_c} \nabla \mathbf{N}_T \right) \right] d\Omega \,,$$

$$\mathbf{f}_g = \int_\Omega \left(\nabla \mathbf{N}_p\right)^T \left(\rho_{ga} \frac{\kappa k_{rg}}{\mu_g} \rho_g \mathbf{g} \right) d\Omega - \int_{\Gamma_g^q} \mathbf{N}_p^T q_{ga} d\Gamma_g^q ,$$

$$\mathbf{C}_{cg} = \int_\Omega \mathbf{N}_p^T \left[\left(\frac{\alpha - n}{K_s} \left(\rho_{gw} S_g + \rho_w S_w \right) + \frac{\rho_w S_w n}{K_w} \right) \mathbf{N}_p \right] d\Omega ,$$

$$\mathbf{C}_{cc} = -\int_\Omega \mathbf{N}_p^T \left[S_w \left(\frac{\alpha - n}{K_s} \left(\rho_{gw} S_g + \rho_w S_w \right) + \frac{\rho_w n}{K_w} \right) \mathbf{N}_p \right] d\Omega + \int_\Omega \mathbf{N}_p^T \left[S_g n \frac{M_w}{RT} \frac{\partial p_{gw}}{\partial p_c} \mathbf{N}_p \right] d\Omega$$

$$+ \int_\Omega \mathbf{N}_p^T \left[\left(\frac{\alpha - n}{K_s} \left(\rho_{gw} S_g p_c + \rho_w S_w p_w - \rho_w S_w p_c \right) + n \left(\rho_w - \rho_{gw} \right) \right) \left(\frac{\partial S_w}{\partial p_c} \mathbf{N}_p \right) \right] d\Omega$$

,

$$\mathbf{C}_{cT} = -\int_\Omega \mathbf{N}_p^T \left[\left(\beta_s (\alpha - n) \left(\rho_{gw} S_g + \rho_w S_w \right) + n \beta_w \rho_w S_w \right) \mathbf{N}_T \right] d\Omega$$

$$+ \int_\Omega \mathbf{N}_p^T \left[S_g n \frac{M_w}{RT} \left(\frac{\partial p_{gw}}{\partial T} - \frac{p_{gw}}{\theta} \right) \mathbf{N}_T \right] d\Omega$$

$$+ \int_\Omega \mathbf{N}_p^T \left[\left(\frac{\alpha - n}{K_s} \left(\rho_{gw} S_g p_c + \rho_w S_w p_w - \rho_w S_w p_c \right) + n \left(\rho_w - \rho_{gw} \right) \right) \left(\frac{\partial S_w}{\partial T} \mathbf{N}_T \right) \right] d\Omega$$

$$+ \int_\Omega \mathbf{N}_p^T \left[\frac{1 - n}{\rho_s} \left(\rho_w S_w + \rho_{gw} S_g \right) \frac{\partial \rho_s}{\partial \Gamma_{dehydr}} \frac{\partial \Gamma_{dehydr}}{\partial T} \mathbf{N}_T \right] d\Omega$$

$$+ \int_\Omega \mathbf{N}_p^T \frac{\rho_w S_w + \rho_{gw} S_g - \rho_s}{\rho_s} \frac{\partial m_{dehydr}}{\partial T} \mathbf{N}_T d\Omega ,$$

$$\mathbf{C}_{cu} = \int_\Omega \mathbf{N}_p^T \left[\alpha \left(\rho_{gw} S_g + \rho_w S_w \right) \mathbf{m}^T \mathbf{L} \mathbf{N}_u \right] d\Omega ,$$

$$\mathbf{K}_{cg} = -\int_\Omega \left(\nabla \mathbf{N}_p\right)^T \left[\rho_g \frac{M_a M_w}{M_g^2} \mathbf{D}_g \left(\frac{p_{gw}}{\left(p_g\right)^2} \nabla \mathbf{N}_p \right) \right] d\Omega$$

$$+ \int_\Omega \left(\nabla \mathbf{N}_p\right)^T \left(\rho_{gw} \frac{\kappa k_{rg}}{\mu_g} \left(\nabla \mathbf{N}_p \right) \right) d\Omega + \int_\Omega \left(\nabla \mathbf{N}_p\right)^T \left(\rho_w \frac{\kappa k_{rw}}{\mu_w} \left(\nabla \mathbf{N}_p \right) \right) d\Omega ,$$

$$\mathbf{K}_{cc} = \int_{\Omega} \left(\nabla \mathbf{N}_p\right)^T \left[\rho_g \frac{M_a M_w}{M_g^2} \mathbf{D}_g \left(\frac{1}{p_g} \frac{\partial p_{gw}}{\partial p_c} \nabla \mathbf{N}_p \right) \right] d\Omega - \int_{\Omega} \left(\nabla \mathbf{N}_p\right)^T \left(\rho_w \frac{\boldsymbol{\kappa} k_{rw}}{\mu_w} \left(\nabla \mathbf{N}_p\right) \right) d\Omega$$

$$, \mathbf{K}_{cT} = -\int_{\Omega} \left(\nabla \mathbf{N}_p\right)^T \left[-\rho_g \frac{M_a M_w}{M_g^2} \mathbf{D}_g \left(\frac{1}{p_g} \frac{\partial p_{gw}}{\partial T} \nabla \mathbf{N}_T \right) \right] d\Omega ,$$

$$\mathbf{f}_c = \int_{\Omega} \left(\nabla \mathbf{N}_p\right)^T \left(\rho_{gw} \frac{\boldsymbol{\kappa} k_{rg}}{\mu_g} \left(\rho_g \mathbf{g}\right) + \rho_w \frac{\boldsymbol{\kappa} k_{rw}}{\mu_w} \left(\rho_w \mathbf{g}\right) \right) d\Omega$$

$$- \int_{\Gamma_w^q} \mathbf{N}_p^T \left(q_w + q_{gw} + \beta_c \left(\rho_{gw} - \rho_{gw\infty} \right) \right) d\Gamma_w^q ,$$

$$\mathbf{C}_{Tg} = -\int_{\Omega} \mathbf{N}_T^T \Delta H_{vap} \left[\rho_w S_w \left(\frac{\alpha - n}{K_s} + \frac{n}{K_w} \right) \mathbf{N}_p \right] d\Omega ,$$

$$\mathbf{C}_{Tc} = \int_{\Omega} \mathbf{N}_T^T \Delta H_{vap} \left[-\rho_w \left(n - \frac{\alpha - n}{K_s} p_c S_w \right) \frac{\partial S_w}{\partial p_c} \mathbf{N}_p \right] d\Omega$$

$$+ \int_{\Omega} \mathbf{N}_T^T \Delta H_{vap} \left[\rho_w \left(\frac{\alpha - n}{K_s} S_w^2 + \frac{n S_w}{K_w} \right) \mathbf{N}_p \right] d\Omega ,$$

$$\mathbf{C}_{TT} = \int_{\Omega} \mathbf{N}_T^T \left(\rho C_p\right)_{eff} \mathbf{N}_T d\Omega + \int_{\Omega} \mathbf{N}_T^T \Delta H_{vap} \left[\rho_w S_w \left((\alpha - n) \beta_s + n \beta_w \right) \mathbf{N}_T \right] d\Omega$$

$$+ \int_{\Omega} \mathbf{N}_T^T \Delta H_{vap} \left[-\rho_w \left(n - \frac{\alpha - n}{K_s} p_c S_w \right) \frac{\partial S_w}{\partial T} \mathbf{N}_T \right] d\Omega + \int_{\Omega} \mathbf{N}_T^T \left[\Delta H_{vap} \frac{\partial m_{dehydr}}{\partial T} \mathbf{N}_T \right] d\Omega$$

$$- \int_{\Omega} \mathbf{N}_T^T \left[\Delta H_{vap} \frac{\rho_w S_w (1 - n)}{\rho_s} \frac{\partial \rho_s}{\partial \Gamma_{dehydr}} \frac{\partial \Gamma_{dehydr}}{\partial T} \mathbf{N}_T \right] d\Omega$$

$$- \int_{\Omega} \mathbf{N}_T^T \left[\Delta H_{vap} \frac{\rho_w S_w}{\rho_s} \frac{\partial m_{dehydr}}{\partial T} \mathbf{N}_T \right] d\Omega - \int_{\Omega} \mathbf{N}_T^T \left[\Delta H_{dehydr} \frac{\partial m_{dehydr}}{\partial T} \mathbf{N}_T \right] d\Omega ,$$

$$\mathbf{C}_{Tu} = -\int_{\Omega} \mathbf{N}_T^T \Delta H_{vap} \alpha \rho_w S_w \mathbf{m}^T \mathbf{L} \mathbf{N}_u d\Omega ,$$

$$\mathbf{K}_{Tg} = \int_{\Omega} \left(\nabla \mathbf{N}_T\right)^T \left[\Delta H_{vap} \left(\rho_w \frac{\boldsymbol{\kappa} k_{rw}}{\mu_w} \left(-\nabla \mathbf{N}_p\right) \right) \right] d\Omega ,$$

$$\mathbf{K}_{Tc} = \int_{\Omega} (\nabla \mathbf{N}_T)^T \left[\Delta H_{vap} \left(\rho_w \frac{\kappa k_{rw}}{\mu_w} (\nabla \mathbf{N}_p) \right) \right] d\Omega ,$$

$$\mathbf{K}_{TT} = \int_{\Omega} (\nabla \mathbf{N}_T)^T \lambda_{eff} \nabla \mathbf{N}_T d\Omega + \int_{\Omega} \mathbf{N}_T^T \left[\left(n S_w \rho_w C_{pw} \frac{\kappa k_{rw}}{\mu_w} (-\nabla p_g + \nabla p_c + \rho_w \mathbf{g}) \right) \cdot \nabla \mathbf{N}_T \right] d\Omega$$
$$+ \int_{\Omega} \mathbf{N}_T^T \left[\left(n S_g \rho_g C_{pg} \frac{\kappa k_{rg}}{\mu_g} (-\nabla p_g + \rho_g \mathbf{g}) \right) \cdot \nabla \mathbf{N}_T \right] d\Omega,$$

and

$$\mathbf{f}_T = -\int_{\Omega} (\nabla \mathbf{N}_T)^T \left[\Delta H_{vap} \left(\rho_w \frac{\kappa k_{rw}}{\mu_w} (\rho_w \mathbf{g}) \right) \right] d\Omega$$
$$- \int_{\Gamma_T^q} \mathbf{N}_T^T \left(q_T + \alpha_c (T - T_\infty) + e\sigma_0 (T^4 - T_\infty^4) \right) d\Gamma_T^q ,$$

With $\mathbf{B} = \mathbf{L}\mathbf{N}_u$, $\mathbf{K}_{ug} = \int_{\Omega} \mathbf{B}^T \alpha (\mathbf{m}^T \mathbf{N}_p) d\Omega$ and $\mathbf{K}_{uc} = -\int_{\Omega} \mathbf{B}^T \alpha (\mathbf{m}^T S_w \mathbf{N}_p) d\Omega$.

In these expressions $\mathbf{N}_u$, $\mathbf{N}_p$ and $\mathbf{N}_T$ are the finite element shape functions and $\mathbf{m} = \{1,1,1,0,0,0\}^T$ is the vector form of the identity tensor **I**.

Fire safety aspects in cultural heritage – a case study in historical Delft

Maria Öhlin Lostetter
TNO, Centre for Fire Research, Delft, the Netherlands
Email: maria.ohlin@tno.nl, Phone: +31 15 276 3493

Arnoud Breunese
TNO, Centre for Fire Research, Delft, the Netherlands

Fire is an important threat to cultural heritage. Therefore 12 fire laboratories and consultants across the EU have joined together for the European Thematic-Network Fire Risk Evaluation to European Cultural Heritage (Fire-Tech). The final goal of this thematic network was to develop a decision making process in order to choose the most cost-effective fire safety measures when upgrading an object. This article presents the results of one of the case studies done in Fire-Tech. This case study consists of testing the decision making process on a building in the Netherlands. The building that was chosen is the Nieuwe Kerk (New Church) in Delft, which consists of three parts, the main church, the tower and a small shop. The total decision model involves seven steps, each will be presented in the article: Analysis of goal and budget; Analysis of the present level of fire safety; Risk Analysis; Possible fire safety actions; Decision model; Decision making; Results and comparison with existing practice. Emphasis will be laid on the risk analysis and on the decision making model. In the risk analysis an event tree approach was used combined with modelling of the fire spread, smoke spread and evacuation calculations. This showed that in the current configuration if there was a fire in the building there was a probability of 35% that people would be stuck in the tower and could only be rescued with a fire ladder and that there was a probability of 20% that the entire church would be destroyed. In the decision making step a number of measures were compared in order to find the most cost-effective solutions for an improvement of the fire safety of the church. This was done using an "Analytical Hierarchy Process" (AHP). In the AHP a number of measures can be compared in order to see which one has the most influence on a top goal (in this study defined as "Fire Safety"). In the AHP "grades of implementation" can be defined for existing fire safety measures as well as planned measures. With these values and the costs of each measure, the most cost-effective solutions to upgrade the fire safety of the building can be realized. This study showed that a number of the top measures, identified through the AHP, are organisational measures and are consequently easy and cheap to apply. This study is to be seen as an example, meaning a number of assumptions concerning the building itself and the acceptance criteria should be validated.

Key words: Cultural Heritage, Fire Safety, Risk analysis, Decision Model

1 Introduction

In the European project Fire-Tech the final goal is to develop an evaluation tool, taking into account all parameters expected to influence decisions when upgrading the fire safety of a cultural heritage building.

A case study into the fire safety of the Nieuwe Kerk in Delft has been made as a part of the Fire-Tech project in order to test the decision model designed in the project. This study includes a number of steps, among other a risk analysis model combined with fire safety engineering and a final decision making process, both that will be presented in this article.

This case study is to be seen as an example of the decision model, meaning a number of assumptions concerning the building itself and the acceptance criteria (i.e the acceptable size of the area within the building that is damaged during fire) may not be correct or validated.

2 Fire-Tech

Twelve fire laboratories and consultants across the EU have joined together for the European Thematic Network Fire Risk Evaluation to European Cultural Heritage (Fire-Tech). This Thematic Network, under the leadership of the University of Ghent, started in 2002 and will end in the beginning of 2005.

The main objective of the thematic network is to develop a decision model taking into account all parameters expected to influence design decisions when looking at the fire protection of cultural heritage buildings. In order to do so a number of pre-steps (or working groups) are necessary. These working groups focus on:

- Existing practices and regulations for fire safety of cultural heritage buildings
- Analyses of fires in cultural heritage
- Fire behaviour of archaic materials
- Fires safety techniques
- Risk analysis of cultural heritage

All information gathered from these steps has been put together in the decision model. A number of case studies have then been performed in order to test and improve the model.

All information and results gathered in the project are accessible in a database on www.firetech.be and will be collected in a booklet, to be published in 2005.

3 Nieuwe Kerk, Delft

The Nieuwe Kerk is situated on the Market Square of the town Delft. It is one of the most important churches in the Netherlands as it contains the monument of William the Silent and the tomb of the Dutch royal family. The total length of the church is 100m and it also has an over 100m high tower. The church and the tower are open to the public during daytime all days except Sundays or on special occasions. On Sundays the church is used for religious service.

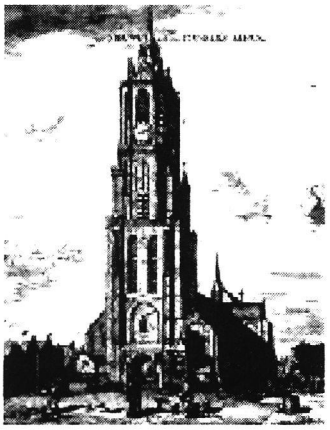

Figure 1: Engraving from 1675. "De Nieuwe Kerk in de 17e eeuw". (http://www.monument.delft.nl)

The tower is 109 m high and contains a staircase that is around 2m wide and has 360 stair steps. The tower has one opening to the shop downstairs, and three openings to higher platforms. There are no external staircases from the higher platforms.

The total ground floor area of the building is approximately 2025 m^2. The ground floor consists of two rooms, one 5 * 5 m^2 large shop and the main church that is approximately 80 * 25 m^2. The main construction of the church is made of masonry and the roof in the church is made of wood. The fire load in the church consists mainly of the wooden benches and the timber of the load-bearing structure (including the roof) of the church itself. In the shop the flammable contents are paper, desks, presents etc. The shop is not of cultural heritage value.

It is assumed that the maximum number of people in the tower, the shop, and the church during public opening hours will be 50, 25, and 100 respectively.

The maximum number of people that will be in the church during a religious service is assumed to be six hundred. However the church occupancy can vary between 300 and 1500. In the rare occasion of a funeral of the Dutch royal family, up to 2000 people will be present in the church.

4 Decision Model

The decision model, developed within Fire-Tech, involves four steps: First of all an analysis of the goal of the study has to be made and the budget available has to be identified (4.1). Thereafter an analysis of the present level of safety of the building will be performed, including a risk analysis (4.2). After this step possible fire safety actions to improve the fire safety of the building will be identified (4.3). Finally the decision making will be performed using an hierarchy model and conclusions will be drawn as to the most cost-effective measures in the building (4.4).

4.1 Analysis of Goal and Budget

In the first step one needs to identify the goal of the study (i.e. what is the need?). The assumed need in the Nieuwe Kerk is to minimize any damage by fire to the building and to people inside the building. One also needs to identify the time and money available for an eventual increase of the fire safety level of the building and for the study. The time available and the money available are not an issue in this example, although cost effectiveness of possible fire safety measures will be considered.

4.2 Analysis of the present level of fire safety

To analyse the present level of fire safety, four points need to be addressed. The first is identifying the fires that have taken place in similar buildings, thereafter the behaviour of eventual critical ancient materials present in the church needs to be analysed. Furthermore the regulations that govern the use of the church need to be clear, the fire safety measures present in the church need to be identified. The information in this chapter can be used to perform a risk analysis (4.3).

4.2.1 Similar fires

In high buildings such as churches falling heavy objects such as church bells or parts of the roof could pose a problem for the firemen's intervention and for the historic contents in the church such as the tomb of William the Silent. Causes of fires in cultural heritage buildings can be seen in the FireTech WG2 report [1].

From a Dutch case, the *Sint Petruskerk* (Saint Peter's Church) in Oisterwijk, it appears that the evacuation of people in the church can be a problem. Close inspection reveals that it took the fire

services approximately 20 minutes to evacuate 100 people with limited mobility from the church during a fire.

4.2.2 Behaviour of archaic materials

More information about the fire behaviour of critical parts of the church, such as the timber roof structure, the masonry walls, the wooden church benches and historical items in the church are needed. In the Fire-Tech project, information on fire behaviour of such material was gathered. Additionally, information was gathered about fire resistance of old doors. This can be used when old doors are important to the compartmentation of the fire, e.g. in the case of the *Nieuwe Kerk* the fire resistance of a separating door between the tower and the shop may be relevant. Also the fire resistance of the exterior doors can be of importance to avoid the spreading of exterior fires (due to arson) to the interior.

4.2.3 Regulations applicable

This church is situated in Delft, the Netherlands. In the Netherlands monuments fall under the "monuments law" and under the Dutch building decree for existing buildings. If a change in a monument needs to be made, a permit is required from the local government, who should consult the Netherlands department for conservation. Also other interests such as public health and safety have to be taken into consideration before the local government will decide on eventual changes.

4.2.4 Fire safety measures present

A number of fire safety measures are present in the church, such as sprinklers. The sprinklers are situated under the roof in the church. They have however to be opened manually by the fire services and vary in age from 70 years old to new. No detection or sprinklers are available in the shop. The fire services have equipment to rescue people from the lowest platform of the tower.

4.3 Risk analysis

Seven steps are involved in the risk analysis. The first step is to identify the objectives of the risk analysis and the acceptance criteria. Thereafter the fire scenarios have to be identified. As a third step the events that can take place during a fire will be identified, and as a fourth step the event tree will be designed. Thereafter the quantification of the fire development and escape times should be made. Using all earlier steps the assessment of damage will be made and finally conclusions will be drawn. Hereafter the 7 steps are discussed in detail. In this study the risk analysis will be performed on the church as it is now to find problem areas. However a risk analysis can also be performed after having identified problem areas and thus including a number of fire safety measures. Hereafter the 7 steps are discussed in detail.

4.3.1 Objectives and Acceptance criteria

No irreversible damage to persons (no persons even slightly injured) and the probability of having damage to more than 4% (in this case 80m²) of the building should be less than 10% in the case of a fire. Damage to the tower will not be taken into account in this report. These acceptance criteria have been chosen by TNO for the purpose of the study and have not been confirmed by the responsible authorities.

4.3.2 Definition of Fire Scenarios

- Scenario 1: fire in the church.

The fire in the church can be caused by arson, by candles or by faulty installations. It is assumed that an initial fire, in a church bench, will develop to surrounding church benches according to a medium growth rate (0,012kW/s²). The fire in the church will be assumed to be fuel limited. According to the Natural fire safety concept (NFSC) [2] an office building will have a RHR of 250kW/m² if the fire is fuel bed controlled. Thus it will be assumed that when 250kW is reached, 1m² is involved in the fire. The fire will be in the growth phase at least during the first twenty minutes, because of the size of the building. Using a zone model to calculate smoke temperatures Halfill [3]calculations showed that the smoke temperature in the church was not high enough to ignite the wooden structure of the roof during the first 20 minutes of the fire.

- Scenario 2: fire in the shop.

The fire in the shop could be caused by a faulty installation or by arson. A rapid fire development is suggested for a shop in NFSC. The fire in the shop will be assumed to have a RHR of 250 kW/m² when it is fuel bed controlled. The amount of combustible material is less than in a normal book, clothes or souvenir shop and therefore this value will be seen as sufficient. The growth phase will go on until a value of approximately 6,25 MW is reached. When the fire reaches this level it is assumed that the fire will spread from the shop compartment to the church, where the fire continues according to a medium fire growth. The fire in the shop is assumed to be stable until 70% of the fuel is burned, this will be after the first 20 minutes.

4.3.3 Selection of Events

As a starting point a developing fire is assumed. Thereafter selection of events (or branches for the event tree) has been done as follows: Fire location - > Time of day -> Fire detected - > Extinguished by staff - > Sprinkler control the fire - > Fire brigade control the fire

Fire location: It is assumed that the probability of the fire to start in the shop is 50% and in the church is 50%.

Time of day: The probability of a daytime fire or a night time fire will be assumed as 70-30 as more people are present during the day than during the night.

Fire detected at early stage: An early stage means at a time early enough to allow extinguishing by staff. The probability of detecting the fire in the church during an early stage will be 70% during the day, and 0% during the night. The probability of detecting the fire in the shop during an early stage will be 70% during the day. During the night because of the burglary alarm in the shop a value of probability of early detection of 50% will be used.

Extinguished by staff: This event only takes place during the daytime and if the fire is successfully detected in an early stage. Even though in these cases the staff is technically in the position to extinguish the fire, it is assumed that the staff has not had any fire fighting training and a value of 50% should be used.

Fire brigade to control the fire: If the fire brigade is able to control the fire the damage will not extend beyond the area where it was when the fire service's operation began to be effective. If the fire services are unsuccessful to extinguish the fire it is assumed that the fire will spread to the entire fire compartment. The probability of the fire brigade to control the fire when they arrive depends also on the detection time. If the staff detects the fire in an early stage, it is assumed that the firemen will be present and effective after 10 min and the assumed probability that they will be able to control the fire is 80%. If the fire is detected by staff at a later stage it is assumed that the firemen will be present and effective after 15min. The probability that the firemen will be able to control the fire will equally be assumed to be 80%.
During the night the time to detection of the fire depends on if passers-by see the fire or if the sprinklers already present inside the roof are activated by the fire. The church is in a busy place in the centre of Delft and it is assumed that a passer-by will see a fire and alarm the fire services within the first 15 minutes. It is then assumed that the firemen will be present and effective after 20 min. The probability that the firemen will be able to control the fire is assumed to be 50%.

4.3.4 Design of Event tree

The information above leads to the following event tree (table 1) that applies to the situation in which no additional fire safety measures are implemented.

Table 1: Event tree for no additional fire safety measures

	Place	Time	Detected Early stage	Extinguished by staff	Extinguished by Fire Brigade	Probability	Nr. Scenario
No additional measures	Shop (0.5)	Day (0.7)	Yes (0.7)	Yes (0.5)	-	0.1225	1
				No (0.5)	Yes (0.8)	0.098	2
					No (0.2)	0.0245	3
			No (0.3)		Yes (0.8)	0.084	4
					No (0.2)	0.021	5
		Night (0.3)	Yes (0.5)		Yes (0.8)	0.06	6
					No (0.2)	0.015	7
			No (0.5)		Yes (0.5)	0.0375	8
					No (0.5)	0.0375	9
	Church (0.5)	Day (0.7)	Yes (0.7)	Yes (0.5)	-	0.1225	10
				No (0.5)	Yes (0.8)	0.098	11
					No (0.2)	0.0245	12
			No (0.3)		Yes (0.8)	0.084	13
					No (0.2)	0.021	14
		Night (0.3)			Yes (0.5)	0.075	15
					No (0.5)	0.075	16

4.3.5 Quantification of Fire Development and Escape times

- Escape:

It is assumed that the staff will detect the fire after three minutes. At that time, the staff will immediately alarm the occupants, and the evacuation will start.

Church: In the church, both during religious service and during the opening hours to the public, the mobility of the occupants can be limited. Given the presence of a large escape door, and a number of other emergency exit doors, it is assumed that during religious service the church can be empty within the time it takes for a person with reduced mobility, sitting at the other end of the church to get out through the main door. The length of the church is 80 m and a speed of 0.5 m/s will be assumed. Also a time of 30 seconds will be allowed to get out of the bench row. A safe approximation of the time to escape is 5 minutes if only a normal number of persons present with reduced mobility are present.

Shop: The evacuation of the shop will be rapid, the people can escape either into the church or out the main entrance, and is assumed to be finished maximum one minute after detection of the fire.

Tower: The tower contains around 360 steps to the highest platform 300 steps to the second platform and 200 steps to the first platform. The steps are very narrow. An initial velocity of 1 step/s is taken for the first 50 steps. After that a velocity of 0.5 steps / s is used until the bottom of the staircase is reached. This means that it will take approximately 11 minutes for the people from the top floor to escape, 9 minutes for the people from the middle platform to escape and 6 minutes for the people from the first platform to escape. The church will be empty before 6 minutes during daytime and thus no congestion will take place at the exit of the tower. It is emphasized again that the actual numbers are exemplary and further validation of the underlying assumptions should be made before general conclusion are drawn.

It is assumed that the fire becomes dangerous for people in the tower because of smoke or fire in the shop when the fire is so large that the staff cannot extinguish it or when firemen cannot control the fire in the church. From this point, no exit is possible from the tower anymore. The evacuation from the tower can be completed within 14 minutes, (3 minutes detection time and 11 minutes escape) according to the calculations above. Therefore it can be safely stated that people present in the tower can always escape if a fire starts in the church if they are warned on time.

In the shop if the staff cannot extinguish the fire people will thus be trapped up in the tower waiting for escape by the high-rise ladder, or for the fire to be extinguished by the fire brigade.

- Fire Development:

The aim of quantifying the fire development is to derive information on how different fire related parameters vary with time. As said in the chapter fie scenarios, 4.3.2, according to NFSC a fuel bed controlled fire inside an office building will have a RHR of 250 kW/m^2. Thus, to make a simplification in this study, for every additional 250 kW that is produced another m^2 is assumed to be involved in the fire. In 4.3.2 a medium fire development was assumed for the church, and in the shop a rapid fire development was assumed until the entire shop was engulfed in flames, thereafter a medium fire growth rate in the church was assumed. This gives the following fire development (see figure 2), with the time represented on the horizontal axis and the area involved in the fire on the vertical axis.

4.3.6 Assessment of Damage

Combining the data from escape, fire development and the event tree the following table is obtained (table 2).

In the table, the 16 different scenarios that follow from the event tree have been characterised by the state of the fire (extinguished, controlled or total damage), the probability of occurrence of the

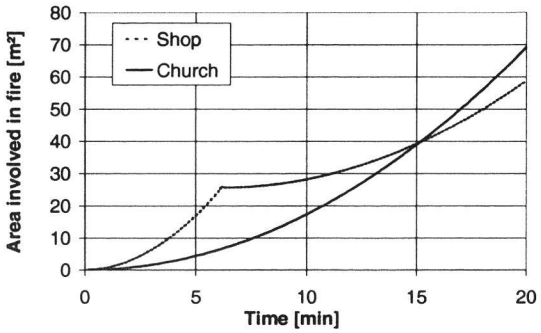

Figure 2: The area involved in the fire versus. time

Table 2: The assessment of damage

Scenario	State	Probability	Consequence [m²] Church	Consequence [m²] Shop	Consequence persons
1	Extinguish by staff	0,1225	-	11	(1)
2	Control by fire brigade	0,098	3	Total Damage	(1)
3	Total Damage	0,0245	Total Damage	Total Damage	(2)
4	Control by fire brigade	0,084	14	Total Damage	(1)
5	Total Damage	0,021	Total Damage	Total Damage	(2)
6	Control by fire brigade	0,06	3	Total Damage	None
7	Total Damage	0,015	Total Damage	Total Damage	None
8	Control by fire brigade	0,0375	33	Total Damage	None
9	Total Damage	0,0375	Total Damage	Total Damage	None
10	Extinguish by staff	0,1225	3	-	None
11	Control by fire brigade	0,098	17	-	None
12	Total Damage	0,0245	Total Damage	Total Damage	None
13	Control by fire brigade	0,084	38	-	None
14	Total Damage	0,021	Total Damage	Total Damage	None
15	Control by fire brigade	0,075	70	-	None
16	Total Damage	0,075	Total Damage	Total Damage	None

(1): Evacuation stopped after 1 min. People left in tower to be evacuated when fire is extinguished or evacuation by high ladder firemen.

(2): Evacuation stopped after 1 min. People left in tower. Evacuation by high ladder firemen.

scenario, the damaged area within the church and the shop, and the consequences for human beings. Since the event tree is based on the situation in which no additional fire safety measures are taken, this also applies to the table.

The previous table can be rearranged to give a clear picture of the probability of a category of scenarios, e.g. the probabilities for damaging a certain floor area, for trapping people in the tower, or other cumulative probabilities.
Cumulative probability versus fire damage area results in the following values in table 3.

Table 3: Probability of fire damage

Hazard	Probability
Total loss of church	22%
70m² church damaged	7,5%
30 –40 m² church damaged	12 %
10-20 m² church damaged	18%
3m² church damaged	28%
No damage to church	12,5%

Cumulative probability versus consequences for persons (i.e. being trapped in the tower) results in the following values (table 4).

Table 4: Probability of consequences for persons

Hazard	Probability
People left in tower to be evacuated by high ladder firemen.	4,5%
People left in tower to be evacuated when fire is extinguished or evacuation by high ladder firemen.	30%
None	65,5%

4.3.7 *Risk evaluation*

The acceptance criteria for this study were that no people should be injured and that the probability of having damage to more than 4% (in this case 80 m²) of the building should be less than 10% in the case of a fire.

One can see that the first acceptance criterion concerning the people can in principle be fulfilled in this case. This acceptance criterion could be checked with the fire brigade, checking how many people they can rescue with their ladder.
One can see that the second acceptance criterion cannot be fulfilled in case of any additional fire safety measures. Therefore a number of measures should be identified to improve the fire safety of the *Nieuwe Kerk*.

4.4 *Possible fire safety actions*

In this chapter a number of measures useful for the protection of people and the building will be identified. The most appropriate measures for this case are listed below in table 5. For a description of the below mentioned measures, refer to the complete report of the *Nieuwe Kerk* in Fire-Tech [4].

Table 5: Possible fire safety actions

Technical Actions	**Technical actions specific for the Nieuwe Kerk**	**Non technical actions**
Automatic fire detection	CCTV	Control of installations
Alarm systems	Burglary alarm	Limit unnecessary flammable items
Visual signals / evacuation plans		Procedures for evacuation of people
Smoke control		Training of personnel
First-aid fire fighting equipment		Contact with fire services
Sprinklers		Guides with visitors in tower
Fire Resistant glazing		"Fire Guards" during large events
Inert insulating materials		Renovation Guidelines
Intumescent materials		

5 Decision making

5.1 *Technical approach*

In this chapter, first of all the structure of the decision method has to be decided on. Questions that need consideration are: What is the main goal or policy? What are the objectives, i.e. how can the policy be attained? What strategies can be used to obtain the objectives? Finally what measures/parameters have been defined. These questions can be considered as a hierarchy, in which the level of consideration ranges from very general (e.g. main goal: fire safety) to very detailed (e.g. one of the possible measures: training of personnel). From each of the levels to the level above there is a need to set a score or an effectiveness of the measure/strategy and objective on the level above.

In the next paragraphs, the allocation and processing of score figures will be shown. The following variables will be used:

S(a,b) the score (importance or effectiveness) of a on b,

I(a,1) the normalised influence of a on the main goal,

G(a) the "grade of implementation"; the extent to which a certain measure is present and effective,

EI the "effectiveness index"; a measure for the overall fire safety,

CE_a the cost effectiveness of measure a.

5.2 *Structure of decision method*

In the following tables, all items have been numbered. The main goal is number 1, both objectives are numbers 2 and 3, the strategies are numbered 4 – 8, and finally the measures are numbered 9 – 27.

Table 6: Main goal

Main Goal	1. Fire Safety of Cultural Heritage Building

Table 7: Objectives

Objectives	2. Protect Building incl. immovable contents	3. Protect People in the building

Table 8: Strategies

Strategies	4. Avoid Ignition	5. Limit fire spread inside compartment	6. Limit fire spread outside compartment	7. Allow escape	8. Allow fire services to act

Table 9: Measures

Measures (9-13)	Sprinklers	First-aid fire fighting equipment	Automatic fire detection	Alarm systems	Visual signals / evacuation plans
(14-18)	Smoke control	Fire resistant glazing	Inert insulating materials	Intumescent materials	CCTV
(19-23)	Training of personnel	Procedures for evacuation	Fire guards during large events	Guides with visitors in tower	Control of installations
(24-27)	Guidelines during renovation	Burglary alarm	Limit flammable items	Contact with fire services	-

It should be noted that in the AHP model the influence of one measure on another is not taken into account. In the list of measures it would thus be useful to note any adverse effect one measure can have on another and take this into account when making a final selection.

Scores Objectives – Main Goal

First of all, it needs to be defined to what extent each of the objectives (protection of the building and of the people) contribute to the main goal (fire safety). In this case it is assumed that it is equally important to protect the building (and its non-moveable contents) and the people inside. Because of the national importance of the building it is chosen to attribute the same importance to the building as to the people inside it. This is an arbitrary choice. Both these objectives can also be used as main goals. The different scores will be as follows:

S(2,1) = 0,5 S(3,1) = 0,5

The score represents the relative importance/effectivity. The notation is S(objective, main goal). The scores show that the importance of both objectives on the main goal are 50% each. Analogous notation will also be used on the lower levels.

Scores Strategy - Objectives

After the decision on the scores of the objectives on the main goal has been made, the scores (effectivity) of the strategies on the objectives have to be decided on.

Concerning the first objective (protecting the building), it is assumed that strategies 4, 5, 6 and 8 are equally important. Strategy 7 has no effect, because allowing escape does not help to protect the building.

S(4,2) =0,25 S(5,2) =0,25 S(6,2) =0,25 S(7,2) =0 S(8,2) =0,25

The second objective concerns the protection of people inside the building. Here strategy 7, allowing escape, is the most important. Thereafter strategies 4, 5 and 8 are equally important. Strategy 6 is the least important. Strategy 6, limit fire spread between compartments is considered less important than the rest because the only separate compartment in the church would be the shop, but if a fire starts in the shop people will be able to get out of the church anyways. If a fire starts in the church it is assumed that people will be able to get out of the shop and the tower and out of the church. It is thus more important to limit the fire spread inside a compartment than between them.

S(4,3) =0,2 S(5,3) =0,2 S(6,3) =0,1 S(7,3) =0,3 S(8,3) =0,2

Thereafter, one lever deeper in the analysis, scores from all measures to the strategies have to be set. These scores can be seen in table 10. The scores for the previous levels were normalised (always

adding up to 1). For the scores of the measures however, a large number of scores needs to be assigned and therefore it would be impractical to normalise them right away. Instead, scores are given on a scale of 0 (no importance) – 10 (ultimate importance). These scores will be normalised hereafter.

Table 10: Scores from measures to strategies

Mea-sure / Stra-tegy	9	10	11	12	13	14	15	16	17	18	19	20	21	22	23	24	25	26	27
4	0	0	0	0	0	0	0	0	0	0	5	0	3	3	9	9	5	7	3
5	9	8	7	0	0	5	0	4	3	3	5	0	4	2	2	4	1	5	5
6	7	3	2	0	0	6	7	5	5	1	3	0	2	1	1	3	0	3	6
7	5	4	7	8	7	6	2	1	1	5	6	9	7	7	3	3	1	3	6
8	7	3	6	4	2	7	5	6	6	4	4	5	3	4	1	1	2	3	9

After all scores on all the levels have been assigned, they are normalised and influence parameters are calculated (I). Whereas a score (S) represents the importance of a low level parameter to another parameter on the level directly above, the influence parameter (I) represents the importance of the low level parameter on the top parameter (main goal). In this way, the influence of all objectives, strategies and measures on the main goal are calculated. The results from this are shown below.

I(2,1)=0,5 I(3,1)=0,5

As given in the scores it has been assumed that the safety of people and the protection of building are equally important in this example.

I(4,1)=0,225 I(5,1)=0,225 I(6,1)=0,175 I(7,1)=0,15 I(8,1)=0,225

From these numbers one can identify the most important strategies for obtaining the overall goal. Avoiding ignition, limiting fire spread within the compartment and contact with firemen are the most important strategies. Thereafter avoiding fire spread between compartments is important and last allowing escape.

From these results the classification of importance of measures is obtained (total 100%) and can be seen in table 11.

Table 11: Classification of importance of measures

n	Measure	I(n,1)	n	Measure	I(n,1)
1	Contact with fire services	8,6 %	11	Guides with visitors in tower	4.8 %
2	Sprinklers	8,0 %	12	Inert insulating materials	4,8 %
3	Renovation Guidelines	7,7 %	13	Intumescent materials	4,5 %
4	Limit flammable items	7,6 %	14	Fire resistant glazing	4,0 %
5	Training of personnel	6,0 %	15	Burglary alarm	3,6 %
6	Smoke control	6,5 %	16	CCTV	3,0 %
7	Control of installations	6,3 %	17	Procedures for evacuation	2,9 %
8	Automatic fire detection	5,8 %	18	Alarm systems	2,4 %
9	Fire guards	5,5 %	19	Visual signals/evacuation plans	1,7 %
10	Fire fighting equipment	5,1 %			

Out of the first five measures it is only sprinklers that will require a major investment. The rest of the measures are organisational measures.

5.3 *Refinement of the technical effectiveness of each measure*

The above calculations were made assuming that in the present situation the measure was not implemented and in a future situation the measure will be fully implemented. In order to have a more refined approach so called "grades of implementation" (G) on a scale of 0 to 1 can be used, to represent both the present and future situations.

E.g. the old sprinkler system, present in the church, may not be very effective and is thus given a G = 0.1. If modern sprinklers would be fit in the church, they would be much more effective but still it might be hard to have reliable and effective sprinklers on a ceiling that is very high; this could be expressed by G = 0.8. Such present and future grade of implementation values have been defined for all possible measures, see table 12.

Present and future grades of implementation

Nr	Measure	Implementation present / future	Nr	Measure	Implementation present / future
1	Sprinklers	0.1 / 0.8	11	Training of personnel	0.3 / 0.9
2	Fire fighting equipment	0.3 / 0.7	12	Procedures for evacuation	0.2 / 1.0
3	Automatic fire detection	0.0 / 0.5	13	Fire guards	0.0 / 0.9
4	Alarm systems	0.0 / 0.8	14	Guides with visitors in tower	0.0 / 0.7
5	Visual signals/evacuation plans	0.2 / 0.8	15	Control of installations	0.3 / 0.6
6	Smoke control	0.0 / 0.8	16	Renovation Guidelines	0.3 / 0.7
7	Fire resistant glazing	0.0 / 0.7	17	Burglary alarm	0.5 / 0.6
8	Inert insulating materials	0.0 / 0.7	18	Limit flammable items	0.6 / 0.9
9	Intumescent materials	0.0 / 0.7	19	Contact with fire services	0.7 / 1.0
10	CCTV	0.4 / 0.5			

Thereafter with the increase of a grade of implementation an increase in the effectiveness index can be found, where the effectiveness index indicates the contribution of each measure to overall fire safety as calculated by AHP. The overall fire safety is represented by the effectiveness index EI, which is calculated as follows:

$$EI = \sum_{n} EI_n$$

$$EI_n = I(n,1) \cdot G(n)$$

$$\Delta EI_n = I(n,1) \cdot \Delta G(n)$$

In these formulae, n is the number of each measure. Using these formulae, again a ranking can be made of all measures based on their likely improvements of the fire safety (ΔEI).

5.4 *Refinement of the cost effectiveness of each measure*

The ranking from the previous paragraph, based on the contribution to EI of each improved measure (ΔG) does not include the costs of a specific measure. Therefore it will give an technically effective measure a high ranking, even if the costs are disproportionately high. In practice it is important to incorporate cost effectiveness in the calculation.

This done by calculating the ratio between improvement of the fire safety over the costs of a measure:

$$CE_n = \Delta EI_n / c(n)$$

in which n is the number of the measure, and $c(n)$ represents the total costs for implementing this measure.

Now it is possible to rank the measures for cost effectiveness. In figure 3, the two rankings (based on technical optimisation and on cost effectiveness optimization) have been compared.

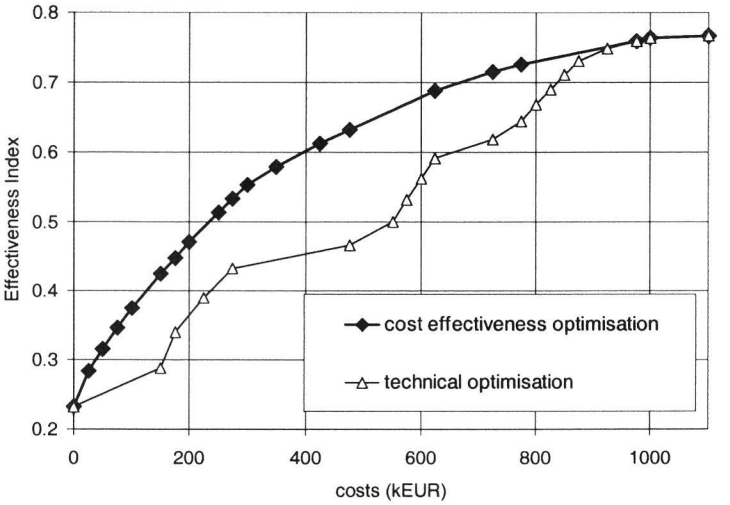

Figure 3: Overall fire safety versus costs with and without cost effectiveness calculation

On the horizontal axis, the figure shows the total costs of a set of measures. On the vertical axis the effectiveness index, achieved with those measures, is shown. The choice of the set of measures is based on the ranking of the measures. The triangular marks represent sets of measures that would be chosen if only the technical optimisation is carried out. The diamond marks represent the sets of measures that would be chosen after carrying out a cost effectiveness calculation.

In the current situation, the EI is 0.23. This can be seen in the figure: in the present situation no costs are made to take additional fire safety measures. At costs=0 both lines show an EI of 0,23, the diamond and triangular marks in the graph representing "empty sets" of additional fire safety measures. If all measures are applied to a credible level (G), the EI will reach 0.77. In the example, this would involve total costs of 1.100 k€. However, with an investment of only 475 k€, the EI can already be improved from 0.23 to 0.63 if the choice of measure is based on a cost effectiveness calculation. If only a technical optimisation is done, the choice of measures would be different and the same investment would give an EI of only 0.47.

6 Results and comparison with existing practice

It is not clear if sprinklers would be acceptable inside the church itself to limit damage to the church and allow escape. In the risk analysis done for the *Nieuwe Kerk* in the Fire-Tech study [5] it has been shown however that sprinklers would limit the damage to the church to an "acceptable" level according to the assumptions made by TNO.

A number of the top ten measures are organisational measures and easy and cheap to apply. Examples are: contact with fire services, guidelines during renovation to avoid ignition, a limitation of unnecessary flammable items and training of personnel.

The criterion of 80m^2 damage in the risk analysis is a tougher recommendation than required by the building decree, which assumes a larger compartment size and will thus in principle allow the entire compartment to burn down. The reason for having the tougher criterion is because of the monumental importance of the church and its contents to the Netherlands.

7 Conclusions

The object of the study, the *Nieuwe Kerk* in Delft, has been used as an example. A number of assumptions concerning the church itself, the effectiveness of measures and the costs involved, should be validated. However the case study has provided a clear example of the possibilities that the methodology, developed within Fire-Tech, has to offer.

The methodology applied in the case study consists of five steps:

1. preliminary steps: definition of the fire safety objectives and the available time and budget.
2. survey of the present fire safety situation: which measures are present in the building?
3. risk analysis
4. survey of possible fire safety measures: which additional measures could be taken?
5. decision making: functional/technical and/or economical optimisation of the choice of measures to be taken. The optimisation is aided by computer models.

In Fire-Tech information has been collected concerning the identification of European regulations, identification of fires in cultural heritage, information regarding archaic materials and information on fire safety techniques. Also, methods for risk analysis and a decision model have been proposed. The case study of the Nieuwe Kerk in Delft has shown that the collected data, together with risk analysis can be combined with a decision model in order to compare a number of fire safety measures and to allow the cost-effective upgrading of a historical building.

Using the method is straightforward but nevertheless requires careful consideration. The all-determining factor is the selection of scores. The scores can be filled in using expert judgement or applying fire safety engineering techniques. The selection of these values can be done by multiple experts. Although these experts are supposed to be familiar both with fire safety and with cultural heritage, the scores assigned to the objectives, strategies and measures can be different. It is noted that the calculated effectiveness index is strongly dependent on expert judgement while entering all scores and grades. This can lead to subjective interpretation and inconsistencies between different individuals filling out the scores and grades.

It should be noted that, even though for any specific case it is possible to calculate an effectiveness index (EI) to represent the overall fire safety, this value of EI can only serve for comparison of different alternative sets of fire safety measures. It is impossible to define a universal threshold value, because in absolute terms the figure has little meaning.

A clear advantage of the AHP method is that it allows the user to oversee a large number of measures and to investigate the sensitivity to specific measures of the overall fire safety level (represented by the effectiveness index). Also, the reasoning behind the choice for a certain set of fire safety measures can be made transparent using this method.

An additional cost effectiveness calculation, as has been added to the spreadsheet AHP-model during the project, can clearly point out which measures per spent Euro contribute most to the overall fire safety level. The case study has shown that this can significantly improve the allocation of budget to an optimised set of fire safety measures.

Through this study this method has shown its potential to determine and upgrade the fire safety level of monumental buildings. It allows to determine the present fire safety level through risk analysis and further to decide on most cost-effective solutions for the upgrading of the building through decision modelling. It is recommended to further use this method for upgrading of cultural heritage buildings.

Acknowledgement
Fire-Tech research project is carried out under the financial support of the EU which is gratefully acknowledged.

References

[1] Cabrita Neves, I., Valente, J., and Ventura, J. ; Fire-Tech WG2 :Analysis of significant fires and Statistical analysis of fire occurrence: 3rd Draft final report, 2004

[2] Twilt, L., et al.; Valorisatie project: Natuurlijk Brandconcept, CEC Overeenkomst 7215-PA/PB/PC -057 (in Dutch)

[3] Oerle, N.J., Janse, E.W. and van de Leur, P.H.E.; TNO report 96-CVB-R0330 (in Dutch)

[4] Breunese, A., Öhlin, S.M. and Twilt, L.; Fire-Tech Case study WG 8 - Example "Nieuwe Kerk"

[5] Öhlin, S.M. and Twilt, L.; Fire-Tech Case study WG 6: Risk Analysis of Cultural Heritage Buildings - Example "Nieuwe Kerk", 2004

Can fatal fires be avoided ? The impact of domestic smoke alarms on human safety

Kjell Schmidt Pedersen
SINTEF NBL as, Trondheim, Norway
Email: kjell.schmidt.pedersen@nbl.sintef.no, Phone: +47 7359 1078

Anne Steen-Hansen
Norwegian University of Science and Technology

This paper presents a summary of the findings from projects at SINTEF NBL concerning the human safety aspect in fires, focusing on fire safety in domestic houses. How domestic smoke alarms affect the safety is chosen as a term of reference. Results from statistical surveys of fire deaths in Norway compared with other countries are used to describe who dies in fires. The use of and requirements for domestic smoke alarms in different parts of the world is briefly presented. The sensibility of ionic and optical smoke detectors in smouldering and flaming fires are analyzed, and an evaluation of the effectiveness of the two detector principles is made based on the test results and expected frequencies of these types of fires. Available time for evacuation is discussed based on expected time to untenable conditions, expected time to flashover, expected time to intervention from fire brigades, and the expected response time for smoke alarms. Different needs to evacuate different groups of occupants (children, elderly people, disabled) are also discussed. An analysis shows that the Norwegian requirement of domestic smoke alarms is highly cost effective. In Norway between 40 and 60 people die in fires every year, and it is estimated that 10 lives is saved every year because of installed domestic smoke alarms. There is, however, an improvement potential for the effectiveness of domestic smoke alarms. Detectors and alarms can be improved technically, requirements to power supply can be set, the installation can be optimized and the extent of use can be increased. All these improvements will increase the probability that an installed smoke alarm really is functioning in case of a fire, both concerning detection and alarm.

Key words: Fire safety, fatal fires, smoke alarms

1 Who dies in fires, why and where does it happen?

1.1 How many persons die in fires?

The number of fire fatalities in a country varies to some degree around an average value from year to year. The Geneva Association has been collecting and systematizing international fire statistics for more than twenty years [1], and the ranking between the countries have more or less been unchanged during the last 10 years, see Figure 1. It is also interesting to notice from the figure that most countries in this list have reported a decrease in number of fire deaths over the period 1992 to 2001. The numbers in the statistics are far from exact, but they are believed to be a fairly good basis for comparison of fire death conditions between different countries.

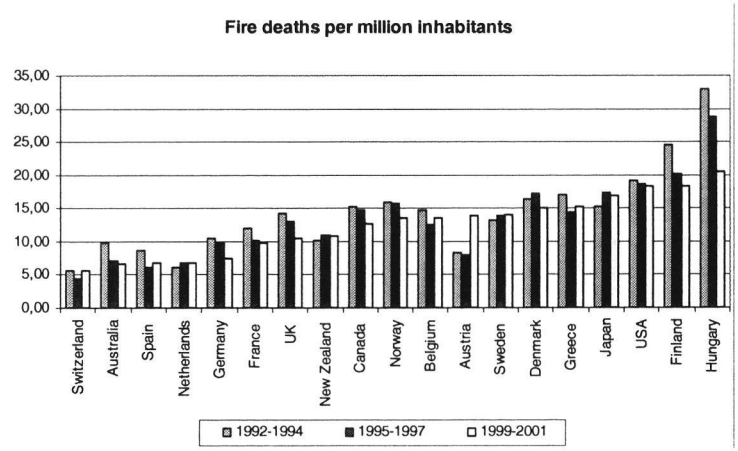

Figure 1: *Number of fire fatalities per million persons in different countries in the periods (1992-1994), (1995-1997) and (1999-2001). The numbers for USA for the latter period include 2791 fatalities following from the World Trade Center disaster 11th September 2001 [1].*

According to the material from The Geneva Association, Switzerland had the lowest rate of fire deaths per population in the period 1999-2001, with a value of 5, 6 fatalities per million inhabitants, closely followed by Australia, Spain and the Netherlands. Hungary was the country on the list with the highest value of fire fatalities, i.e. 20.6 per million people. Norway had the lowest number of deaths among the Nordic countries, with 13.4 per million inhabitants.

The fatalities reported in these statistics are not confined to deaths resulting from fires only in buildings, but include fatalities resulting from fires with a great variety of locations. It is, however, assumed here that a relative ranking between different countries will be roughly the same as shown in Figure 1 when considering solely fires in buildings.

1.2 *Who die in fires?*

Several studies in different countries have been undertaken where fire fatalities are analysed with respect to why, how and where fires start, and concerning how the victims in these fires can be described. In Norway, SINTEF NBL has performed two research projects on this field. One project analysed the fire fatalities in the period 1970-1979 [2], while the other project analysed Norwegian fire deaths in the period 1978-1992, and compared the results with the results from the first project [3]. Later on, an analysis of the impact of different actions against fire was performed, and the effect of smoke detectors on the number of fire fatalities was one of the research objectives. An analysis of factors describing fire victims was one of the methods [4, 5, 6].

About 2/3 of the fire victims are men. This is an international phenomenon. In the Norwegian studies, it was shown that the number of victims per fatal fire is decreasing, i.e. it is most likely that people die alone in a fire. There is a tendency that the proportion of women dying alone in a fire is increasing, and the age of female victims is increasing.

There are many elderly persons among the Norwegian fire victims. Most victims are alone when the fire starts, many of these are elderly people. A large portion of the victims were not able to rescue themselves, because they were in a physically or mentally reduced condition. Such victims could be

- intoxicated by drugs or alcohol
- physically handicapped
- mentally disturbed
- very young children

Only 20 % of the fire victims in Norway in the period 1978-1992 were anticipated as able to evacuate themselves without assistance from others [3].

One interesting finding was that there are relatively few injuries from building fires. There are about three times as many fire injuries in Norway as fire fatalities. Of these, about 17 % are seriously injured [5]. This is in sharp contrast to traffic fatalities, where there are considerable more injures per fatality, and where a large portion of the injuries are serious, which leads to large personal suffering and high expenses for the community. Most fire injuries are caused by inhalation of smoke. There are few fire injuries among elderly people (aged 70 years or more) – only 7 % of fire injuries are registered in this group.

In Norway there will be about 3 fire injuries and 26 building fires per every recorded fire fatality. The corresponding numbers from Australia in the period 1989-1994 was 10 injuries and 143 building fires per fatality [7], i.e. a much smaller probability of fatalities and injuries per building fire than in Norway.

Elderly persons

Elderly persons resemble a large group of fire victims, and the proportion of this group compared to all fire deaths has been increasing. In the period 1985-1989, 30 % of the fire victims were older than 70 years. In the period 1990-1994, the ratio of elderly victims had increased to 33 %, and in the period 1995-1998, 35 % of victims in building fires were 70 years or older. This trend is shown in Figure 2.

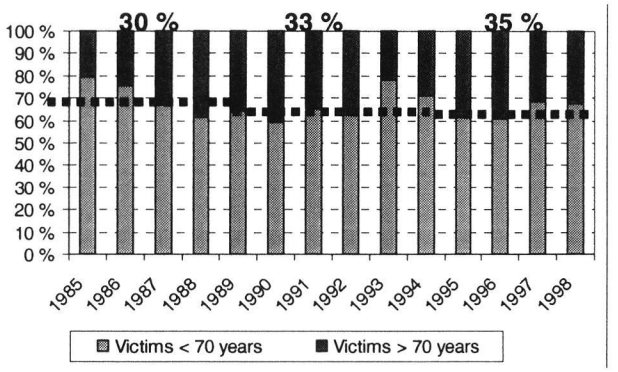

Figure 2: Fire victims aged 70 years or more, compared to fire victims less than 70 years of age in the period 1985-1998. The dashed line shows the averaged ratio of victims aged 70 years or more. This ratio was 30 % in the period 1985-89, 33 % in the period 1990-94 and 35 % in the period 1995-98 [5].

Persons intoxicated by alcohol or drugs

30 % of the fire victims in the period 1970-1979 were intoxicated by alcohol or drugs, 17 % of them heavily affected. The ratio of intoxicated fire victims in the period 1978-1992 has increased to 36 %, whereof 19 % were heavily affected. A larger proportion of fire victims in the larger cities are affected by drugs or alcohol than in less urban areas.

The proportion of intoxicated fire victims is large also in other countries, A Danish study of fire deaths in the period 1988-1993 reported that 62 % of the victims had alcohol in their blood [8]. In a study of fire deaths in London between 1996 and 2000, 40 % of the victims tested for the presence of alcohol were found to have high levels of alcohol in the blood [9].

Physically disabled persons

In Norway about 10-20 % of the fire victims are handicapped, and analyses in Sweden and Denmark also conclude that sick and disabled persons are highly represented among the fire victims [8, 9,10].

Mentally unstable and suicidal persons

About 20 % of the fire victims in the period 1979-1992 were mentally disturbed to different degrees. The proportion of this group of victims had increased significantly compared to the period 1970-1979. It is reasonable to believe that some of these victims committed suicide; for some of the cases this was confirmed through statements from witnesses, in other cases the anticipation was based on strong indications.

Persons being alone when the fire started

Both the Norwegian and the Danish surveys show that a large part of the victims were close to the location where the fire started, and that they were alone. About 35-40 % of the victims were in the same room as the fire started in, and 14 % were in the next room [2, 3]. In about one third of the fires, only one person was present at fire start, and this person died. In Denmark, it was stated that 57 % of fire victims lived alone [8].

Sleeping children and young adults

An Australian project shows that most young children do not awake from the sound of smoke alarms [11], and therefore will need help to wake up in case of a fire. One cannot rely on that children will be alerted by a smoke alarm when they are at sleep. Another Australian project shows that many adults aged 18-24 years also would have problems by getting awake by the sound of a smoke alarm [12]. It has also been shown that many sleeping persons will hear the smoke alarm, but do not understand that the sound means that a fire is on, and will go back to sleep [13]. Smoke alarms, as tested in these projects, may therefore not function as the only means to warn people about a fire at night. To work properly as an alarm device, the alarms may need some modifications, e.g. of alarm signal (frequency, sound level, connection to other devices etc).

A survey was performed amongst 33 persons in Trondheim who had experienced a fire in their homes [14]. The majority of these people were alerted by sounds and smell from the fire. Only 6 of the 33 persons were first made conscious about the fire by the smoke alarms, and 5 of these 6 persons were asleep when the alarm sounded. A total of 14 persons were asleep. Sounds and smell from the fire were alerting more than half of the sleeping people in the analyzed fires. This is a strong indication that smoke alarms may have their greatest effect on alerting sleeping people, and that other signals than the smoke alarm will give most people awake a first awareness of the fire.

There was no available information about function and installation of the smoke alarms in these fires.

Socioeconomic and geographical factors

Several studies, both international and Norwegian, have shown that the frequency of domestic fires are larger in some populations than in others. In a Norwegian study the following factors were identified as being significantly related to the frequency of domestic fires [15]:

- Number of disabled pensioners.
- Number of convicted persons.
- County (The three most northern counties in Norway have a fire frequency three times as high as in the rest of the country).
- High age (the fire frequency is higher for persons aged 75 years or more than for the rest of the population).

The latter finding implies that if a fire starts in an old person's dwelling, the probability to die is higher than if a fire starts in a younger person's home.

A Danish study shows that the fire frequency is higher for persons with low income than for other persons [16]. In block apartments where the median income is low, the fire frequency is 27 % higher than if income had no effect. On the other hand it was not possible to show that a high income will significantly lower the fire frequency.

An Australian study found a significant correlation between fire frequency and income, lodgers and areas with high age (65-85 years) [7].

1.3 Where do fatal building fires start?

Fatal fires are most likely to happen in urban areas. An interesting finding in the Norwegian statistical material was that the proportion of fatal fires in urban areas had increased from 66 % in 1970-1979 to 73 % in 1987-1992.

In the period 1970-1992, 82 % of the fatal building fires in Norway took place in dwellings [3]. Of these dwelling fires, 60 % were in single family homes, 28 % in row houses and multi-family houses, and 12 % were fires in flats in apartment blocks. This means that fatal fires most often happen at home.

The three most likely places for a fatal fire to start are in the living room, in the bedroom and in the kitchen. However, there has been a change in the location of the point of fire origin in the Norwegian fatal fires over the 15 analyzed years. This is shown in Table 1 below.

Table 1: The location of the fire origin in fatal building fires in Norway in the periods 1970-1979 and 1987-1992 [3].

Location of fire origin	1970-1979	1987-1992
Bedroom	30 %	20 %
Kitchen	10 %	17 %
Living room	26 %	39 %

The numbers in Table 1 imply that there has been a shift towards that fatal fires are more likely to start in living rooms and kitchens, and that fires starting in bedrooms are less common than earlier. We believe that this is a consequence of a higher consciousness about the hazard of smoking in bed, combined with a general reduction in the number of smokers.

1.4 *Where do the victims die?*

About one third of the victims in the Norwegian fatal fires in 1970-1992 were found in the same room as the point of fire origin. Most victims of the remaining 2/3 were found near the fire room, at the same floor of the building.

In the first 10 year of the period, 22 % of the victims were found in bed, while the same proportion was 12 % over the last six years from 1987 to 1992. This corresponds well to the finding that the bedroom as the point of fire origin decreased over the same period.

1.5 *What kills people in building fires?*

Most fire victims, over 50-60 %, die of smoke, mainly because of carbon monoxide inhalation. This has been concluded through studies of fatal fires in several countries [2, 3, 8,17].

In the Norwegian study, it was found that the number of mentally unstable persons had increased among the victims, and that there was a tendency to an increase in the number of victims where one suspected that suicide had caused the fire death. The increase in this number was from 1 % in the period 1978-1980 to 7 % in 1990-1992. The number of victims in this material is, however, small, so these results will only be valid as an indication.

2 The effectiveness of different detector principles

We know from statistical surveys, like the ones mentioned in references [2, 3], that people dying in fires suffer a lonely death.
Some fires start as smouldering fires and develop into flaming fires, while others are plain flaming fires from the very start. Based on the fire reports constituting the background for our statistical analyses, it is not easy to distinguish between these two types of fires. If the fire remains smouldering it easily shows on the fire scene. In a smouldering fire the combustion occurs on the surface of the fuel and the process is dependant on the diffusion of air to the combustion zone and diffusion of combustion products from the combustion zone.
A major discussion occurred in Norway in 1988 concerning the choice of principles by which the different domestic smoke alarms and detectors work. Some claimed that a lot of fires start as smouldering fires, and that the detector based on the ionic detection principle detect the smoke far too late, i.e. beyond fatality conditions. This allegation was taken seriously because 95 % of the already installed smoke detectors and alarms were based on the ionic principle and it was the most common fire protection measure in private homes. At that time it was furthermore discussed to require installation of at least one domestic smoke alarm in all private homes. This became mandatory in 1990.

A crucial question to answer was: How frequent are these smouldering fires that eventually turn into flaming fires, and thus are categorized as flaming fires? A smouldering fire could remain as such for a long period of time, creating life threatening conditions. Smouldering fires will create only a small rise in temperature and are soundless, which means that sleeping victims will not notice the fire and wake up. These victims could even be dead before the smouldering fire turned into the flaming phase. Since a lot of the analyzed fatal fires occurred while people were sleeping [2, 3] this problem had to be surveyed.

Since there is no way to establish the number of flaming fires which started as smouldering fires from the fire scene itself, at least not based on the normal fire reports from the police, this number had to be established in an indirect manner. One can anticipate that in a normal household, smouldering fires can occur in upholstered furniture and mattresses made of expanded polyurethane. To establish a smouldering fire in such a material, one has to start the fire by applying a glowing ignition source, like a burning cigarette. One cannot exclude other materials and/or ignition sources, but most of the smouldering fires will be in the category mentioned above. After going through the statistical material discussed in [2, 3], combining first ignited material and cigarettes, we established that the number of fatal smouldering fires will maximum be 25 % of the total number of fatal fires. This is considered to be a conservative number.

As a consequence of this discussion, SINTEF NBL decided to perform a series of tests using different detectors and smoke alarms in smouldering and flaming scenarios. Several different types of smoke detectors were tested together with heat detectors. These tests were performed in 1989 by SINTEF NBL together with detector producers, insurance companies and Norwegian Fire Protection Association [18]. The test room was arranged like a patient room in a hospital with normal bedding components with no addition of flame retardants. The registered moments for alarm were evaluated against criteria for safe occupancy conditions associated with CO-concentrations, visibility and temperatures. The safe occupancy criteria were based on the recent year's research results. Unsafe occupancy concerning CO-concentrations is considered to be beyond the accumulated dose of CO (measured in ppm·min) leading to incapacitation. Some of the test results are shown in Figure 3, Figure 4 and Figure 5 below.

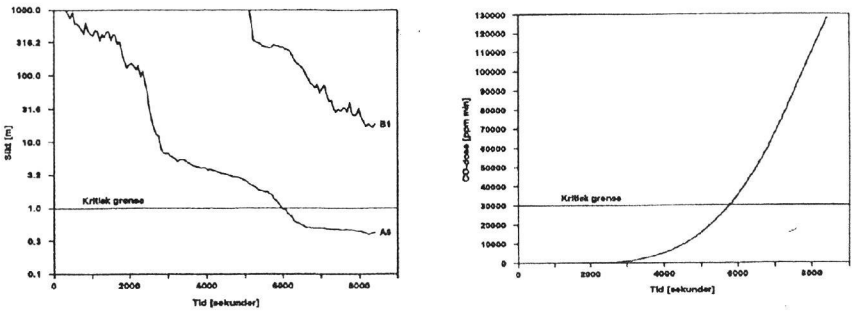

Figure 3: Smouldering fire development. Left diagram: reduction in visibility [m] in the fire room (A6) and in the adjacent room (B1) versus time [s]. The critical limit for visibility, defined as 1.0 m, is indicated. Right diagram: accumulated CO-dose [ppm·min] in the fire room versus time. The critical limit for CO-dose, defined as 30 000 ppm·min, is indicated.

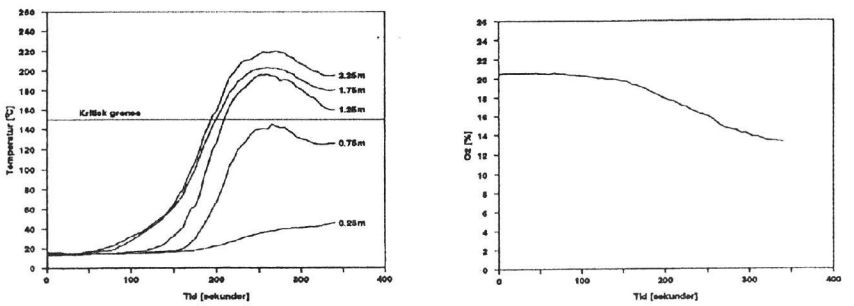

Figure 4: Flaming fire development. Left diagram: temperature [°C] measured at different levels above the floor versus time. The critical temperature limit, defined as 150 °C, is indicated. Right diagram: Oxygen concentration [Vol%] at ceiling level in the fire room versus time.

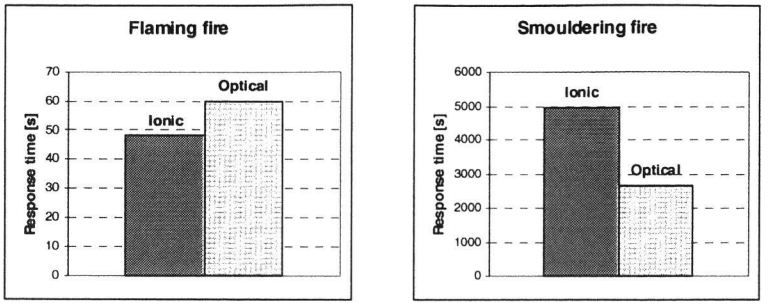

Figure 5: Response time [s] for optical and ionic smoke alarms in a flaming fire and in a smouldering fire. The smoke alarms were located in the ceiling in the fire room. Note the large difference in time scales for response time in the two types of fire.

In the tests with smouldering fires critical conditions were reached after 5-6000 seconds after fire start. Both the optical smoke alarms and detectors responded before life threatening conditions were reached. The ionic based alarms and detectors did not give adequate protection in case of smouldering fires in these tests.

In the flaming fires the critical temperatures in the smoke layer were reached 200-240 seconds after the fire start. The alarms and detectors based on the ionic principle reacted slightly faster than the alarms and detectors of the optical type. The differences are considered to be marginal. These results are in accordance with results from a recent extensive project at NIST in US, where several smoke detectors were tested in a variety of fire conditions [19]. Fire tests in domestic bedrooms showed times to smoke detector response in the magnitude of what was experienced in the SINTEF NBL tests in the simulated patient room.

From these test results one could clearly conclude that smoke alarms in dwellings preferably should be based on the optical detector principle, if only one type should be applied.

At the end of the 1980's 95 % of the domestic smoke alarms were based on the ionic principle. Considering this information, and the fact that smouldering fires are likely to start as a result of ignition by glowing cigarettes, one could state that people should be sufficiently safe if one could avoid such fire starting conditions. This implies that one first of all should avoid that people are smoking in their beds.

However - all this information, recommendations and finally official prescriptions will most likely not reach the individuals of the population most threatened by domestic fires, being elderly single alcoholised men, as shown in [2, 3].

3 Time to flashover and available time for evacuation

SINTEF NBL performed a series of analyses of occurred fires over the period 1978-82 to retrieve data that could be used as a basis for revision of prescriptions [20, 21]. One of the factors studied was the different times to flashover in the rooms of fire origin. The rooms or occupancies were of different sizes and involved different activities. Half the number of fires involved flashover times less than 10 minutes. Smaller rooms, like patient rooms in hospitals or living rooms in private homes, gave flashover times in the order of 6 minutes. Later investigations of occurred fires reveal that the flashover times for dwellings, hospital rooms and the like, after the flaming stage is reached, are 5-10 minutes. The majority of these flashover times are closer to 5 than 10 minutes.

Among the above mentioned analyses performed by SINTEF NBL in 1978-82, one study concentrated on hospital fires only [22]. 4 actual hospital fires occurring in the project period were closely analysed and the project team issued a comparison of the findings in Norway with results from international studies [23]. The 4 actual fires included 2 incidents that were classified as catastrophes (i.e. resulting in more than four fatalities). The following conclusions could be drawn from the studies of the hospital fires concerning the actual fire risk for hospitals:

- The three main factors of importance for the fire safety of the patients are alarm, actions taken by the personnel, and the reaction-to-fire properties of the bedding components or other interior materials. The actions taken by the personnel include fighting the initial fire, assist evacuation and closing doors to the fire room.
- A critical situation can occur in a patient room only three minutes after bedding components without any flame retardants have been ignited by a small flame. A critical situation means a situation that is not controllable by the personnel.
- The smoke spread potential represented by an open door is paramount and should attract much more attention than it has done (this is unfortunately the case even today in 2005). Fire protection and preparedness is concentrating on smoke spread potential of ventilation ducts, dampers when ducts are penetrating walls, and the procedure to stop the ventilation system in the case of fire. Stopping the ventilation system was a major mistake in the case of the fire on the passenger ship "Scandinavian Star" 7th April 1990, where 158 persons died [24]. As long as the air inlet lines are separated from the air outlet lines it is important to let the ventilation system run to avoid spread through the system by natural pressure differences.

- An automatic detection and alarm system alone is not giving any guarantee for the patient's safety. This must be closely linked to the personnel's possibilities to act.
- The difference in response time between heat detectors and smoke detectors is of vital importance to the patients' safety when bedding components without any flame retardants are used.
- Quick and adequate actions from the personnel are heavily dependant on the instructions and training given to the personnel.

All these findings from the analyses of the unfortunate hospital fires led to changes in the prescriptions, making it mandatory to install automatic smoke detection systems in hospitals with more than ten beds. It furthermore led to a major campaign throughout the country to instruct and train hospital personnel in how to meat a start fire and manage to control it.

SINTEF NBL performed a cost-benefit study of the public fire brigades in 1988-89 [25]. This study showed that the fire brigades usually arrived at the fire scene at the time when the fire room or the building reached flashover, or shortly after this moment. This means that the fire brigades in many cases will arrive too late to be able to rescue persons from the fire room, and that measures against fire with a fast response time are necessary to increase the human safety.

From all the above mentioned statistical analyses, case based studies and cost-benefit studies, one conclusion concerning human safety is evident: *The major difference between failure or success for saving human lives lays in the possibility of the occupants to have an early responding, audible and understandable alarm, and the possibility to perform quick and adequate actions of fire fighting and assisted evacuation.*

Based on these findings and following expert panel discussions, the Norwegian fire prescriptions were radically changed. From 1990 it was mandatory to have smoke alarms (one battery driven smoke alarm as a minimum) and hand held extinguishing units (portable powder extinguishers or water hoses) in every dwelling, both in existing as well as in new units [26]. At that time this was a very unusual claim to include in public prescriptions. As shown in [5] this was lucrative in terms of saved lives compared with the total installation costs for all the dwelling units in Norway.

In a survey performed by NFPA in the US, the available time to escape was analysed concerning how it would affect human safety in home fires [27]. One conclusion was that roughly half of the fire deaths and two-thirds of the injuries in dwelling fires in the US could be prevented if the times to escape were sufficiently lengthened. Smoke alarm was identified as a necessary measure for saving most sleeping victims.

4 Many countries require smoke detectors in dwellings

Although many countries have had no legislation regarding installation of domestic smoke alarms, the prevalence of such alarms has been quite high for many years. National information campaigns over the last have been the main reason for this widespread use of smoke alarms. Some countries will not accept installation of ionization smoke detectors, because the radio active sources in the detectors represent a large problem for waste treatment when old smoke alarms are discarded. Below, requirements in some nations are briefly presented.

Norway: Smoke alarms have been required in both new and existing residential buildings since 1991. This requirement also includes holiday homes and cottages. At least one approved smoke alarm shall be installed in each dwelling, and shall be heard in all bedrooms when the doors are closed [26]. There are no specific requirements to which type of detector that should be installed, or to the type of power supply system, but recommendations on different solutions are given in the guidelines to the regulations [28].

Denmark: 1st of December 2004 the new fire safety regulations in the building regulations for small buildings came into force. The regulations are applicable for single family houses with a maximum of two floors and a basement. One of the new requirements is the prescription of a smoke alarm system for each dwelling. The system shall be coupled to the mains, and shall be equipped with a battery backup system [29].

Sweden: All buildings shall be equipped with safety measures that prevents fire from starting and developing, and that restrict fire damage [30]. On this background, the Swedish Rescue Services Agency issued a general recommendation on installation of smoke alarms in all residential buildings in 2004 [31]. At least one functioning alarm should be installed in each floor, and precautions to ensure a continuous power supply are recommended.

Finland: All residences in Finland, both existing and new (including summer cottages and other holiday houses), must be equipped with fire detectors [32]. This decree came into force 1 September 1999, and the detectors had to be installed within a year. There must be at least one detector in each storey, and it must be kept in working order (the batteries must be functional etc.). The occupant of the residence is responsible for the installation and maintenance. Battery is the required power source. If the detector is wire operated, it must be provided with a battery backup.

United Kingdom: According to the Building regulations from 2000, dwellings shall be provided with devices for the early warning of fire [33]. A general recommendation about placing smoke alarms in

connection with bedrooms, and installing at least one detector in each floor is given. Smoke alarms can be wired or battery operated.

The Netherlands: Smoke detectors have been required in new dwellings in the Netherlands since 2003. Detectors shall be of the non-ionic type, and shall be coupled to the electrical mains system [34]. There are no requirements for smoke alarms in existing dwellings.

The United States: Smoke detectors have been increasingly common in domestic households over the last three decades, and it is estimated that 93, 6 % of homes across the US had a smoke alarm installed in 1995 [35], and at least 95 % in 2000 [19]. The high prevalence is a result of different strategies: public education, legislations, improved technology and smoke-alarm-giveaway programs. Several states in the US have legislation requiring domestic smoke alarms.

5 How many homes have smoke alarms installed? How many alarms work?

Nearly all Norwegian dwellings, i.e. more than 97 %, have smoke alarms installed. Surveys have shown, however, that only 60-80 % of these smoke alarms would function as required in a fire [5]. There are less smoke alarms, and also less working alarms, in dwellings where there have been a fire. In dwellings where there has been a fatal fire, the number of functioning smoke detectors is even lower.

In a survey of statistical information from 365 Norwegian fatal fires in the period 1997-2003, where a total of 420 victims died [36], it was found that

- 25 % of the dwellings had a working smoke alarm installed
- 21 % had no smoke alarm or a non-functioning smoke alarm installed
- For 38 % there was no information available whether a smoke alarm was installed or not.

In a Swedish survey it was found that a working smoke alarm was absent in 75 % of fatal fires in Sweden in 2002 [37]. In Norway dwellings in row houses are best covered by smoke alarms [5]. Single-family homes have a coverage near the national average for Norway, while flats in block buildings have the lowest number of smoke alarms installed. Holiday homes are also poorly covered.

In all the Nordic countries there are most smoke alarms installed in single-family homes, and fewer in flats. Information campaigns have resulted in the high level of smoke detectors in Sweden, Denmark and Finland. It looks like, however, that Norway, through prescriptions, has obtained a

higher degree of smoke alarm coverage than the other Nordic countries. Denmark and Sweden have not had any requirements for installation of this equipment before recently.

6 Is there room for improvements?

It is impossible to state the exact number of lives that smoke detectors have saved. The falling trend in number of fatalities in building fires is shown in

Figure 6. This figure shows that the average number of fire fatalities per million inhabitants has decreased from 16.4 in the end of the 1980's to 14.1 in the end of the 1990's. Related to a Norwegian population of about 4.5 million people, this means that approximately 10 lives are saved every year compared to the number of fatalities in the late 1980's.

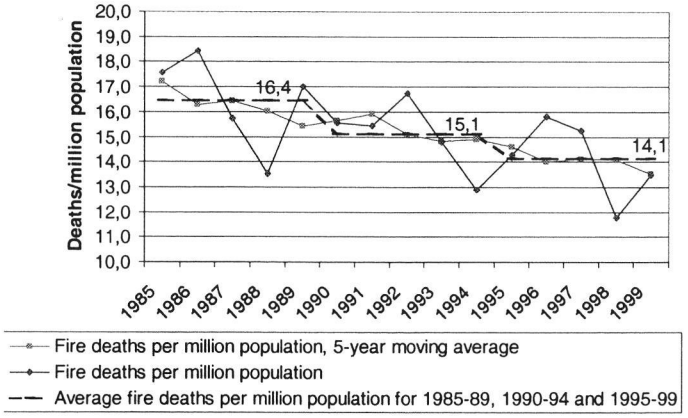

Figure 6: 5-years moving average of fire deaths per million population in Norway, yearly number of fire deaths per million inhabitants and the average number of fire deaths per million inhabitants for 1985-89, 1990-94 and 1995-99.

SINTEF NBL has performed a study [5, 6] concerning the cost–benefit effects of these requirements. This study shows that the requirements are cost effective. A rough estimate on the cost-effectiveness is based on the following assumptions:

- 2 smoke detectors per housing unit with 10 years of operating time
- 2 batteries per housing unit per year
- 2 millions housing units
- a statistic life is worth 18 millions NOK (2000-value)

Based on these premises the yearly cost is estimated to be 120 millions NOK, while the benefit per year is estimated to be 180 millions NOK. This gives a net annual profit of 60 millions NOK, or expressed as a benefit-to-cost ratio of 1.5: 1.

This estimate only includes the benefit of saved lives. In addition smoke alarms will limit material losses by detecting fires at an early stage.

Reports from the Norwegian fire brigades show that mobile fire extinguishing equipment in dwellings prevent fire spread in 15 % of the domestic fires every year. We have no statistical information that indicates the potential material loss if the fire extinguishing equipment had not prevented the fire from spreading, but we could assume that fire-extinguishing equipment reduces the insurance companies' compensation of fire losses with 15 % per year. The estimate is based on the following assumptions:

- One portable extinguisher per housing unit with 10 years of operating time.
- 2 millions housing units.
- Compensation from the insurance companies for material losses in dwelling fires per year is 1 500 millions NOK (in1999) [38].

The resulting cost per year is estimated to be 100 millions NOK, while the annual benefit is estimated to be 225 millions NOK. The resulting benefit-to-cost ratio will then be approximately 2:1.

Data and experience from domestic fires over the last 10 years show that the coverage and function of smoke alarms imply an improvement potential. Improvements will arise from the following main actions:

- *Secure the power supply*
  The main reason that smoke alarms do not function is missing or flat batteries. By connecting the smoke alarms to the mains or by using long-life batteries (10 years operating time), the probability that the smoke alarm will function increases considerably. The need to change battery will decrease, which will be beneficial for some groups of persons where this may be a problematic operation (for instance elderly persons).
- *Connect the smoke alarms in series*
  Install more than one smoke alarm and connect them in series. This will secure an early detection and warning of fire. Full-scale experiments indicate that approximately 2 minutes of extra evacuation time can be achieved if more smoke alarms are installed, instead of having one smoke detector in each dwelling [7].
- *Improve follow-up and inspection*

Higher priority should be given to follow-up and inspection of the fire safety in dwellings. A possible solution is that the fire brigade, chimneysweepers or insurance companies carry out inspections to check that the required equipment is properly installed and that it functions. This may, however, be perceived as unnecessary monitoring and guardianship. Another solution is that every house owner has to document that he or someone else has verified the equipment.

- *Special actions for elderly persons and other groups at risk*
  We recommend inspection programs to be carried out to assist elderly persons and disabled persons to maintain the smoke alarms.

Primarily, smoke alarms will help persons that are able to evacuate without assistance. Only 20-30% (approximately 15-20 persons) of the Norwegian fire victims belonged to this group before the requirements came into force [2, 3]. We have assumed that some of the victims categorised with "unknown condition" in the SINTEF NBL analyses actually would be self-reliant. An established effect of approximately 10 persons saved per year is already demonstrated through our analysis. That indicates that the maximal yearly potential for further reduction in the number of fire deaths in Norway is approximately 10 persons, based on the prerequisite that every Norwegian household have smoke detectors that function in case of a fire.

7 Conclusive remarks

The SINTEF NBL studies [2, 3, 20, 22] clearly show that 70-80 % of the fatalities occur in dwelling units; i.e. private homes and cottages, and that people die one by one. Traditionally, building prescriptions and building codes are not addressing measures or requirements for protection of human lives as they are normally threatened in fires. Prescriptions and codes will in the first place protect against catastrophic fires, and will protect third parties from damages from the buildings on fire.

The requirements in the fire prescriptions of 1990 [26] are, however, addressing the daily fire threat to people by requiring at least one smoke alarm and a hand held extinguisher in every dwelling unit. Norway has a population of approximately 4.6 million people per January 2005. This means that the demonstrated effect from installation of smoke alarms and hand held extinguishers is 2.2 lives per million inhabitants. The estimated full potential of these measures against fire is estimated to be 4.4 saved lives per million persons.

References

[1] The Geneva Association (2004): 'World Fire Statistics. Information Bulletin of the World Fire Statistics', No. 20, October 2004. http://www.genevaassociation.org/ (January 2005).

[2] Pedersen, K. Schmidt og Lundberg, S.(1982): 'Menneskelig sikkerhet ved brann i bygning. En statistisk undersøkelse av branner i Norge med tap av menneskeliv.' (Human safety in building fires. A statistical analysis of Norwegian fatal fires). *SINTEF-report STF25 A82008.* Norwegian fire research laboratory, SINTEF, Norway.

[3] Hansen, A.S. (1994): 'Dødsfall som følge av brann i bygninger. En analyse av dødsbranner i perioden 1978-1992' (Fire deaths. An analysis of fatal fires in the period 1978-1992). *SINTEF-report STF25 A94008.* Norwegian fire research laboratory, SINTEF, Norway.

[4] Hansen, A. S., Hovden, J. (1998): 'Do smoke detectors and portable extinguishers in residences affect fire safety?' *1. International Symposium on Human Behaviour in Fire, Belfast, UK, September 1998.* ISBN 1 85923 103 9, pp 135-143.

[5] Mostue, B.Aa. (2000): 'Evaluering av tiltak mot brann. Har røykvarslere, håndslokkingsapparater og sprinkleranlegg hatt effekt på brannsikkerheten i Norge?' (Evaluation of actions against fire. Have domestic smoke detectors, manual extinguishers and sprinkler systems affected the fire safety level in Norway?) *SINTEF-report STF22 A00853,* Norwegian Fire Research Laboratory, SINTEF, Norway.

[6] Mostue, B.Aa., Hansen, A.S., Pedersen, K.S. (2001): 'Smoke detectors and fire extinguishing equipment in residences – evaluation after ten years with prescriptions.' *Interflam 2001, 9th International fire science & engineering conference, Edinburgh, UK. Conference proceedings Volume 1,* ISBN 09532312 9 1, pp 269-278.

[7] Beever, P. og Britton, M. (1998): 'Research into Cost_Effective Fire Safety Measures for Residential Buildings.' Victoria University of Technology, Melbourne, Australia, 1998.

[8] Leth, P. (1998): 'Omkommet i brand' (Fire fatalities), *PhD dissertation,* Aarhus Universitet, Denmark.

[9] Holborn, P.G. Nolan, P.F., Golt, J. (2003): 'An analysis of fatal unintentional dwelling fires investigated by London Fire Brigade between 1996 and 2000.' *Fire Safety Journal* 38 (2003) pp 1-42.

[10] Svenska Brandförsvarsföreningen (2000): '110 omkom i brander under 1999.' (110 persons died in fires in 1999). *Brand och Räddning* no 1 2000, p 10. Stockholm, Sweden.

[11] Bruck, D. (1999): 'Non-awakening in children in response to a smoke detector alarm.' Department of Psychology, Victoria University, Melbourne, Victoria, Australia.

[12] Bruck, D., Horasan, M. (1995): 'Non-arousal and Non-action of Normal Sleepers in Response to a Smoke Detector Alarm.' Victoria University, Australia.

[13] Grace, T. (1997): 'Improving the Waking Effectiveness of Fire Alarms in Residential Areas.' *Fire Engineering Research Report: 97/13*, Canterbury University, New Zealand. http://www.civil.canterbury.ac.nz/fire/pdfreports/Grace.pdf (January 2005).

[14] Aanensen, M., Østbye, I.E. (1998): 'Adferd i boligbranner.' (Behaviour in domestic fires). A master of science project report, Norwegian University for Science and Technology, Trondheim, Norway.

[15] The Norwegian Directorate for Fire and Explosion Prevention (Direktoratet for brann- og eksplosjonsvern), Statistics Norway (Statistisk sentralbyrå), Parexel Medstat Research (1999): 'Samfunnet og brannhyppighet. Prosjektrapport. '(The community and the frequency of fires. Project report.), Tønsberg, Norway.

[16] Ryborg, S.(2000): 'Sammenhæng mellem indkomst og brand.' (Correlation between income and fire). *Brandværn og sikring* 2/00, p. 17. Foreningen af Kommunale Beredskapschefer og Dansk Brandteknisk Insititut, Copenhagen, Denmark.

[17] Harwoos, N., Hall, J.R (1989): 'What kills in fires, smoke inhalation or burns?' *Fire Journal* 83(3), p 28, May/June 1989.

[18] Meland, Ø. og Lønvik, L.E. (1989): 'Deteksjon av røyk. Rapport fra fullskala brannforsøk i Vesterskaun skole januar 1989.' (Detection of smoke. Full scale fire tests in January 1989). *SINTEF report STF25 A89010*, Norwegian Fire Research Laboratory, SINTEF, Norway.

[19] Bukowski, R.W. et al (2004): 'Performance of Home Smoke Alarms. Analysis of the Response of Several Available Technologies in Residential Fire Settings'. *NIST Technical Note 1455*. National Institute of Standards and Technology, Fire Research Division, Building and Fire Research Laboratory, Gaithersburg MD. http://smokealarm.nist.gov/HSAT.pdf (January 2005).

[20] Pedersen, K.S., Lundberg, S. (1982): 'Branners utvikling og skaderesultat. Analyser av de forskjellige faktorenes betydning på bakgrunn av inntrufne branner.' (Development and damage potential of fires. Analysis of the impact of the different factors based on occurred fires). *SINTEF report STF25 A82007*, Norwegian Fire Research Laboratory, SINTEF, Norway.

[21] Pedersen, K.S., Lundberg, S. (1982): 'Branner; systematisering og analyse. Delrapport 4. Vurdering av krav i lover og forskrifter.' (Analysis of fire safety requirements in the building prescriptions). *SINTEF report STF25 A82005*, Norwegian Fire Research Laboratory, SINTEF, Norway.

[22] Pedersen, K.S., Lundberg, S. (1980): 'Branner, systematisering og analyse. Delrapport 2. Sykehus- og sykehjemsbranners tidlige fase.' (The early phase of hospital fires). *SINTEF- report STF25 A80005*, Norwegian Fire Research Laboratory, SINTEF, Norway.

[23] Lundberg, S.(1981): 'Brannsikring av sykehus. Bygningstekniske løsninger; seksjonering, varsling og sprinkleranlegg sett i relasjon til personalets muligheter for slokking og redning.' (Fire protection of hospitals. Analysis of the build in safety and its importance concerning the

possibility for the staff to perform fire fighting and evacuation assistance). *SINTEF report STF25 A81006*, Norwegian Fire Research Laboratory, SINTEF, Norway.

[24] Schei, T. (ed.) (1991): 'The Scandinavian Star disaster of 7 April 1990 : report of the committee appointed by royal decrees of 20 April and 4 May 1990 : submitted to the Ministry of Justice and the Police in January 1991.' *Norwegian official reports ; NOR 1991: 1 E.* ISBN: 82-583-0236-1 (h.) Oslo, Norway.

[25] Kørte, J.(1989): 'En analyse av det norske brannvesen.' (A cost–benefit analysis of the Norwegian Public Fire Brigade). *SINTEF report STF25 A89003*, Norwegian Fire Research Laboratory, SINTEF, Norway.

[26] Directorate for civil protection and emergency planning (Direktoratet for samfunnssikkerhet og beredskap) (2002): Forskrift om brannforebyggende tiltak og tilsyn (Regulations relating to fire-preventive measures and fire inspection), Tønsberg, Norway. www.dsb.no (January 2005).

[27] Hall, J.R. Jr. (2004): 'How many People Can Be Saved from Home Fires if Given More Time to Escape?' *Fire Technology*, 40, pp117-126.

[28] Directorate for Civil Protection and Emergency Planning (Direktoratet for samfunnssikkerhet og beredskap) (2004): 'Veiledning til forskrift om brannforebyggende tiltak og tilsyn.' (Guidelines to Regulations relating to fire-preventive measures and fire inspection). www.dsb.no (January 2005).

[29] National Agency for Enterprise and Construction (Erhvervs- og Byggestyrelsen) (2004): 'Tillæg 6 til Bygningsreglement for småhuse 1998.' (Appendix 6 to Building regulations for small houses 1998). Copenhagen, Denmark. http://www.ebst.dk/file/2220/tillaeg6_smaahuse_br98.pdf (January 2005).

[30] Swedish Ministry of Defence (Försvarsdepartementet)(2003): 'Lag (2003:778) om skydd mot olyckor.' (Regulations about protection against accidents). Valid from 2004-01-01. Stockholm, Sweden. http://www.notisum.se/rnp/sls/lag/20030778.htm (January 2005).

[31] The Swedish Rescue Services Agency (Statens räddningsverk) (2004): 'Statens Räddningsverks allmänna råd och kommentarer om brandvarnare i bostäder.' (The Swedish Rescue Services Agency's general advice and recommendations concerning fire alarms in dwellings). *Statens räddningsverks författningssamling, SRVFS 2004:2.* ISSN 0283-6165. Stockholm, Sweden. http://www.srv.se/RSDoc/SRVFS_2004-2.pdf (January 2005)

[32] Inrikesministeriet, Räddningsavdelningen (Department for Rescue Services, Finland) (1999): 'A:59 Brandvarnares tekniska egenskaper och placering.' (Smoke alarms: technical requirements and installation). Helsinki, Finland. http://www.pelastustoimi.net/ (January 2005).

[33] Office of the Deputy Prime Minister (2002): 'Building regulations 2000. Fire Safety. Approved document B1. Means of warning and escape. 2000 edition consolidated with 2000 and 2002 amendments.' http://www.odpm.gov.uk/stellent/groups/odpm_buildreg/ (January 2005).

[34] The Netherlands Ministry of Spatial Planning, Housing and Environment (VROM) (2003): 'Regeling Bouwbesluit 2003.' (Dutch Building Regulations). Den Haag, the Netherlands. http://www.vrom.nl/ (January 2005).

[35] Stevenson, Mark R., Lee, Andy H. (2003): 'Smoke alarms and residential fire mortality in the United States: an ecologic study.' *Fire Safety Journal* 38 (2003) 43-52.

[36] Liebe, G (2004): Presentation at the 12th International Fair of Fire Fighting Equipment PYROS 2004, Brno, Czech Republic May 2004.

[37] Stålbrand, K (2003): 'Antalet döda i brander fortsatt högt!' (The number of fire fatalities is still high). *Brand och Räddning* no 1 2003, p 6. Stockholm, Sweden.

[38] FNH Finansnæringens hovedorganisasjon (2000): 'Brannårsaksstatistikk. Foreløpige tall for 1999. Endelige tall for 1998.' (Norwegian Financial Services Association. Statistics on causes of fire. Preliminar numbers for 1999. Final numbers for 1998). Oslo, Norway.

Sponsored by:

Bouwen met Staal

Centre Technique Industriel de la Construction Métallique

DGMR

Efectis

Delft University of Technology

LBP

Peutz

Promat

Rockwool

Sintef NBL

Stybenex

TNO

VVBA

TNO Environment and Geosciences

Centre for Fire Research

P.O. Box 49

2600 AA Delft

The Netherlands

www.tno.nl